R-08-109

Explorative analyses of microbes, colloids, and gases together with microbial modelling

Site description model SDM-Site Laxemar

Lotta Hallbeck, Karsten Pedersen
Microbial Analytics Sweden AB

August 2008

Svensk Kärnbränslehantering AB
Swedish Nuclear Fuel
and Waste Management Co
Box 250, SE-101 24 Stockholm
Tel +46 8 459 84 00

ISSN 1402-3091
SKB Rapport R-08-109

Explorative analyses of microbes, colloids, and gases together with microbial modelling

Site description model SDM-Site Laxemar

Lotta Hallbeck, Karsten Pedersen
Microbial Analytics Sweden AB

August 2008

Preface

The overall objectives of the hydrogeochemical description for the Laxemar-Simpevarp area are to establish a detailed understanding of the hydrogeochemical conditions at the site and to develop models that fulfil the needs identified by the safety assessment groups during the site investigation phase. Issues of concern to safety assessment are radionuclide transport and technical barrier behaviour, both of which are dependent on the chemistry of groundwater and pore water and their evolution with time.

The work has involved the development of descriptive and mathematical models for groundwaters in relation to rock domains, fracture domains and deformation zones. Past climate changes are the major driving force for hydrogeochemical changes and therefore of fundamental importance for understanding the palaeohydrogeological, palaeohydrogeochemical and present evolution of groundwater in the crystalline bedrock of the Fennoscandian Shield.

Understanding current undisturbed hydrochemical conditions at the proposed repository site is important when predicting future changes in groundwater chemistry. The causes of copper corrosion and/or bentonite degradation are of particular interest as they may jeopardise the long-term integrity of the planned SKB repository system. Thus, the following variables are considered for the hydrogeochemical site descriptive modelling: pH, Eh, sulphur species, iron, manganese, carbonate, phosphate, nitrogen species, total dissolved solids (TDS), isotopes, colloids, fulvic and humic acids and microorganisms. In addition, dissolved gases (e.g. carbon dioxide, methane and hydrogen) are of interest because of their likely participation in microbial reactions.

In this series of reports, the final hydrogeochemical evaluation work of the site investigation at the Laxemar site, is presented. The work was conducted by SKB's hydrogeochemical project group, ChemNet, which consists of independent consultants and university researchers with expertise in geochemistry, hydrochemistry, hydrogeochemistry, microbiology, geomicrobiology, analytical chemistry etc. The resulting site descriptive model version, mainly based on available primary data from the extended data freeze L2.3 (November, 30 2007). The data interpretation was carried out during November 2007 to September 2008. Several groups within ChemNet were involved and the evaluation was conducted independently using different approaches ranging from expert knowledge to geochemical and mathematical modelling including transport modelling. During regular ChemNet meetings the results have been presented and discussed.

The original works by the ChemNet modellers are presented in four level III reports containing complementary information for the bedrock hydrogeochemistry Laxemar Site Descriptive Model (SDM-Site Laxemar, R-08-93) level II report.

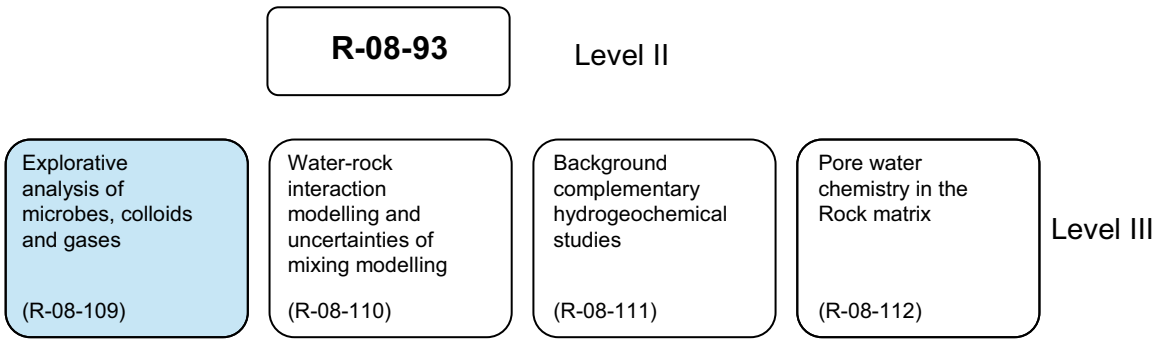

There is also a fifth level III report: Fracture mineralogy of the Laxemar area by Sandström et al. R-08-99.

This report focuses on microbiology, colloids and gases

- *Microbes (Chapter 1):* Several methods must be used to characterise active microbial communities in groundwater. Microbial parameters of interest are the total number of cells (TNC) and the presence of various metabolic groups of microorganisms. Different microbial groups influence the environment in different ways, depending on what metabolic group is dominant. Typically, the following redox couples are utilized by bacteria in granitic groundwater: H_2O/O_2, NO_3^-/N_2, $Mn^{2+}/Mn(IV)$, $Fe^{2+}/Fe(III)$, S^{2-}/SO_4^{2-}, CH_4/CO_2, CH_3COOH/CO_2, and H_2/H^+. The data will indicate the activity of specific microbial populations at particular sites and how they may affect the geochemistry.
- *Colloids (Chapter 2):* Particles in the size range from 1 to 1×10^{-3} μm are regarded as colloids. Their small size prohibits them from settling, which gives them the potential to transport radionuclides in groundwater. The aim of the study of colloids in the Laxemar 2.3 site investigation was to quantify and determine the composition of colloids in groundwater samples from the boreholes. There are both inorganic and organic colloids, and the site investigation measured both types.
- *Gases (Chapter 3):* Dissolved gases in groundwater contribute to the mass of dissolved species. The distribution and composition of dissolved gases in deep groundwater are important to understand in the safety assessment of a deep geological nuclear waste repository: Micro bubbles of gas may potentially transport radionuclides from the repository to the surface. Oxygen, hydrogen sulphide and carbon dioxide are parts of fundamental redox couples that participate in several solid-aqueous phase transformations such as the precipitation of ferric iron oxides, iron sulphide and calcite. Methane and hydrogen, may serve as sources of energy to various microbiological processes.

Contents

Microbial abbreviations:

TNC = total number of cells
ATP = adenosine-tri-phosphate
CHAB = cultivable heterotrophic aerobic bacteria
NRB = nitrate-reducing bacteria
IRB = iron-reducing bacteria
MRB = manganese-reducing bacteria
SRB = sulphate-reducing bacteria
AA = autotrophic acetogens
HA = heterotrophic acetogens
AM = autotrophic methanogens
HM = heterotrophic methanogens
MOB = methane-oxidising bacteria

1 Microbiology and microbial model

1.1 Introduction

Microbial metabolic activities greatly influence groundwater chemistry. To understand current undisturbed conditions at the proposed repository site, the following parameters are of interest for hydrogeochemical site description modelling: pH, Eh, sulphur species, iron(II), manganese(II), carbonate, phosphate, nitrogen species, total dissolved solids (TDS), colloids, fulvic and humic acids, dissolved organic carbon (DOC), and microorganisms. As well, the dissolved gases carbon dioxide, methane, and hydrogen may participate in microbial reactions. Furthermore, a full understanding entails being able to predict how conditions will change during repository construction and during the ensuing phases of the storage of spent nuclear waste. This part of the report will deal with the microbial data from the site investigation in the Laxemar-Simpevarp area.

Several methods must be used to characterize active microbial communities in groundwater. Microbial parameters of interest are the total number of cells (TNC) and the presence of various metabolic groups of microorganisms /Pedersen, 2001/. The groups cultured for the microbial part of the site investigation were cultivable heterotrophic aerobic bacteria (CHAB), nitrate-reducing bacteria (NRB), iron-reducing bacteria (IRB), manganese-reducing bacteria (MRB), sulphate-reducing bacteria (SRB), auto- and heterotrophic methanogens (AM and HM), and auto- and heterotrophic acetogens (AA and HA). These groups use the following redox couples commonly observed in groundwater: H_2O/O_2, NO_3^-/N_2, $Mn^{2+}/Mn(IV)$, $Fe^{2+}/Fe(III)$, S^{2-}/SO_4^{2-},

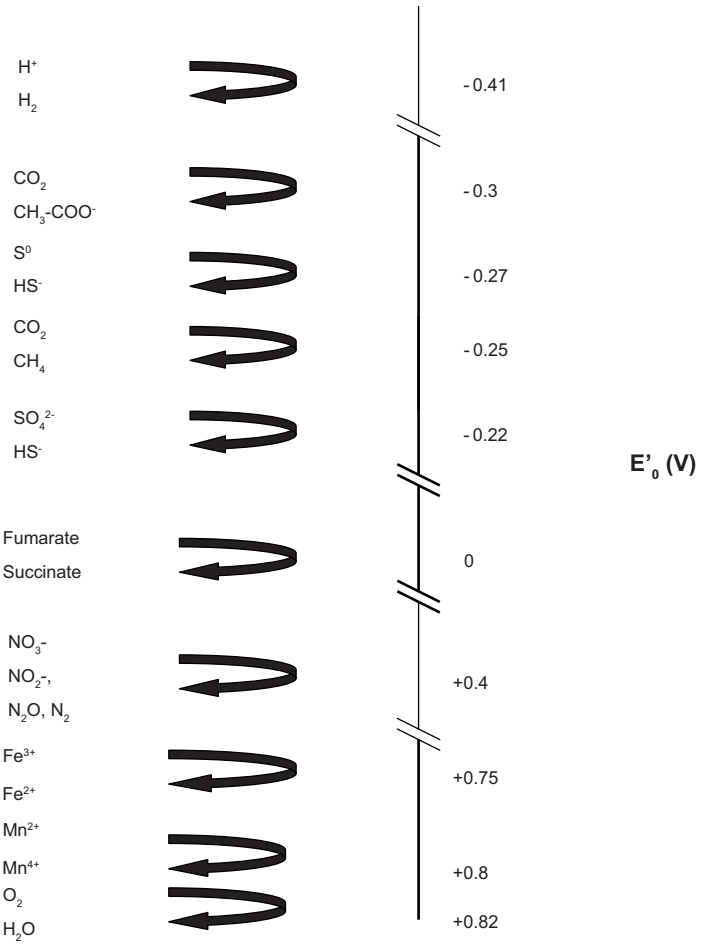

Figure 1-1. *Redox couples in microbial processes found in deep groundwater.*

CH_4/CO_2, CH_3COOH/CO_2, and H_2/H^+ (Figure 1-1). The data will indicate the activity of specific microbial populations at particular sites and how they may affect the geochemistry. Counting the different metabolic groups was done using the most probable number of cells (MPN) method, a statistical cultivation method for counting the most probable number of cells of different cultivable metabolic groups of microorganisms /Greenberg et al. 1992, Hallbeck and Pedersen 2008/.

1.2 Characterising the influence of different metabolic groups of microorganisms

Microbial decomposition and the production of organic material depend on the energy sources and electron acceptors present /Madigan and Martinko 2006/. Organic carbon and methane and reduced inorganic molecules, including hydrogen, are possible energy sources in the subterranean environment. During the microbial oxidation of these energy sources, microbes preferentially use electron acceptors in a particular order (Figure 1-2): first oxygen, and thereafter nitrate, manganese(IV), iron(III), sulphate, sulphur, and carbon dioxide are used. Simultaneously, fermentative processes supply the metabolizing microorganisms with, for example, hydrogen and short-chain organic acids. As the solubility of oxygen in water is low, and because oxygen is the preferred electron acceptor of many bacteria that use organic compounds in shallow groundwater, anaerobic environments and processes usually dominate at depth in the subterranean environment.

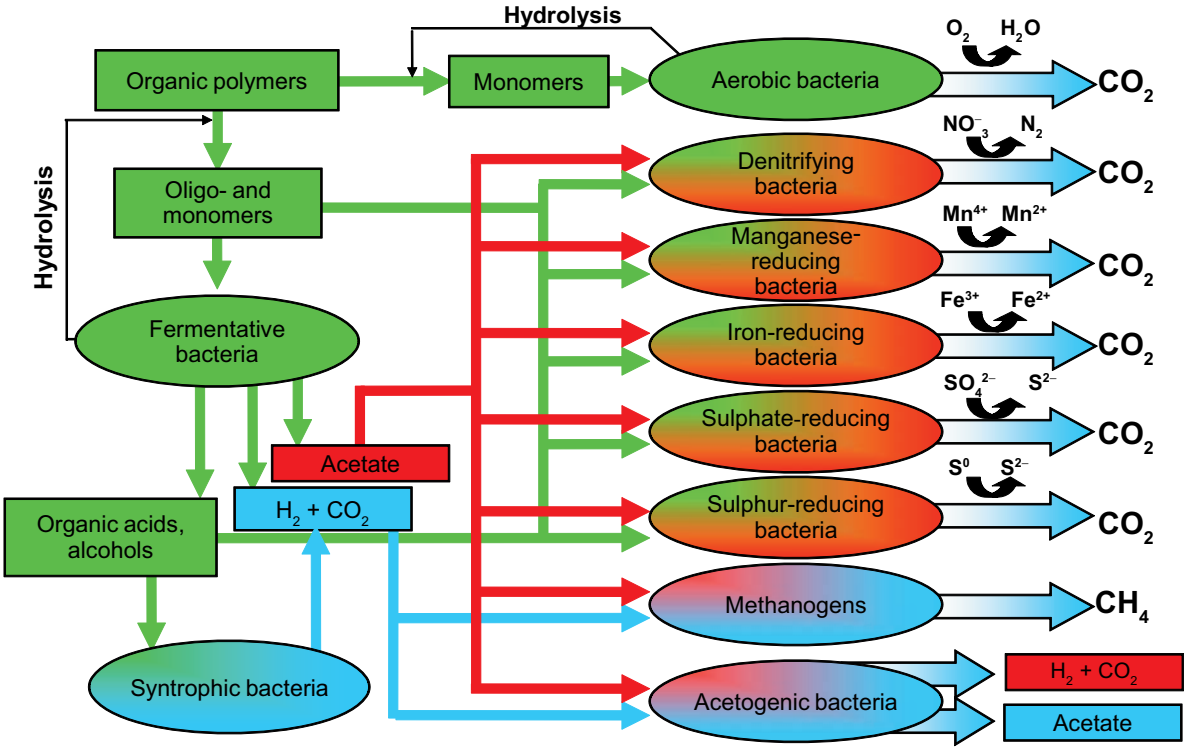

Figure 1-2. *Possible pathways for the flow of carbon in the subterranean environment. Organic carbon is respired with oxygen, if present, or else fermentation and anaerobic respiration occur using an array of different electron acceptors.*

Different microbial groups influence the environment in different ways, depending on what metabolic group is dominant. Table 1-1 lists the activities of these groups and their possible effects on their environment. These microbial processes generally lower the redox potential, E_h. Most of the microbially mediated reactions will not occur in a lifeless groundwater environment without the presence of the catalyzing enzymes of the microorganisms. However, the concentrations of reduced electron acceptors alone will not reveal when, where, or the rate at which the individual microbial processes occur. The microbial methods applied, i.e. TNC and MPN, will be used to estimate the total number of cells and their diversity, which in turn indicate what microbial processes dominate in a particular groundwater. To gain a full understanding of the microbial influence on the system, measurements of the rates of the different metabolic processes are also needed.

Table 1-1. Activities and effects of the different physiological groups of microorganisms found in deep groundwater.

Metabolic group of microorganisms	Activities	Effects on the environment
Aerobes	Oxidation of organic material by oxygen reduction	Depletion of oxygen and organic material; increase in alkalinity; lowering of redox potential
Anaerobes	Oxidation of organic material along with the reduction of compounds other than oxygen	See below for each specific group of bacteria
Nitrate-reducing bacteria	Oxidation of organic material along with nitrate reduction	Depletion of organic material and nitrate; increase in nitrogen gas and/or nitrite and alkalinity; lowering of redox potential
Iron-reducing bacteria	Oxidation of organic material along with ferric iron reduction	Depletion of organic material and ferric iron; increase in ferrous iron concentration and alkalinity; lowering of redox potential
Manganese-reducing bacteria	Oxidation of organic material along with manganese(IV) ion reduction	Depletion of organic matter and manganese(IV); increase in manganese(II) concentration and alkalinity; lowering of redox potential
Sulphate-reducing bacteria	Oxidation of organic material along with sulphate reduction	Depletion of organic matter and sulphate; increase in sulphide concentration and alkalinity; lowering of redox potential
Methanogenesis		
Heterotrophic methanogens	Convert short-chain organic material to methane and carbon dioxide	Depletion of organic material; increase in methane gas and carbon dioxide (alkalinity) concentrations; redox not influenced
Autotrophic methanogens	Oxidation of hydrogen gas and reduction of carbon dioxide to methane gas	Depletion of hydrogen gas and alkalinity; increase in methane gas concentration; redox lowered
Acetogenesis		
Heterotrophic acetogens	Convert organic material to acetate	Depletion of organic material other than acetate; increase in acetate concentration; redox not influenced
Autotrophic acetogens	Oxidation of hydrogen gas along with reduction of carbon dioxide to acetate	Depletion of hydrogen gas and alkalinity; increase in acetate concentration; redox lowered

1.3 Available data

This report uses data from the extended data freeze 2.3 (November 30, 2007) for the Laxemar-Simpevarp area. Microbiological data were available from 14 sections of the following six boreholes: KSH01A, KLX03A, KLX08A, KLX13A, KLX15A, and KLX17A /Pedersen 2004, Pedersen 2005c, Pedersen 2007/. In this report, microbial data are analysed in relation to the chemistry and gas data important to the various microbial processes. Information regarding the extent of MPN culturing of samples from the various boreholes can be found in Table 1-2. The use of culturing methods was expanded over the site investigation period, so results for some of the metabolic groups are missing for samples taken early on. All the different MPN media were used for samples from borehole KLX08A to KLX17A (Table 1-2).

While exploring the chemistry data, data from some sections were found to be of poor quality /Smellie and Tullborg 2009/. The sections where microbial data were sampled were boreholes KLX03 at 700 m depth, KLX08 at 150 m, KLX08 at 320 m, and KLX17A at 548 m. We decided to include these data in the microbial report since so few microbial data are available. Special care was taken when these data were evaluated.

1.4 Quality controls for the most probable number analysis

The reproducibility of the sampling and analysis procedures used in the site investigations both in Laxemar and Forsmark, was tested using a pressure sampling vessel (i.e. PVB sampler) /Hallbeck and Pedersen 2008/. The 353.5–360.0 m section of Forsmark site investigation borehole KFM06A was sampled on 14 March 2005 using two PVB samplers installed at the same time. It was also deemed important to test reproducibility over time in borehole sections that were expected to harbour stable and reproducible populations. This was done in two boreholes at the MICROBE site in the Äspö Hard Rock Laboratory (HRL) tunnel, denoted KJ0052F01

Table 1-2. The MPN of different metabolic groups tested for in groundwater from the boreholes in the Laxemar-Simpevarp area.

Metabolic group	KSH01A, 153 m	KSH01A, 242 m	KSH01A, 556 m	KLX03A, 171 m	KLX03A, 380 m	KLX03A, 700 m	KLX03A, 922 m	KLX08A–KLX17A
Cultivable heterotrophic aerobic bacteria (CHAB)	–	–	–	–	–	–	–	X
Nitrate-reducing bacteria (NRB)	–	–	–	–	–	–	X	X
Iron-reducing bacteria (IRB)	X	X	X	X	X	X	X	X
Manganese-reducing bacteria (MRB)	X	X	X	X	X	X	X	X
Sulphate-reducing bacteria (SRB)	X	X	X	X	X	X	X	X
Autotrophic methanogens (AM)	–	X	X	X	X	X	X	X
Heterotrophic methanogens (HM)	–	X	X	X	X	X	X	X
Autotrophic acetogens (AA)	–	X	X	X	X	X	X	X
Heterotrophic acetogens (HA)	–	X	X	X	X	X	X	X

and KJ0052F03 /Pedersen 2005a/. Groundwater from the borehole sections was sampled using PVB samplers on two occasions, 26 October 2004 and 9 February 2005. The PVB samplers were attached to the flows from each borehole section, and groundwater was circulated overnight under in situ pressure, temperature, and chemistry conditions. Early in the morning, the samplers were closed, detached, and transported to the laboratory in Göteborg; analysis started the same afternoon, before 14.00. All parts of this procedure resembled the sampling of sections of the Forsmark deep boreholes, except that in this case the samplers were not operated remotely from the ground surface; instead, personnel standing next to the PVB samplers in the tunnel manually operated the samplers using adjustable spanners.

1.4.1 Tests for reproducibility of the pressure vessel method

The results of the MPN analyses of groundwater samples taken simultaneously in the Forsmark section in borehole KFM06A at a depth of 357 m reproduced very well (Table 1-3). The lower and upper 95% confidence intervals for the MPN method applied to five parallel tubes equalled approximately one-third and three times the obtained values, respectively /Greenberg et al. 1992/. There was a small bias towards higher numbers in PVB sampler number 1. The maximum discrepancy between the samples was observed for SRB and equalled a factor of two, well within the 95% confidence interval of the MPN analysis. The TNC determinations and ATP analyses also displayed good reproducibility, as pertains to the sampling procedure, transportation logistics, and MPN inoculation, cultivation, and analysis for each physiological group of microorganisms, i.e. TNC, CHAB, and ATP. The second test explored the reproducibility of two different analytical rounds on groundwater from two different borehole sections and of repeated sampling over time. This test also included the effects of different personnel involved and different preparations of chemicals and media. In general, groundwater from the two borehole sections had very different result profiles that reproduced well (Table 1-4). The MPN's of MRB, SRB, and AM differed most between the sampling times, while the MPN's of AA and HM indicated high reproducibility.

Table 1-3. The total numbers of cells, ATP, and most probable numbers of various physiological groups of microorganisms in groundwater sampled using two different PVB samplers, samples were taken simultaneously on 14 March 2005 at the same location in borehole KFM06A, from the 353.5−360.0 m depth section.

Analysis[a] and physiological group	Sample		
	KFM06A:1	KFM06A:2	KFM06A:1/ KFM06A:2
TNC × 10^4 (cells mL^{-1})	7.2 (1.7)[b]	5.2 (1.7)	1.4
ATP × 10^4 (amol mL^{-1})	1.51 (0.07)	9.54 (0.05)	1.6
IRB (cells mL^{-1})	30 (10–120)[c]	23 (9–86)	1.3
MRB (cells mL^{-1})	13 (5–39)	30 (10–130)	0.54
SRB (cells mL^{-1})	0.8 (0.3–2.4)	0.4 (0.1–1.7)	2.0
AA (cells mL^{-1})	30 (10–130)	24 (10–94)	1.3
HA (cells mL^{-1})	24 (10–94)	24 (10–94)	1.0
AM (cells mL^{-1})	< 0.2	0.2 (0.1–1.1)	< 1.0
HM (cells mL^{-1})	0.2 (0.1–1.1)	0.4 (0.1–1.7)	0.5

[a] TNC = total number of cells, ATP = adenosine-tri-phosphate, CHAB = cultivable heterotrophic aerobic bacteria, IRB = iron-reducing bacteria, MRB = manganese-reducing bacteria, SRB = sulphate-reducing bacteria, AA = autotrophic acetogens, HA = heterotrophic acetogens, AM = autotrophic methanogens, HM = heterotrophic methanogens, and MOB = methane-oxidizing bacteria. [b] Standard deviation, n = 6. [c] Lower and upper 95% confidence limits.

Table 1-4. The most probable numbers of various physiological groups of microorganisms in two different boreholes sampled on 14 October 2004 and 9 February 2005.

Physiological group[a] (cells mL^{-1})	KJ0052F01:1	KJ0052F01:2	KJ0052F01:1/ KJ0052F01:2
IRB	< 0.2	< 0.2	1
MRB	< 0.2	< 0.2	1
SRB	300 (100–1,300)[b]	1,600 (600–5,300)	0.19
AA	1,600 (600–5,300)	1,600 (600–5,300)	1
HA	1,600 (600–5,300)	1,600 (600–5,300)	1
AM	17 (7–48)	5 (2–17)	3.4
HM	2.3 (0.9–8.6)	2.3 (0.9–8.6)	1
	KJ0052F03:1	**KJ0052F03:2**	**KJ0052F03:1/ KJ0052F03:2**
IRB	< 0.2	0.8 (0.3–2.4)	< 1
MRB	5.0 (2–17)	1.1 (0.4–2.9)	4.6
SRB	2.3 (0.9–8.6)	5 (2–17)	0.46
AA	5 (2–17)	17 (7–48)	0.30
HA	8 (3–25)	11 (4–30)	0.73
AM	2.3 (0.9–8.6)	0.4 (0.1–1.5)	8.0
HM	1.3 (0.5–3.8)	< 0.2	> 1

[a] TNC = total number of cells, ATP = adenosine-tri-phosphate, IRB = iron-reducing bacteria, MRB = manganese-reducing bacteria, SRB = sulphate-reducing bacteria, AA = autotrophic acetogens, HA = heterotrophic acetogens, AM = autotrophic methanogens, HM = heterotrophic methanogens. [b] Lower and upper 95% confidence limits.

1.4.2 Detection limits and uncertainties in the microbiological methods used

The detection limit of the MPN method is 0.2 cells mL^{-1}. The lower and upper 95% confidence intervals of the MPN method applied to five parallel tubes equalled approximately one-third and three times the obtained value, respectively /Greenberg et al. 1992/. The detection limit of the TNC method is 1×10^3 mL^{-1}. The results are normally distributed and the uncertainty is 10% if enough cells are counted.

1.5 Evaluation of the microbial biomass data

1.5.1 Analysis of microbial biomass

For almost two decades, the microbial biomass in granitic rock aquifers of the Fennoscandian Shield has been analysed in terms of total and viable numbers /Pedersen 2001/; total number estimates have ranged from 10^3 to 10^6 cells mL^{-1}, while viable number estimates have ranged from 10^0 to 10^5 cells mL^{-1}. Between 0.00084 and 14.8% of the total numbers have been cultivated and detected using most probable number (MPN) methods /Haveman and Pedersen 2002a/. Although low viable numbers have been detected relative to the total numbers observed, in vitro radiographic and radiotracer estimates have suggested that the absolute majority of the total cells observed using microscopy was viable /Pedersen and Ekendahl 1990, 1992ab/. Consequently, there was a significant gap between estimates of potentially viable total numbers and evidently viable cultivable numbers. Hence, a method for estimating the total amount of viable biomass in groundwater was sought. A recent investigation found that analysing

the ATP concentration in shallow and deep Fennoscandian groundwater (including Laxemar groundwater) using a commercially supplied assay supplied needed information about the metabolic state and bio-volume of the bacteria present /Eydal and Pedersen 2007/. The assay appeared robust and reliable and had a detection range that included all samples analysed. The analysed ATP concentrations were found to correlate both with the microscopic counts and with the volume and metabolic status of the investigated pure culture and groundwater cells. The results suggested that bacterial populations in deep groundwater vary significantly in size, and that metabolic activity is a function of prevailing environmental conditions.

ATP was first analysed in Laxemar groundwater in autumn 2004. When ATP is analysed concomitantly with TNC, a good correlation is normally obtained. In Laxemar, the correlation was significant at $p \leq 0.05$, with $p = 0.003$ (Figure 1-3). As ATP is an energy transport compound present in all living cells, measuring its concentration indicates the biovolume and metabolic state of the biomass in any system. A groundwater containing many active cells should thus have a higher ATP concentration than one containing few such cells. If the cells are large, this will increase the content of ATP per cell. It has been demonstrated that the ATP/TNC ratio is a good indicator of the metabolic activity of cells in groundwater /Eydal and Pedersen 2007/. The average ATP/TNC ratio for nine Laxemar groundwater determinations was 0.93 (Figure 1-4), and for 166 deep Fennoscandian shield groundwater determinations was 0.43. The ATP value from borehole KLX08A, 150 m depth, is not included in this value; this value was 22 amol mL^{-1}, and there must be some error, either in the ATP measurement or the TNC value for this section. One explanation of this might be that the samples from this section were not representative, as discussed above (see section 1.3). The value of 0.93 suggests that the populations analysed in Laxemar were somewhat more active than the average Fennoscandian shield population. As the investigation by /Eydal and Pedersen 2007/ provided no details as to the data distribution, we did not test whether this difference was significant.

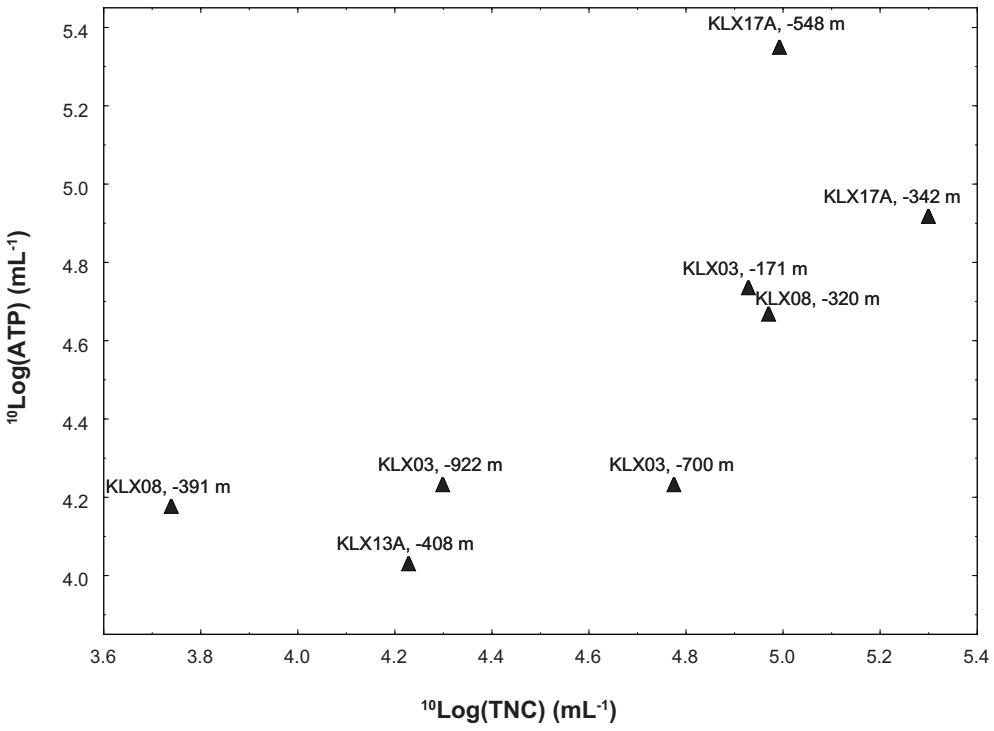

Figure 1-3. *The relationship between the total number of cells (TNC) and ATP concentration in Laxemar groundwater. Statistics:* $^{10}Log(ATP) = 1.5 + 0.66 \times {}^{10}Log(TNC)$, $r = 0.75$, *significant at* $p = 0.003$, $n = 8$. *Data from extended freeze 2.3 (November 30, 2007).*

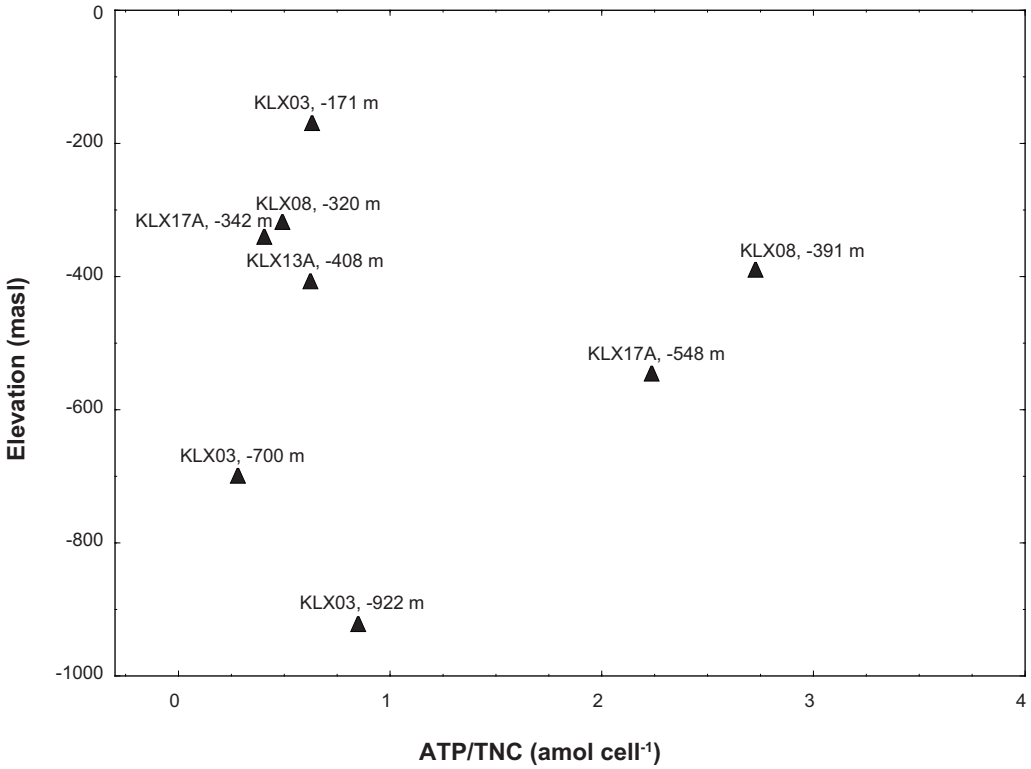

Figure 1-4. *The ATP concentrations per total number of cells (TNC) distributed over depth in Laxemar groundwater.*

A special case is the possible occurrence of microbes that grow attached to aquifer surfaces (i.e. biofilms), a phenomenon repeatedly observed in groundwater from other sites /Ekendahl and Pedersen 1994/. Such biofilms will increase their cell numbers until they reach steady state. The hypothetical cell numbers and activities of attached versus unattached bacteria in a 0.1 mm wide fracture have previously been compared (see Table 4.5 in /Pedersen 2001/) and the results are reported in Appendix 2 of Hydrogeochemical evaluation: Preliminary site description Laxemar subarea – version 1.2 /SKB 2006/. This report demonstrated the potential importance of attached versus unattached microorganisms in underground environments. The studied microorganisms attached to artificial surfaces generally exhibited greater activity per cell than did the unattached microorganisms. Taken together with the cell numbers, there was up to five orders of magnitude more activity on the surfaces than in the groundwater itself. It is still an open question whether attached bacteria are common and active on groundwater flow surfaces under pristine conditions.

1.5.2 Dissolved organic carbon and total number of cells

Dissolved organic carbon (DOC) and the total number of cells (TNC) are parameters that usually display parallel trends. DOC provides a basis for microbial populations, at least in ecosystems fed by photosynthetically produced carbon compounds, i.e. systems in contact with the ground surface. In deeper groundwater containing chemolithotrophic microorganisms, the connection between DOC and TNC is not necessarily so strong.

The data for DOC in Laxemar groundwater displayed large variation. The highest value was 22 mg L^{-1} in KLX03 at a depth of 171 m. All other data were distributed between 13 mg L^{-1} in groundwater from a depth of 380 m in KLX03 to below the detection limit of 0.1 mg L^{-1} (Figure 1-5). The DOC concentrations in groundwater from Laxemar are generally higher than in deep groundwater at Forsmark or in shallow groundwaters, from depths of 1–10 m, at Forsmark.

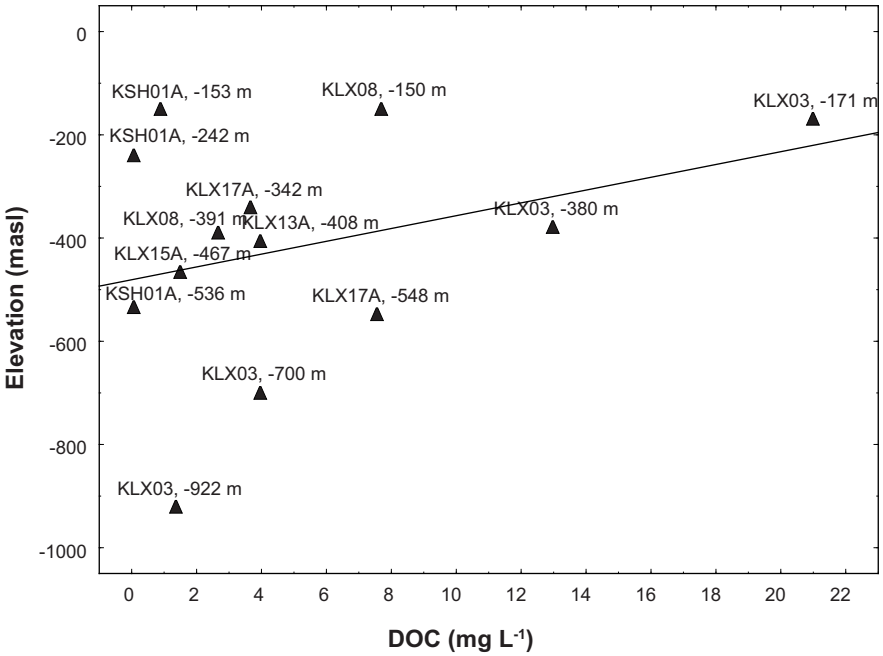

Figure 1-5. *Dissolved organic carbon (DOC) versus depth. Symbols for DOC at 0.1 denote data below the detection limit of 0.1 mg DOC L^{-1}. Data from extended freeze 2.3 (November 30, 2007).*

Figure 1-6 shows that the TNC's in the boreholes were all below 10^5 mL^{-1}, except in two samples, one from borehole KSH01A, 153 m depth, and KLX17A, 342 m depth. The lowest TNC, below 1×10^4 mL^{-1}, was from a depth of 391 m in borehole KLX08A. These data are in the range of the cell numbers earlier found in boreholes in the Fennoscandian Shield /Pedersen 2001/. The DOC values follow a decreasing trend with depth, in agreement with the results of earlier studies /Pedersen 2001/. There was no significant ($p > 0.05$) correlation between DOC and TNC (Figure 1-7) in Laxemar.

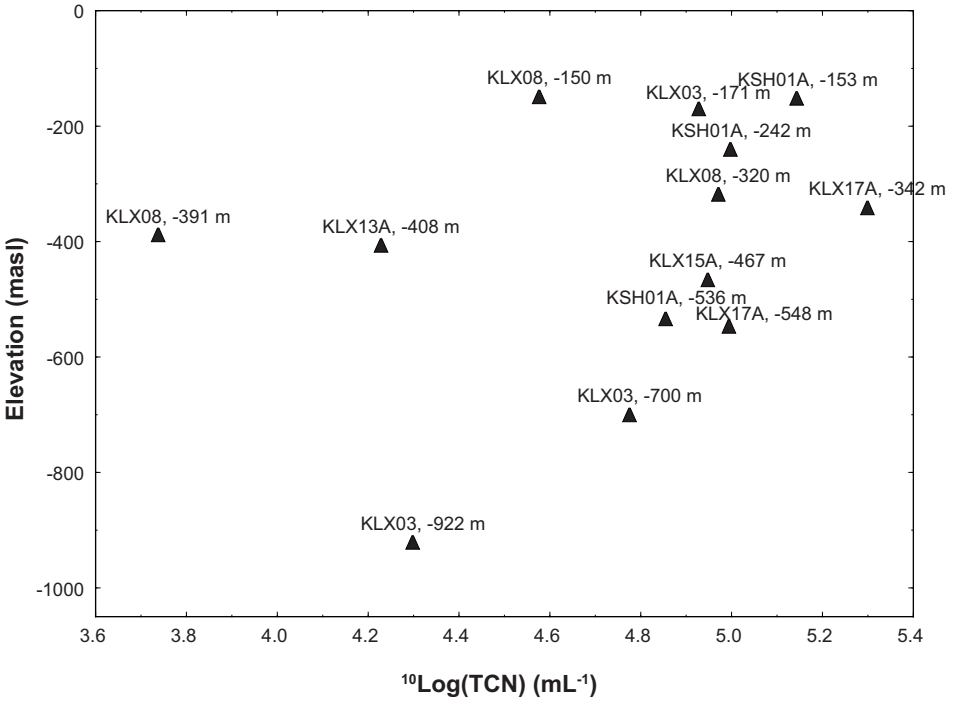

Figure 1-6. *Total number of cells (TNC) versus depth. Data from extended freeze 2.3 (November 30, 2007).*

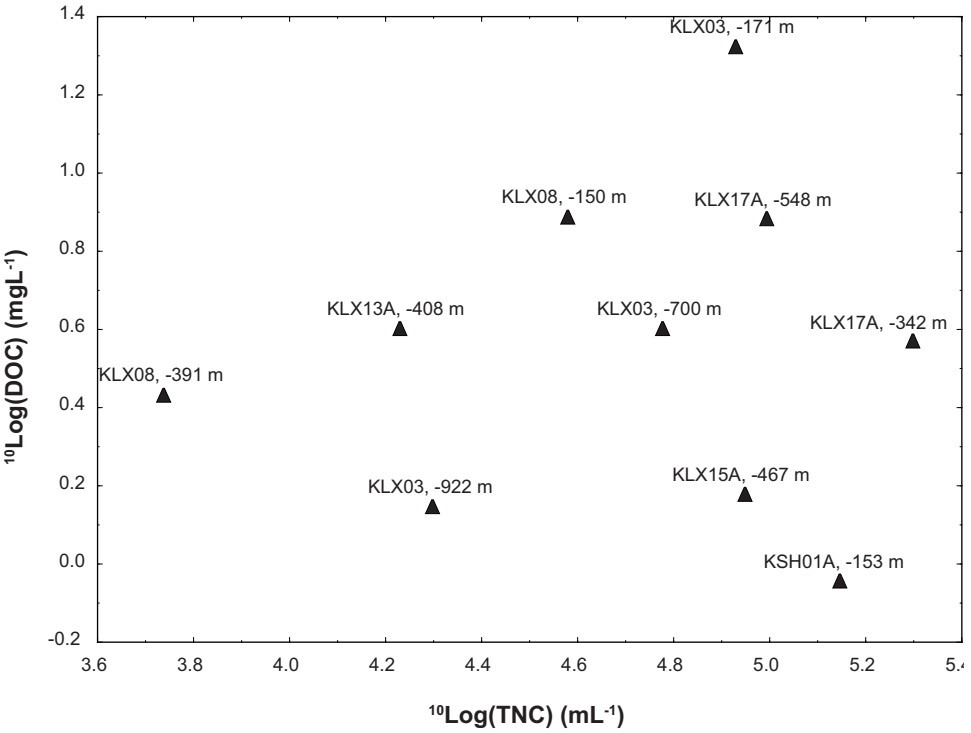

Figure 1-7. *The relationship between total number of cells (TNC) and dissolved organic carbon (DOC). Symbols for DOC at –1 denote data below the detection limit of 1 mg DOC L^{-1}. Data from extended freeze 2.3 (November 30, 2007).*

1.5.3 Relationships between microbiology and organic material

To understand the size distribution of the organic material in groundwater, samples from several sections of seven boreholes were subjected to fractionation filtration (see Table 1-5). Defined cut-off filters of 1,000 and 5,000 Dalton (D) were used (one D is equivalent to the mass of one hydrogen atom, i.e. 1.67×10^{-24} g). Fulvic acids are smaller than humic acids and have molecular weights below 1,000 D. Humic acids, on the other hand, have molecular weights up to several hundred thousand D. The 1,000–5,000 D fraction is considered to represent colloidal organic material. The results of the filtration indicated that most of the organic material was smaller than 1,000 D in size but that some was in the > 5,000 D fraction. Organic material in the 1,000–5,000 D fraction was found in five sections.

Table 1-5. Organic material (mg L^{-1}) in groundwater sampled from boreholes in the Laxemar-Simpevarp area, measured for three fractions using fractionation filtration and DOC measurements.

Borehole section	< 1,000 D (mg L^{-1})	1,000–5,000 D (mg L^{-1})	> 5,000 D (mg L^{-1})	DOC (mg L^{-1})
KSH01A, 153 m	1.0 ± 0.1	n.d.[1]	0.06 ± 0.04	0.9–1.5
KSH01A, 536 m	1.0 ± 0.1	n.d.	0.04 ± 0.03	< 1–1.1
KLX03, 171 m	8.30 ± 0.9	n.d.	12.8 ± 1.5	20
KLX03, 380 m	5.90 ± 0.8	1.40 ± 0.1	n.d.	d.m.[2]
KLX03, 922 m	1.40 ± 0.2	n.d.	1.40 ± 0.2	1.4
KLX08, 150 m	2.70 ± 0.4	2.90 ± 0.3	0?	7.5
KLX08, 320 m	2.40 ± 0.3	1.40 ± 0.4	3.30 ± 0.4	4.0
KLX08, 390 m	1.90 ± 0.2	0.49 ± 0.09	0.20 ± 0.10	2.5
KLX15, 467 m	1.50 ± 0.2	d.m.	d.m.	1.5
KLX17, 342 m	1.80 ± 0.2	1.60 ± 0.2	n.d.	3.7

[1] n.d. = not detected; [2] d.m. = data missing /Wacker et al. 2003, 2004ab/.

The presence of organic colloids was not correlated with high MPN's for the different physiological groups of microorganisms (not shown). In addition, it must be considered that molecules with a molecular weight of 1,000 D are relatively large. These molecules could easily contain 20 or more carbon atoms. For example, complex binding molecules produced by microorganisms have approximately 40 carbon atoms together with nitrogen, oxygen, and hydrogen atoms /Johnsson et al. 2006/.

1.5.4 Cultivable heterotrophic aerobic bacteria

Analysis of CHAB indicated an increasing trend with depth (see Figure 1-8). This analysis started with borehole KLX08 (Table 1-4), so there are no CHAB data for the boreholes sampled earlier. It should be noted that the number of CHAB was very high, i.e. above 10,000 mL^{-1}, in borehole KLX15A, 467 m depth. In this section, high MPN's were found for many of the different groups of microorganisms (Figure 1-28). Some CHAB are facultative anaerobes, which means that they can live without oxygen and instead use nitrate as the electron acceptor, as can be seen in the high NRB value (see Figure 1-9) The weak increasing trend of CHAB with depth was not statistically significant at $p > 0.05$ ($p = 0.06$) (Table 1-16).

1.6 Nitrate-reducing bacteria

Analysis of NRB was introduced in the MPN analyses starting from that of borehole KLX03 at 700 m depth (Table 1-4); the results of this analysis are shown in Figure 1-9. NRB numbers displayed an increasing trend with depth but were not, however, statistically significant ($p > 0.05$) (Table 1-1). The highest value was found in borehole KLX15A at a depth of 467 m. Nitrate reducers reduce nitrate with organic material to nitrogen gas or, in some species, to nitrite. The nitrate concentrations in groundwater in Laxemar were generally very low. Several genera and species that are nitrate reducers can also use other electron acceptors, such as oxygen, ferric iron, and manganese(IV); one such genus is *Shewanella* /Meyers and Nealson 1990/. Therefore, the presence of nitrate reducers in a sampled section does not necessarily indicate that nitrate reduction is occurring.

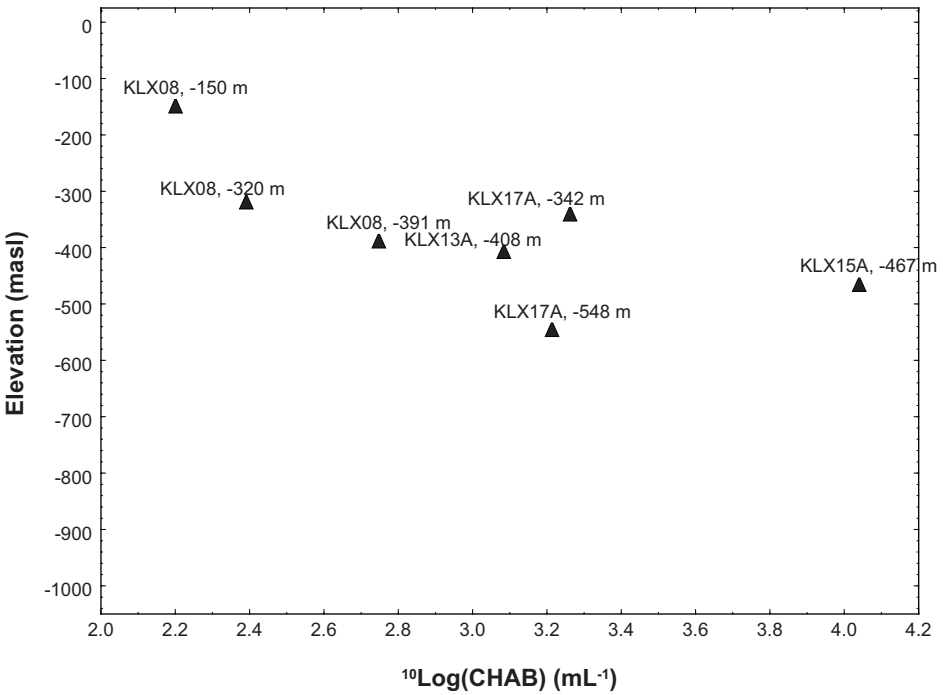

Figure 1-8. *The relationship between cultivable bacteria (CHAB) and depth. r = –0.54, not significant at p ≤ 0.05 (p = 0.06), n = 7. Data from extended freeze 2.3 (November 30, 2007).*

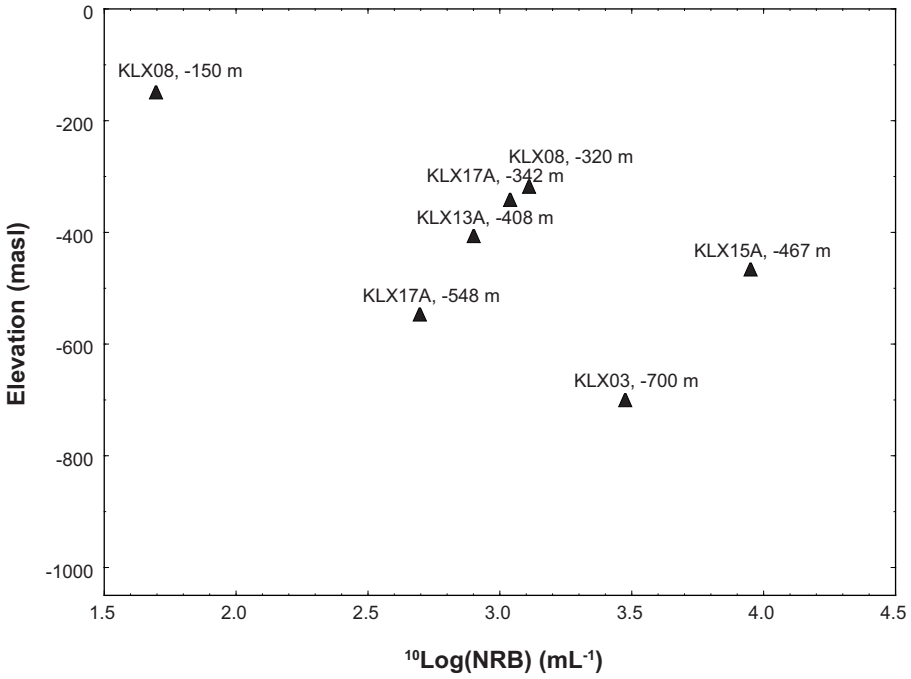

Figure 1-9. *The relationship between nitrate-reducing bacteria (NRB) and depth. The correlation was not significant at $p \leq 0.05$ ($p = 0.12$), $n = 7$. Data from extended data freeze 2.3 (November 30, 2007).*

The CHAB were analysed under aerobic conditions, unlike all other cultivation methods used here, which were performed under anaerobic conditions. As stated above, many bacteria are known to be facultative anaerobes, i.e. they can switch from aerobic respiration using oxygen to anaerobic respiration using nitrate and often also ferric iron and manganese(IV) as alternative electron acceptors /Madigan and Martinko 2006/. Microorganisms in groundwater must be adapted to anoxic conditions but, if oxygen should appear, it is advantageous for the microbe to be able to switch to oxygen respiration. Indigenous groundwater microorganisms should consequently be detectable as both CHAB and NRB, while contaminants from the surface should have a smaller tendency to do so. Comparing the CHAB data to the NRB data indicated a reasonably good correlation (Figure 1-10), suggesting that the microorganisms analysed as CHAB were generally indigenous. The high CHAB and NRB values from KLX15A at a depth of 467 m illustrate this phenomenon. Many of the bacteria that grew on the plates and in the culture tubes used in the analyses were probably facultative anaerobes.

1.7 Iron-reducing bacteria and Fe^{2+}

The highest numbers of IRB were found in boreholes KLX15A, at a depth of 467 m, and KLX17A, at depths of 342 and 548 m, where they reached 140, 240, and 280 IRB mL^{-1}, respectively (see Figure 1-11). There was no significant trend in the relationship between number of IRB and depth in Laxemar (see Table 1-6) or between concentrations of ferrous iron and depth (see Figure 1-12). Iron mainly occurred in the groundwater in a ferrous state, and if sulphide was present, ferrous iron may have precipitated as ferrous sulphide and become adsorbed to surfaces in fractures. This could explain why the correlation between the concentration of Fe^{2+} and IRB was weak for some samples (Figure 1-13). A model of the influence of microorganisms on groundwater geochemistry must consider ferrous iron and sulphide production simultaneously. These two components will interact depending on pH and Eh. Ferric iron will probably mostly be found mineralised on fracture surfaces.

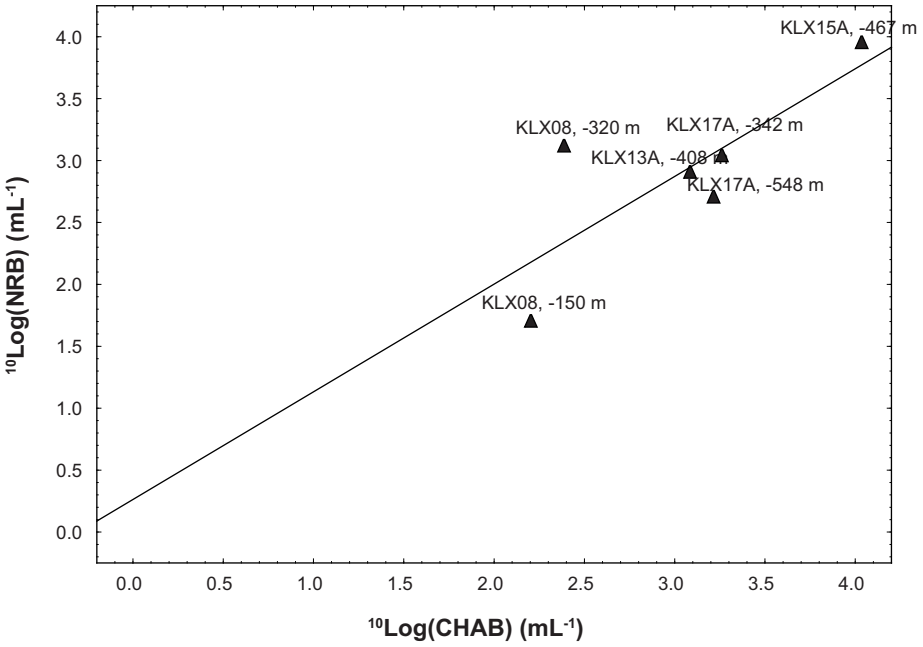

Figure 1-10. *The relationship between the number of nitrate-reducing bacteria (NRB) and the number of cultivable bacteria (CHAB). Statistics:* $^{10}Log(NRB) = -0.2624 + 0.87 \times {}^{10}Log(CHAB)$, *r = 0.79, not significant at p ≤ 0.05 (p = 0.06), n = 6. Data from extended data freeze 2.3 (November 30, 2007).*

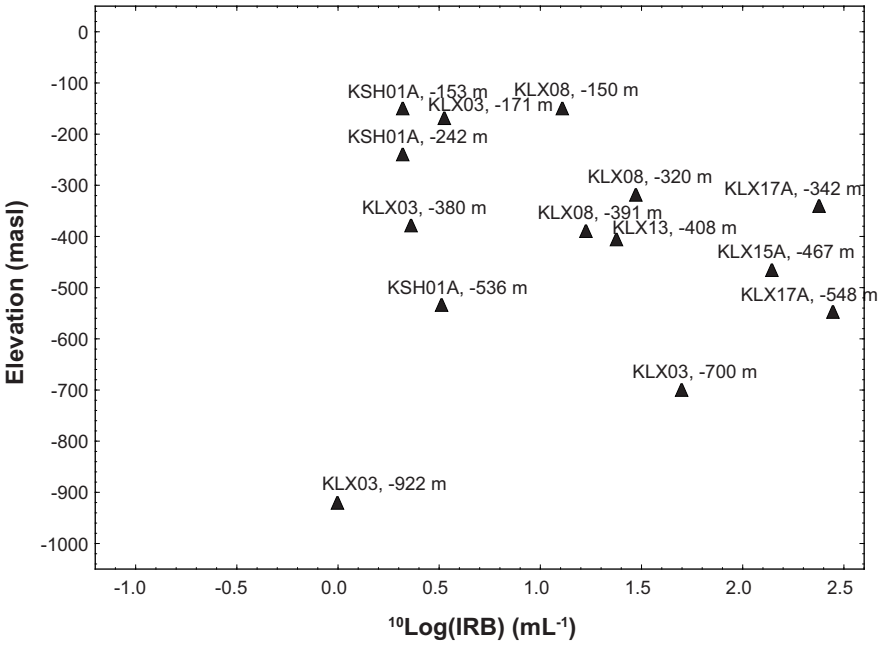

Figure 1-11. *The relationship between the number of iron-reducing bacteria (IRB) and depth. Statistics: Depth = 241 + 105 ×* $^{10}Log(IRB)$, *r = –0.49, not significant at p ≤ 0.05 (p = 0.09), n = 13. Data from extended freeze 2.3 (November 30, 2007).*

The relatively high numbers of IRB in the 300–600 m depth interval are interesting, as most of the sampled groundwaters also contain high numbers of SRB in this interval (see section 1.9). It does not seem that there is competition between the two metabolic groups, but that this interval simply contains high numbers of active microorganisms in general. This is true for KLX17A, which had the one of the highest measured ATP/TNC values.

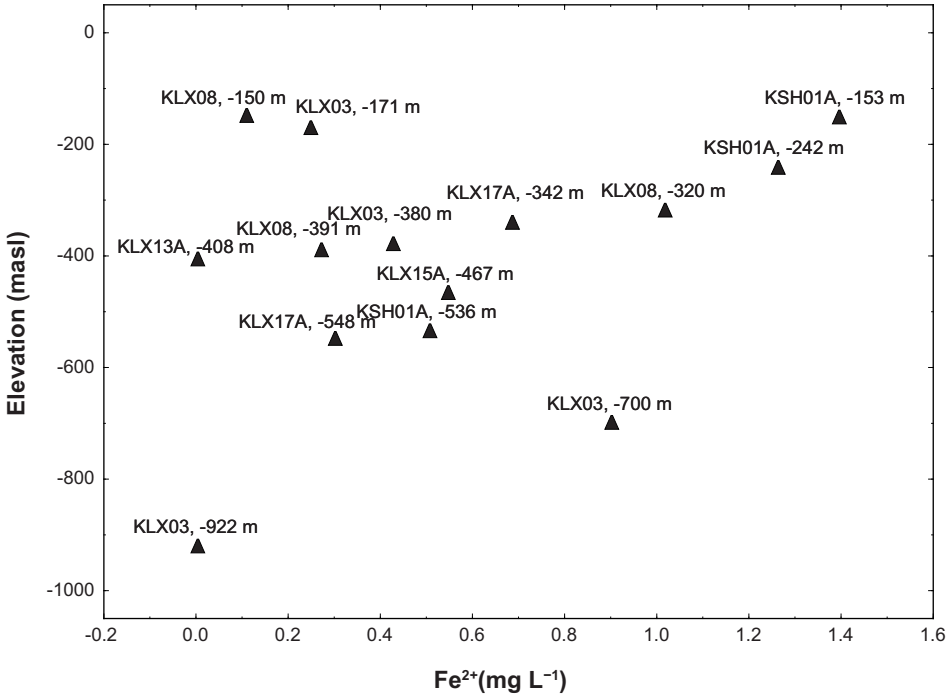

Figure 1-12. *The relationship between the concentration of Fe^{2+} and depth. Statistics: Depth = 496 + 156 × (Fe^{2+}), r = 0.26, not significant at p ≤ 0.05 (p = 0.09), n = 14. Data from extended freeze 2.3 (November 30, 2007).*

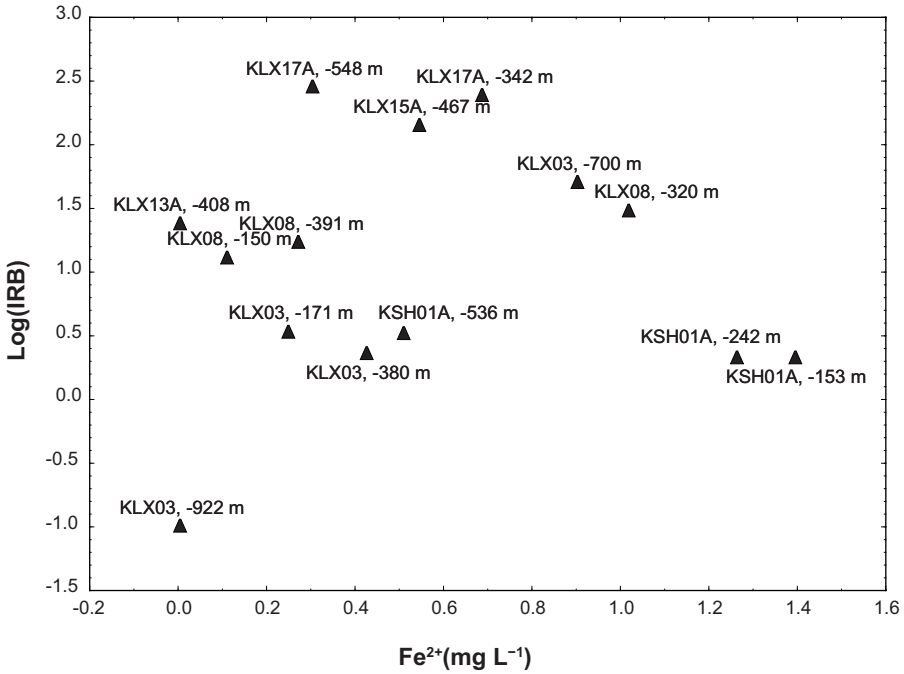

Figure 1-13. *The relationship between the concentration of Fe^{2+} and log iron-reducing bacteria. Statistics: $^{10}Log(Fe^{2+}) = 1.01 + 0.10 \times {}^{10}Log(IRB)$, r = 0.04, not significant at p ≤ 0.05 (p = 0.88), n = 14, all available data were included. Symbols for IRB at –1 denote data below the detection limit of 0.2 cells mL^{-1}. Data from extended freeze 2.3 (November 30, 2007).*

1.8 Manganese-reducing bacteria and manganese

In natural water in the pH 5–8 range, Mn(IV) occurs mostly in precipitates as insoluble MnO_2, manganese found in solution in such environments therefore consists of Mn^{2+} ions. The highest values of manganese in groundwater were found in borehole KSH01A, which is located in the Simpevarp subarea (see Figure 1-14). The highest value in the Laxemar area was found in borehole KLX15A, at 467 m depth, with here it reached 0.55 mg L^{-1}. No clear decreasing trend of Mn with depth can be seen in Laxemar. As discussed above with reference to IRB, MRB are part of the groundwater community that degrade organic matter from the surface or use acetic acid produced by acetogens; they are therefore an important part of the process that lowers the redox potential in groundwater by oxidizing organic matter with oxidized manganese compounds.

The highest numbers of MRB were found in boreholes KLX03 at 380 m depth, KLX15A at 467 m, and KLX17A at 548 m (Figure 1-15), where 100–1,000 cells per millilitre were found. When the MRB number was compared with Mn^{2+} concentration, a correlation could not be demonstrated (Table 1-6), which reflects a fairly large scatter among the observations at the analysed depths.

Many of the MRB can also reduce ferric iron. Therefore, an excellent correlation was found between IRB and MRB numbers (Figure 1-16). These organisms can toggle between the electron acceptors ferric iron and manganese(IV) depending on availability. This correlation also attests to the stability and reproducibility between the different physiological MPN groups cultivated.

1.9 Sulphate-reducing bacteria, sulphate and sulphide

The number of SRB was highest at a depth of 548 m in KLX17A at 3×10^3 mL^{-1} (see Figure 1-17). Thus, the number of SRB peaks at a depth of 300–600 m; this peak almost coincides with the highest amounts of DOC and TNC (Figure 1-5 and Figure 1-6). These parameters were also high at a shallower depth of approximately 200 m. A significant relationship between depth and numbers of SRB could not be established (Figure 1-17). The SRB data were scattered over the sampled depth range.

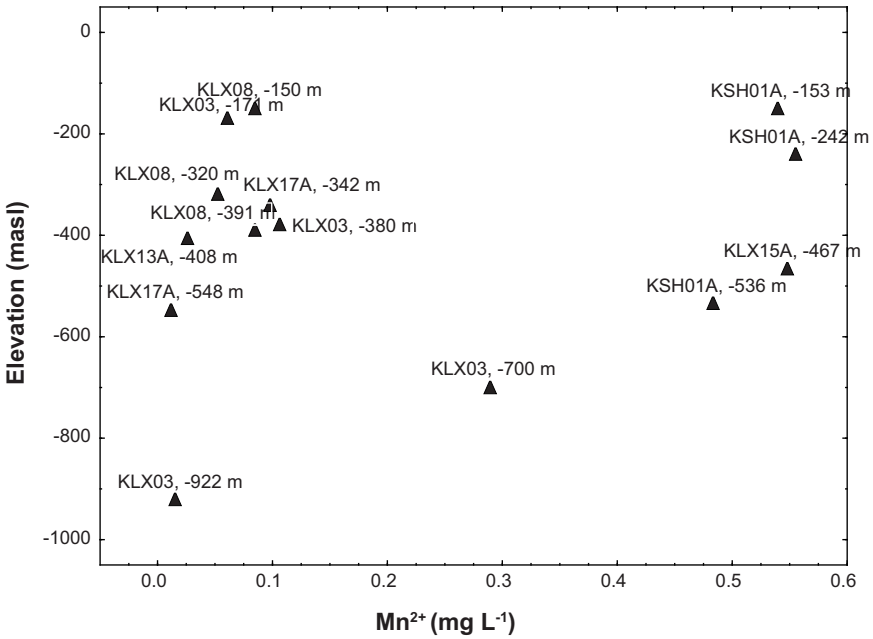

Figure 1-14. *The relationship between Mn^{2+} concentration and depth. Statistics: Depth = 442 + 253 × (Mn^{2+}), r = 0.16, not significant at $p \leq 0.05$ ($p = 0.16$), n = 1. Data from extended freeze 2.3 (November 30, 2007).*

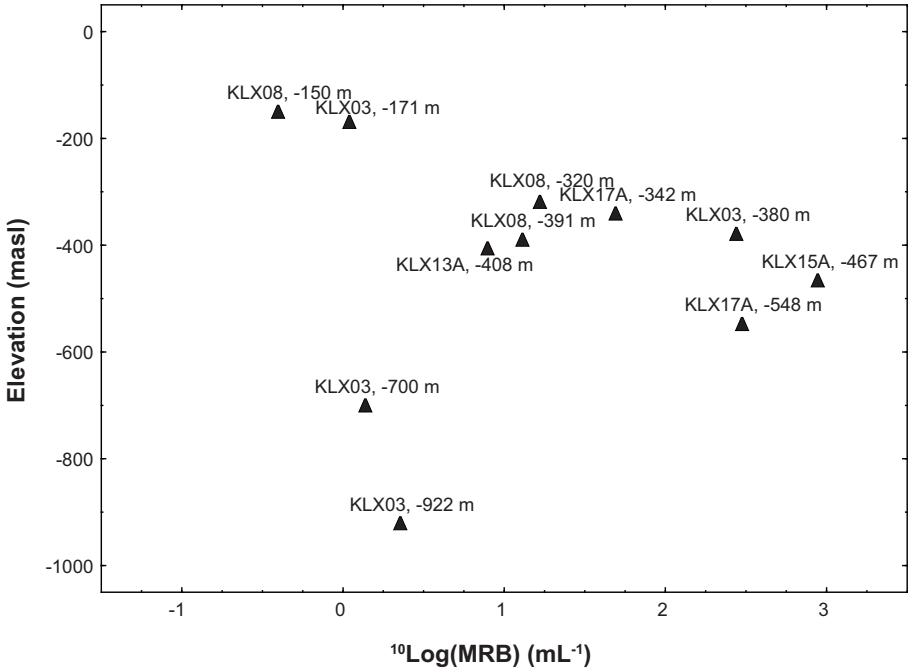

Figure 1-15. *The relationship between the number of manganese-reducing bacteria (MRB) and depth. Statistics: Depth = 384 + 35 × ^{10}Log(MRB), r = –0.21, not significant at p ≤ 0.05 (p = 0.46), n = 14. Data from extended freeze 2.3 (November 30, 2007).*

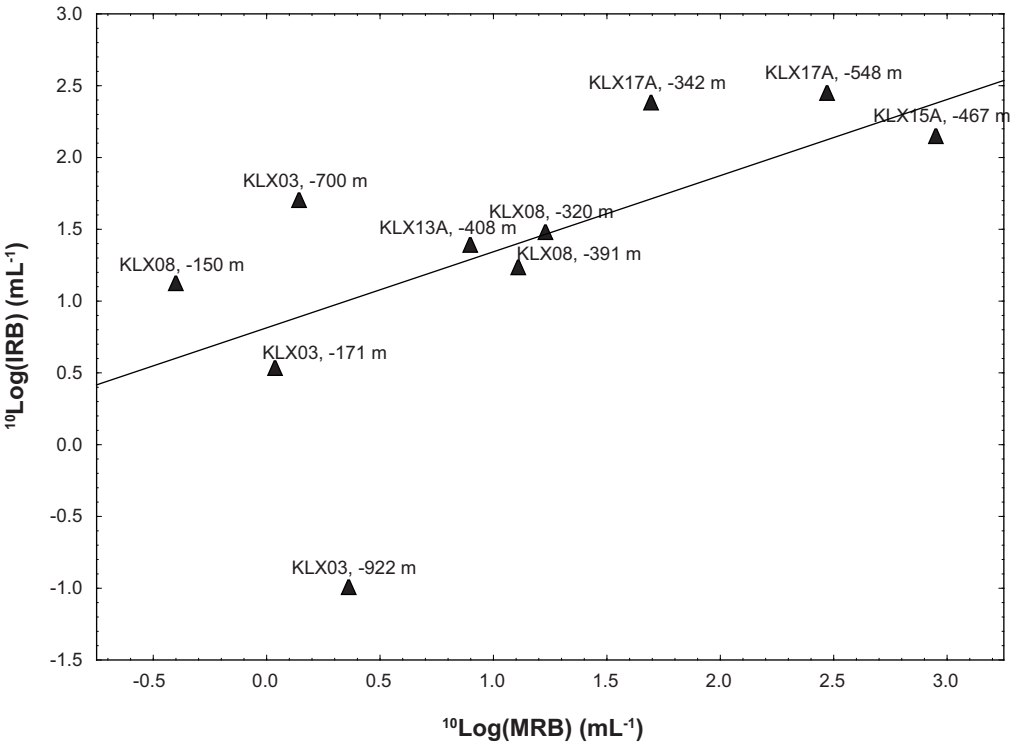

Figure 1-16. *The relationship between the number of manganese-reducing bacteria (MRB) and the number of iron-reducing bacteria (IRB). Statistics: ^{10}Log(IRB) = 0.86 + 0.40 × ^{10}Log(MRB), r = 0.63, significant at p = 0.01, n = 14. Symbols at –1 denote data below the detection limit of 0.2 cells mL^{-1}. Data from extended freeze 2.3 (November 30, 2007).*

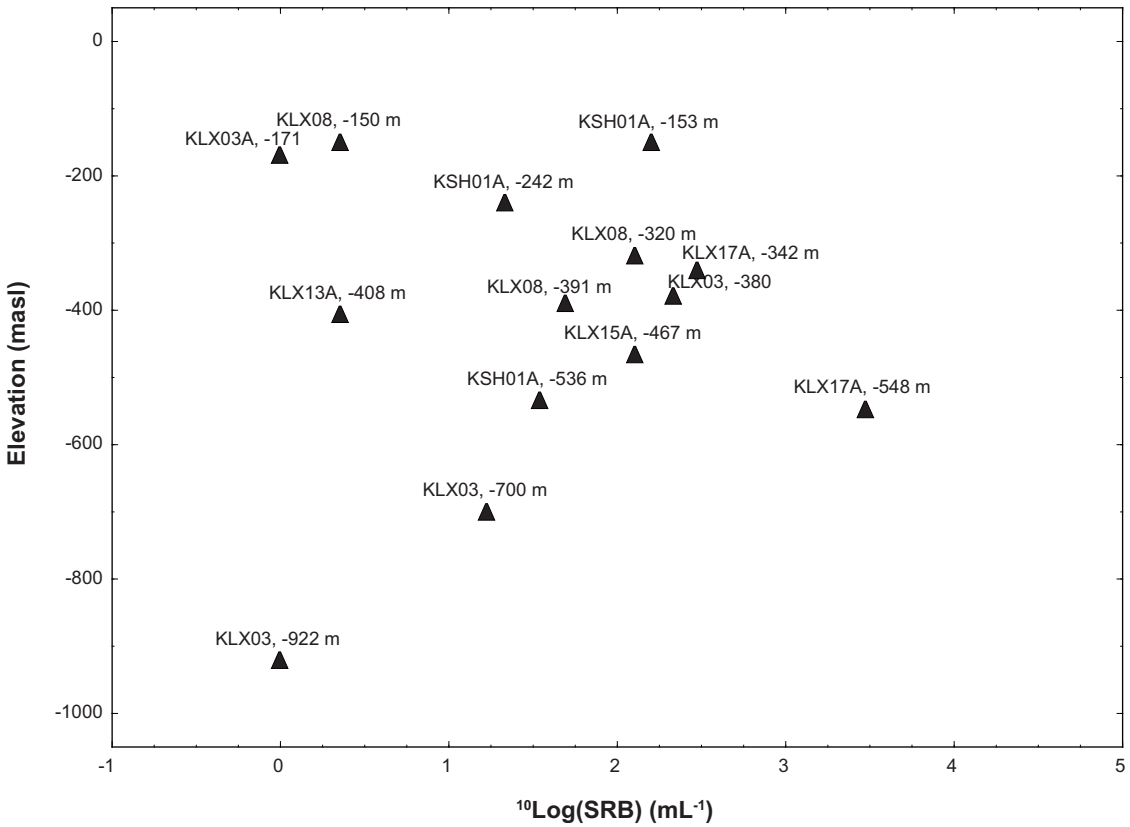

Figure 1-17. *Most probable number of cells (MPN) of sulphate-reducing bacteria (SRB) versus depth in the Laxemar area. Symbols for SRB at –1 denote data below the detection limit of 0.2 cells mL^{-1}. Data from extended freeze 2.3 (November 30, 2007).*

The presence of SRB in groundwater in Laxemar was accompanied by very low sulphide values, close to the detection limit of approximately 0.002 mg L^{-1} as shown in Figure 1-18. It could be that amorphous iron sulphides form and precipitate in fractures if the groundwater is rich in ferrous iron. The highest sulphide values were found in groundwater from below 900 m. The ferrous iron concentration is low in the deep groundwater in Laxemar. There was a significant correlation between sulphate and depth in Laxemar. Despite this, the groundwater with the highest MPN of SRB, from borehole KLX17A at 548 m depth, has a low sulphate content, 6.2 mg L^{-1}, compared with groundwater from other borehole sections at the same depth, for example, KSH01A, KLX15A, and KLX08 (Figure 1-19). The boreholes were pumped at a pumping rate of approximately 200 mL min^{-1} before sampling for analysis of SRB and sulphide. Prolonged pumping may introduce a disturbance that influences the numbers of SRB and that washes out sulphide from the groundwater system. This effect has been documented at the MICROBE site in the Äspö HRL /Pedersen 2005b, Hallbeck and Pedersen 2008/. Pumping may also trigger FeS precipitation, due to ferrous iron production by IRB, which may be stimulated by increased flow in the sampled fractures. Because of the large risk of such disturbances, the SRB and sulphide values are unfortunately not reliable for predictive modelling of microbial processes.

1.10 Methanogens

Figure 1-20 presents the MPN of the two different types of methanogens, autotrophic (AM) and heterotrophic (HM), plotted against depth. The highest number of methanogens observed was 500 mL^{-1} for HM at a depth of 380 m in KLX03; the amount of methane here was 0.62 mL L^{-1}, corresponding to 31 µM. Additionally, the highest number of AM, i.e. 30 mL^{-1}, was found in this section. All other data were at or below 1 cell mL^{-1}, so no trend versus depth could be seen. No isotopic data are available for the measured methane, so it is difficult to determine its origin; however, the C1/(C2 + C3) ratio (see section 3.4.4, “Methane and higher hydrocarbons”) implies that the methane is either biogenic or a mixture of biogenic and abiogenic methane.

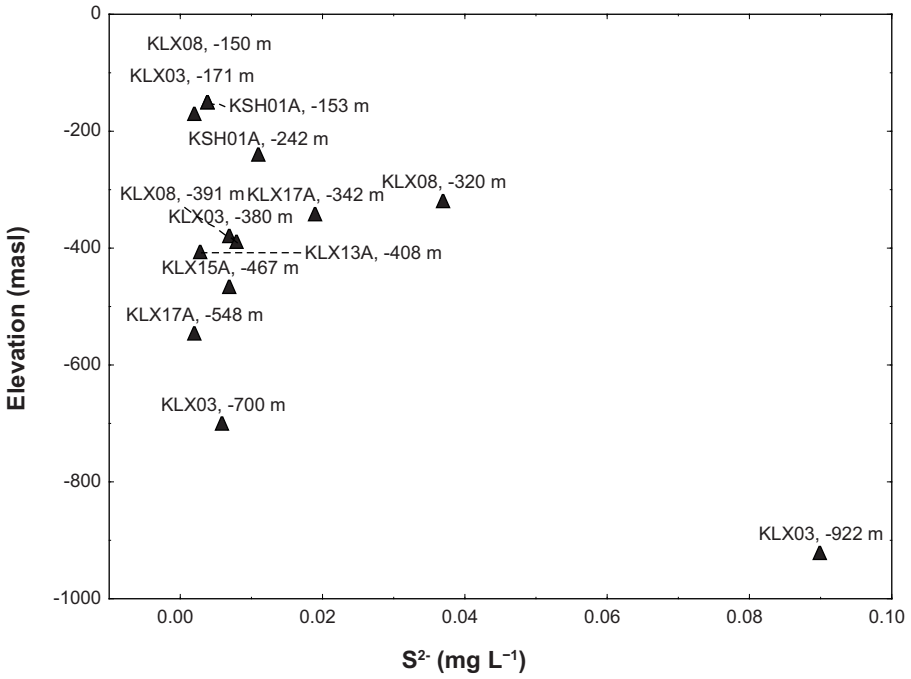

Figure 1-18. *Sulphide concentration versus depth in the Laxemar area. Symbols for sulphide at 0.001 denote data below the detection limit of 0.002 mg L^{-1}. Data from extended freeze 2.3 (November 30, 2007).*

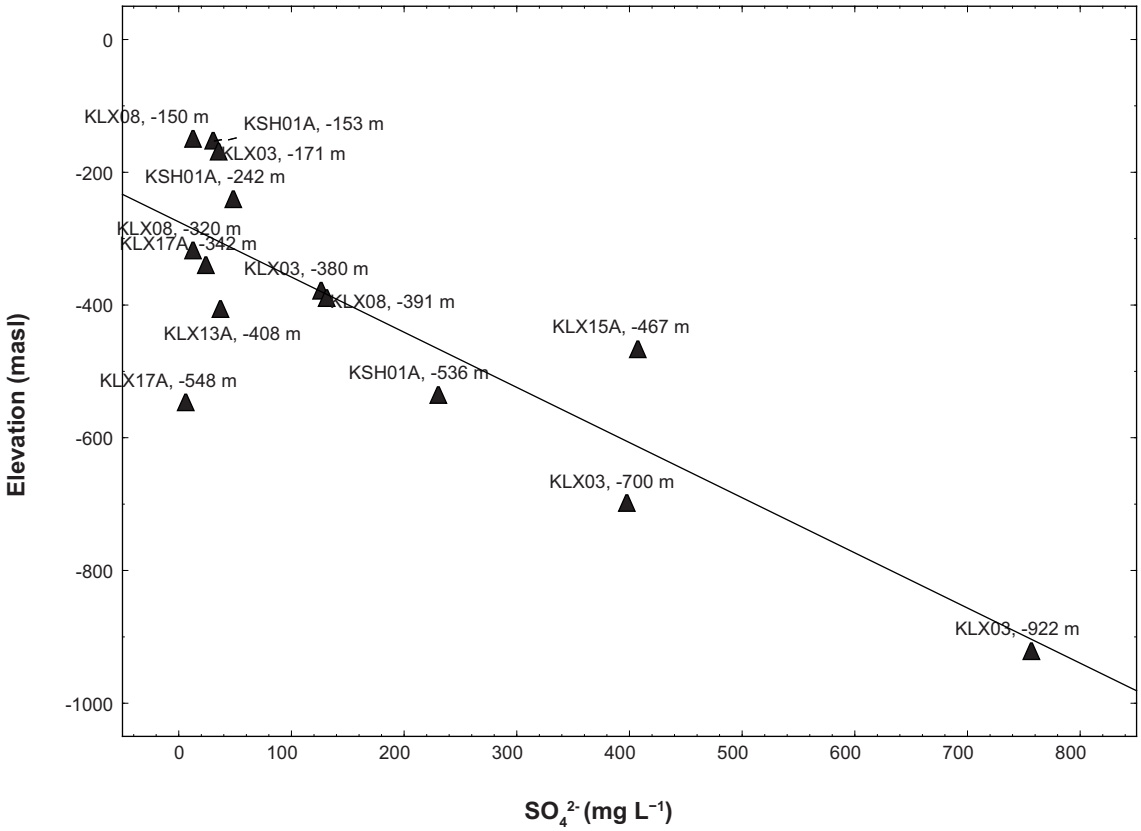

Figure 1-19. *Sulphate concentration versus depth in the Laxemar area. Statistics: $(SO_4^{2-}) = -275 - 0.83 \times X$, $r = -0.84$, significant at $p = 0.0002$, $n = 14$. Data from extended freeze 2.3 (November 30, 2007).*

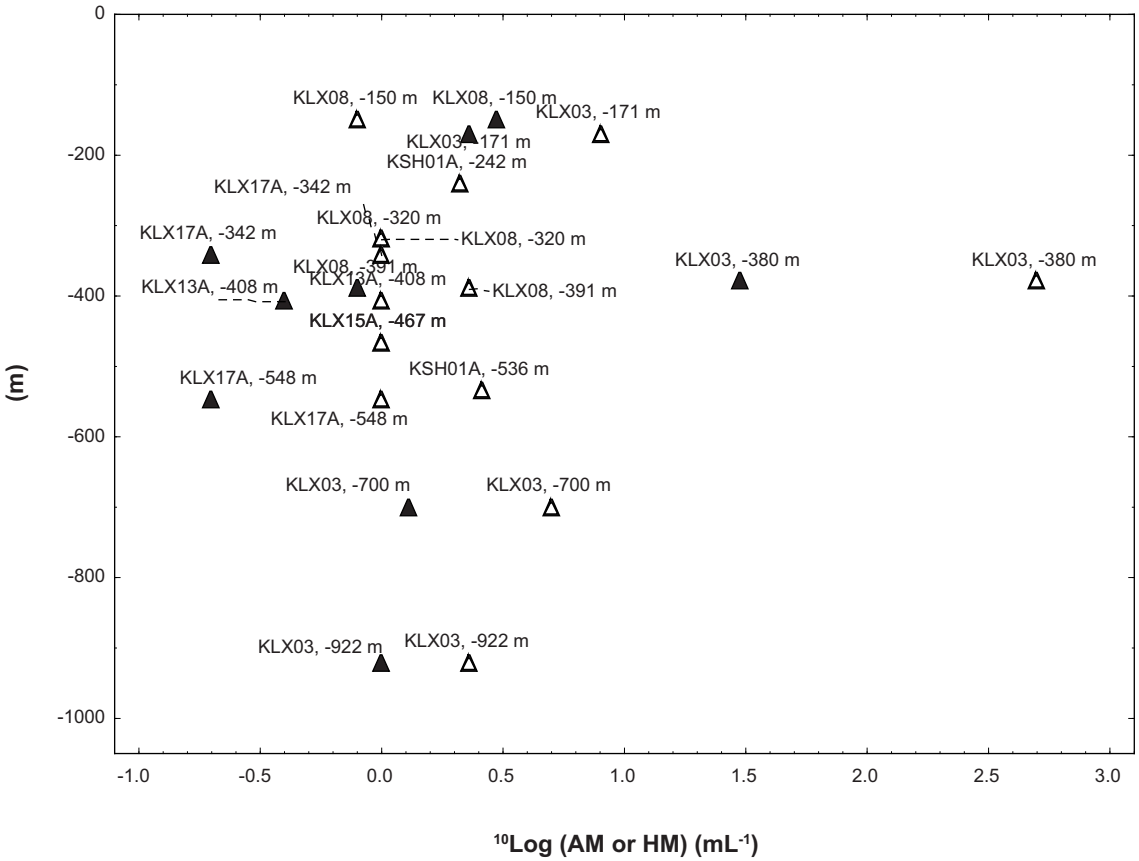

Figure 1-20. *Most probable numbers of cells (MPN) of auto- and heterotrophic methanogens (AM and HM) versus depth in boreholes in the Laxemar area. Solid triangles = autotrophic methanogens, open squares = heterotrophic methanogens. Symbols at –1 denote data below the detection limit of 0.2 cells mL^{-1}. Data from extended freeze 2.3 (November 30, 2007).*

1.11 Acetogens

Acetogenic activity results in acetate production. Acetogens were the dominant microorganisms in the sections studied; there were often one or two orders of magnitude more acetogens than the second most common organism type. Many acetogens are both heterotrophic and autotrophic. The highest numbers were found in boreholes KLX08, KLX15A, and KLX17A in the depth range between 200 and 600 m (see Figure 1-21). There was no significant relationship between the numbers of acetogens and depth (Table 1-6). Some of the metabolic groups analysed using MPN may overlap in numbers. At the onset of this investigation it was unclear whether AA and HA would differ in numbers. The acetogens are known to be a diverse group of organisms that may switch between different metabolic states /Drake et al. 2002/. Comparing the MPN numbers of AA and HA demonstrates that they correlate well, i.e. $p = 0.012$ (Figure 1-22). So far, acetate data have not been available, though acetate could well be an important parameter to measure. One problem is that, because acetate is one of the organic molecules most used by microbes, its concentration in groundwater is probably below the detection limits of available analyses.

1.12 Total number of cells versus most probable number

The MPN method for enumerating microorganisms in deep Fennoscandian shield groundwater was first used for analysing methanogens and acetogens in Äspö HRL groundwater /Kotelnikova and Pedersen 1998/. Later, the method was further developed, and it has been used to analyse more types of microorganisms in deep groundwater from Finland /Haveman et al. 1999, Haveman and Pedersen 2002a/, including from Olkiluoto, and from the natural nuclear reactors in Bangombé,

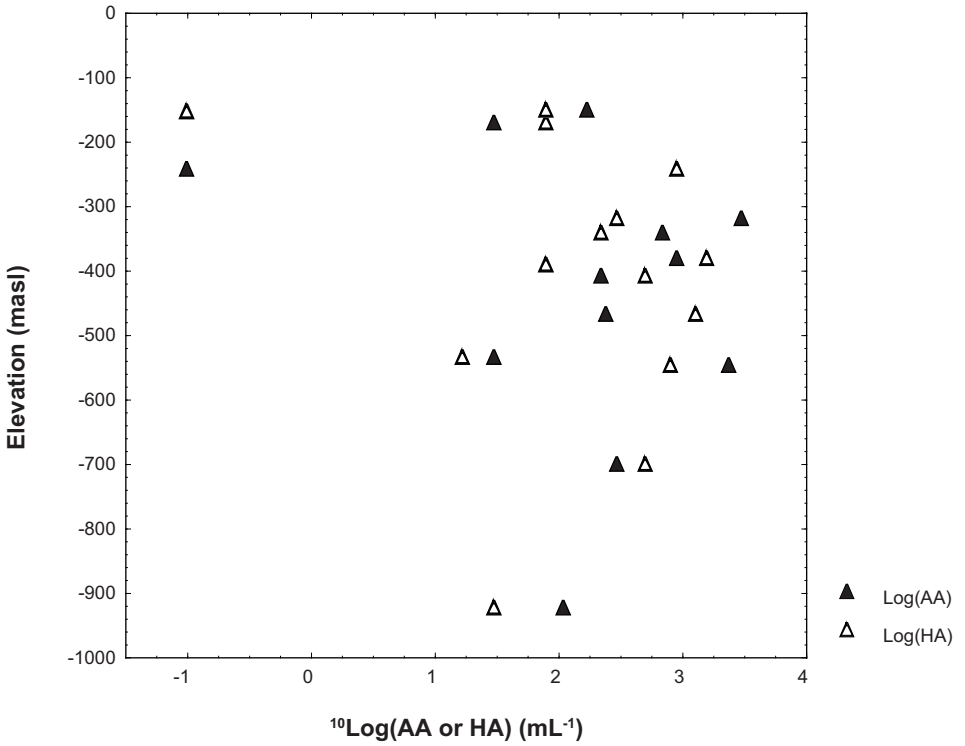

Figure 1-21. *Most probable numbers of cells (MPN) of auto- and heterotrophic acetogens (AA and HA) versus depth at six depths in boreholes in the Laxemar area. Solid symbols = heterotrophic acetogens, open symbols = autotrophic acetogens. Symbols at –1 denote data below the detection limit of 0.2 cells mL^{-1}. Data from extended freeze 2.3 (November 30, 2007).*

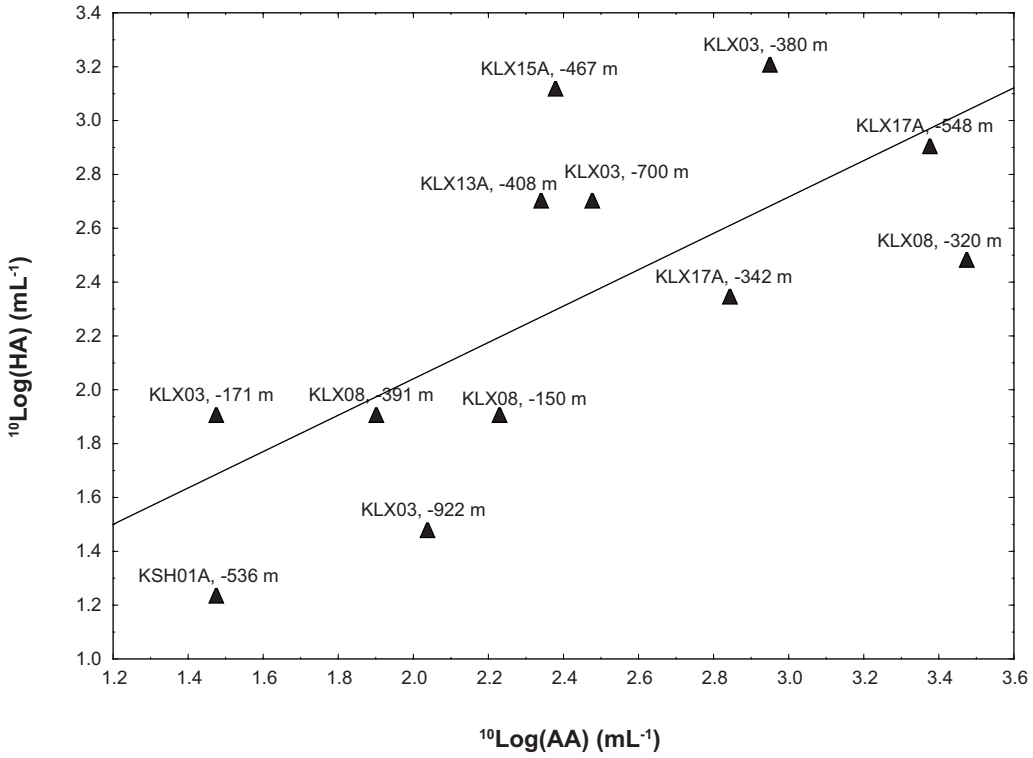

Figure 1-22. *The relationship between autotrophic (AA) and heterotrophic (HA) acetogens. Statistics: $^{10}Log(AA) = 0.69 + 0.68 \times {}^{10}Log(HA)$, r = 0.70, significant at p = 0.012, n = 11. Data from extended freeze 2.3 (November 30, 2007).*

Gabon, Africa /Haveman and Pedersen 2002b/. The method has been modified and changed over time. As the numbers of samples and types of organisms analysed have increased, the manual preparation of single tubes, as used for analysing methanogens and acetogens in Äspö HRL groundwater /Kotelnikova and Pedersen 1998/, has had to give way to methods that could handle the approximately 300 MPN tubes needed during each Laxemar field sampling campaign.

The expression "the great plate count anomaly" was coined by /Staley and Konopka 1985/ to describe the difference in orders of magnitude between the numbers of cells from natural environments that form colonies on agar media (CHAB) and the numbers countable by means of microscopic examination (TNC). In general, only 0.01–0.1% of bacterial cells sampled from various environmental aquatic systems produce colonies when using standard plating techniques, so, as expected from the relevant literature results, there was no significant correlation between TNC and CHAB data for Laxemar groundwater (Table 1-6). The anaerobic cultivation methods presented here represent the culmination of almost 10 years of development, testing, and adaptation for deep groundwater. This is reflected in the maximum MPN cultivability of 14% of the TNC in the sample from borehole KLX15A at 467 m depth and the 0.12–14% MPN cultivability range in all groundwater samples (Figure 1-23). The use of multiple, liquid anaerobic media has obviously overcome much of the discrepancy found between TNC and cultivations that use agar media only. However, it should be understood that there may still be microorganisms in the groundwater not cultivable using the applied methods. One example is that of anaerobic methane-oxidizing bacteria (ANME), which, as of the time of writing, have escaped successful cultivation by the world microbiology community. ANME have been observed in environmental samples but their successful cultivation in the laboratory has yet not been described in the literature.

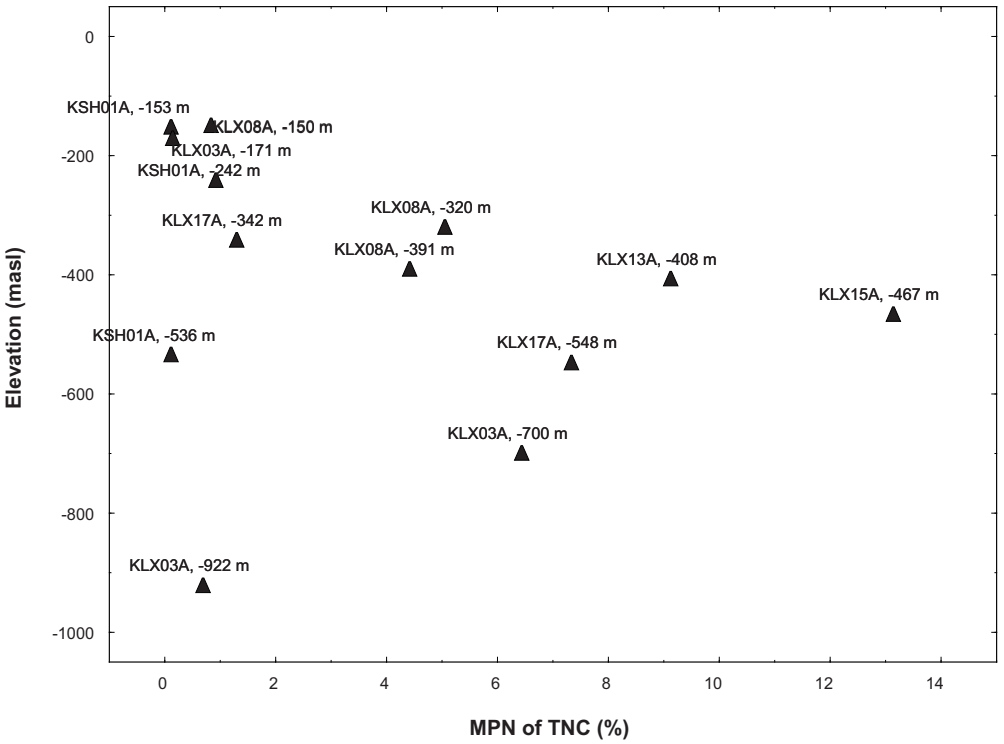

Figure 1-23. *Percentages of the total number of cells cultured using MPN in the analysed sections of boreholes in the Laxemar area. Nitrate-reducing bacteria were included in analyses of KLX03 (700 m depth), KLX08, KLX13A, KLX15A, and KLX17A. Data from extended freeze 2.3 (November 30, 2007).*

1.13 Correlations between variables deemed important for microbiological conceptual models

The dataset from Laxemar 2.3 includes a large range of variables and many cases. The following is a correlation matrix constructed for the variables deemed important for understanding microbial processes (Table 1-6). As demonstrated previously, crosswise correlations between the different cultivation and biomass results were generally good. Many of these parameters also displayed good correlations with TOC and DOC. The drill water residual (DWR) was not found to correlate with any of the included variables. Several of the chemical variables, such as log ferrous iron and manganese and sulphate, displayed good correlation with depth, as expected, because the amount of dissolved species generally decreases with depth. These are examples of nested variables, implying that some caution should be taken when evaluating multiple correlation matrices before conclusions are drawn about how some variables affect others. The correlation matrix in Table 1-6 should be regarded as a guide to possible relationships that can be further evaluated, as is done next.

Table 1-6. Correlation matrix of analysed variables related to microbial processes and, therefore, potentially correlated. For each correlated pair, the correlation coefficient, r, is given followed by the number of observations and the significance level, p, for the correlation. Pairwise missing data deletion was applied. Correlations marked in red are significant at p < 0.0500. Data from extended freeze 2.3 (November 30, 2007).

Variable	Variable (m)	Log(TNC)	Log(ATP)	Log(CHAB)	Log(NRB)	Log(IRB)	Log(MRB)
(m)		.2916 *n* = 13 *p* = .334	.3111 *n* = 9 *p* = .415	–.7258 *n* = 7 *p* = .065	–.6452 *n* = 7 *p* = .118	–.0627 *n* = 14 *p* = .831	–.0673 *n* = 11 *p* = .844
Log(TNC)	.2916 *n* = 13 *p* = .334		.7541 *n* = 8 *p* = .031	.3073 *n* = 7 *p* = .503	.3176 *n* = 7 *p* = .488	.2091 *n* = 13 *p* = .493	.3284 *n* = 10 *p* = .354
Log(ATP)	.3111 *n* = 9 *p* = .415	.7541 *n* = 8 *p* = .031		.3402 *n* = 5 *p* = .575	–.5488 *n* = 5 *p* = .338	.2822 *n* = 9 *p* = .462	.7466 *n* = 9 *p* = .021
Log(CHAB)	–.7258 *n* = 7 *p* = .065	.3073 *n* = 7 *p* = .503	.3402 *n* = 5 *p* = .575		.7918 *n* = 6 *p* = .061	.7171 *n* = 7 *p* = .070	.8609 *n* = 7 *p* = .013
Log(NRB)	–.6452 *n* = 7 *p* = .118	.3176 *n* = 7 *p* = .488	–.5488 *n* = 5 *p* = .338	.7918 *n* = 6 *p* = .061		.4595 *n* = 7 *p* = .300	.5801 *n* = 7 *p* = .172
Log(IRB)	–.0627 *n* = 14 *p* = .831	.2091 *n* = 13 *p* = .493	.2822 *n* = 9 *p* = .462	.7171 *n* = 7 *p* = .070	.4595 *n* = 7 *p* = .300		.4636 *n* = 11 *p* = .151
Log(MRB)	–.0673 *n* = 11 *p* = .844	.3284 *n* = 10 *p* = .354	.7466 *n* = 9 *p* = .021	.8609 *n* = 7 *p* = .013	.5801 *n* = 7 *p* = .172	.4636 *n* = 11 *p* = .151	
Log(SRB)	.0616 *n* = 14 *p* = .834	.4599 *n* = 13 *p* = .114	.7245 *n* = 9 *p* = .027	.4148 *n* = 7 *p* = .355	.3297 *n* = 7 *p* = .470	.5175 *n* = 14 *p* = .058	.8193 *n* = 11 *p* = .002
Log(AA)	.0122 *n* = 12 *p* = .970	.3919 *n* = 11 *p* = .233	.5759 *n* = 9 *p* = .105	–.0357 *n* = 7 *p* = .939	.0592 *n* = 7 *p* = .900	.5569 *n* = 12 *p* = .060	.5577 *n* = 11 *p* = .075
Log(HA)	.1712 *n* = 13 *p* = .576	.3408 *n* = 12 *p* = .278	.4894 *n* = 9 *p* = .181	.7751 *n* = 7 *p* = .041	.7913 *n* = 7 *p* = .034	.4105 *n* = 13 *p* = .164	.7438 *n* = 11 *p* = .009

Variable	Variable (m)	Log(TNC)	Log(ATP)	Log(CHAB)	Log(NRB)	Log(IRB)	Log(MRB)
Log(AM)	.2084	–.1994	.1416	–.4681	–.1971	–.6740	–.0838
	n = 11	*n* = 10	*n* = 9	*n* = 7	*n* = 7	*n* = 11	*n* = 11
	p = .539	*p* = .581	*p* = .716	*p* = .289	*p* = .672	*p* = .023	*p* = .807
Log(HM)	.0004	–.0751	.3140	–.0210	.4095	–.4784	.1662
	n = 13	*n* = 12	*n* = 9	*n* = 7	*n* = 7	*n* = 13	*n* = 11
	p = .999	*p* = .817	*p* = .411	*p* = .964	*p* = .362	*p* = .098	*p* = .625
MPN/TNC	–.2506	–.1389	–.1374	.7322	.7023	.6689	.6823
	n = 13	*n* = 13	*n* = 8	*n* = 7	*n* = 7	*n* = 13	*n* = 10
	p = .409	*p* = .651	*p* = .746	*p* = .061	*p* = .079	*p* = .012	*p* = .030
Eh Chemmac	–.1190	.0487	–.4881	–.8607	.3011	–.5003	–.5425
	n = 11	*n* = 10	*n* = 7	*n* = 5	*n* = 6	*n* = 11	*n* = 8
	p = .728	*p* = .894	*p* = .266	*p* = .061	*p* = .562	*p* = .117	*p* = .165
Log(SO_4^{2-})	–.6464	–.3337	–.5805	.5777	.7425	–.3158	–.0048
	n = 14	*n* = 13	*n* = 9	*n* = 7	*n* = 7	*n* = 14	*n* = 11
	p = .012	*p* = .265	*p* = .101	*p* = .174	*p* = .056	*p* = .271	*p* = .989
Log(Fe^{2+})	.4235	.6251	.5207	.0821	.3700	.1781	.3399
	n = 14	*n* = 13	*n* = 9	*n* = 7	*n* = 7	*n* = 14	*n* = 11
	p = .131	*p* = .022	*p* = .151	*p* = .861	*p* = .414	*p* = .542	*p* = .306
Fe^{2+}(mg L^{1})	.3223	.6079	.2144	.0467	.5628	–.0612	.2364
	n = 14	*n* = 13	*n* = 9	*n* = 7	*n* = 7	*n* = 14	*n* = 11
	p = .261	*p* = .028	*p* = .580	*p* = .921	*p* = .188	*p* = .835	*p* = .484
Mn^{2}+ (mg L^{-1})	.1550	.4008	–.1897	.7031	.6985	–.1898	.3662
	n = 14	*n* = 13	*n* = 9	*n* = 7	*n* = 7	*n* = 14	*n* = 11
	p = .597	*p* = .175	*p* = .625	*p* = .078	*p* = .081	*p* = .516	*p* = .268
Log(Mn^{2+})	.3005	.3614	–.1363	.3941	.5450	–.1762	.1493
	n = 14	*n* = 13	*n* = 9	*n* = 7	*n* = 7	*n* = 14	*n* = 11
	p = .297	*p* = .225	*p* = .727	*p* = .382	*p* = .206	*p* = .547	*p* = .661
S^{2-} (mg L^{-1})	–.6301	–.1920	–.2592	–.3032	.1810	–.3293	–.1850
	n = 13	*n* = 12	*n* = 9	*n* = 7	*n* = 7	*n* = 13	*n* = 11
	p = .021	*p* = .550	*p* = .501	*p* = .509	*p* = .698	*p* = .272	*p* = .586
Log(S^{2-})	–.4666	–.0804	–.2329	–.1784	.3095	–.1987	–.0314
	n = 13	*n* = 12	*n* = 9	*n* = 7	*n* = 7	*n* = 13	*n* = 11
	p = .108	*p* = .804	*p* = .546	*p* = .702	*p* = .499	*p* = .515	*p* = .927
DOC	.3305	.0921	.4824	–.6170	–.8732	–.0686	–.1753
	n = 13	*n* = 12	*n* = 8	*n* = 6	*n* = 6	*n* = 13	*n* = 10
	p = .270	*p* = .776	*p* = .226	*p* = .192	*p* = .023	*p* = .824	*p* = .628
Log(DOC)	.3089	.0801	.6126	–.6882	–.8612	.0214	–.1604
	n = 11	*n* = 10	*n* = 8	*n* = 6	*n* = 6	*n* = 11	*n* = 10
	p = .355	*p* = .826	*p* = .106	*p* = .131	*p* = .028	*p* = .950	*p* = .658
DWR (%)	–.1699	–.3396	–.6552	.2400	.3858	.2285	–.1099
	n = 11	*n* = 10	*n* = 9	*n* = 7	*n* = 7	*n* = 11	*n* = 11
	p = .618	*p* = .337	*p* = .055	*p* = .604	*p* = .393	*p* = .499	*p* = .748
Log(Fe^{2+})/S^{2-}	–.0957	.3507	.2427	.0345	.3422	–.1267	.1922
	n = 13	*n* = 12	*n* = 9	*n* = 7	*n* = 7	*n* = 13	*n* = 11
	p = .756	*p* = .264	*p* = .529	*p* = .942	*p* = .452	*p* = .680	*p* = .571
Stacked log(MPN)	–.4586	.7272	.9860	.6817	.5919	.8977	.9131
	n = 7	*n* = 7	*n* = 5	*n* = 6	*n* = 7	*n* = 7	*n* = 7
	p = .301	*p* = .064	*p* = .002	*p* = .136	*p* = .162	*p* = .006	*p* = .004

Variable	Variable						
	Log(SRB)	Log(AA)	Log(HA)	Log(AM)	Log(HM)	MPN/TNC	E_h Chemmac
(m)	.0616	.0122	.1712	.2084	.0004	–.2506	–.1190
	n = 14	*n* = 12	*n* = 13	*n* = 11	*n* = 13	*n* = 13	*n* = 11
	p = .834	*p* = .970	*p* = .576	*p* = .539	*p* = .999	*p* = .409	*p* = .728
Log(TNC)	.4599	.3919	.3408	–.1994	–.0751	–.1389	.0487
	n = 13	*n* = 11	*n* = 12	*n* = 10	*n* = 12	*n* = 13	*n* = 10
	p = .114	*p* = .233	*p* = .278	*p* = .581	*p* = .817	*p* = .651	*p* = .894
Log(ATP)	.7245	.5759	.4894	.1416	.3140	–.1374	–.4881
	n = 9	*n* = 9	*n* = 9	*n* = 9	*n* = 9	*n* = 8	*n* = 7
	p = .027	*p* = .105	*p* = .181	*p* = .716	*p* = .411	*p* = .746	*p* = .266
Log(CHAB)	.4148	–.0357	.7751	–.4681	–.0210	.7322	–.8607
	n = 7	*n* = 7	*n* = 7	*n* = 7	*n* = 7	*n* = 7	*n* = 5
	p = .355	*p* = .939	*p* = .041	*p* = .289	*p* = .964	*p* = .061	*p* = .061
Log(NRB)	.3297	.0592	.7913	–.1971	.4095	.7023	.3011
	n = 7	*n* = 7	*n* = 7	*n* = 7	*n* = 7	*n* = 7	*n* = 6
	p = .470	*p* = .900	*p* = .034	*p* = .672	*p* = .362	*p* = .079	*p* = .562
Log(IRB)	.5175	.5569	.4105	–.6740	–.4784	.6689	–.5003
	n = 14	*n* = 12	*n* = 13	*n* = 11	*n* = 13	*n* = 13	*n* = 11
	p = .058	*p* = .060	*p* = .164	*p* = .023	*p* = .098	*p* = .012	*p* = .117
Log(MRB)	.8193	.5577	.7438	–.0838	.1662	.6823	–.5425
	n = 11	*n* = 11	*n* = 11	*n* = 11	*n* = 11	*n* = 10	*n* = 8
	p = .002	*p* = .075	*p* = .009	*p* = .807	*p* = .625	*p* = .030	*p* = .165
Log(SRB)		.6885	.5088	–.2111	.0556	.2946	–.2632
		n = 12	*n* = 13	*n* = 11	*n* = 13	*n* = 13	*n* = 11
		p = .013	*p* = .076	*p* = .533	*p* = .857	*p* = .329	*p* = .434
Log(AA)	.6885		.6947	–.1521	–.0075	.4112	–.4394
	n = 12		*n* = 12	*n* = 11	*n* = 12	*n* = 11	*n* = 9
	p = .013		*p* = .012	*p* = .655	*p* = .982	*p* = .209	*p* = .237
Log(HA)	.5088	.6947		.1204	.2336	.7070	–.0599
	n = 13	*n* = 12		*n* = 11	*n* = 13	*n* = 12	*n* = 10
	p = .076	*p* = .012		*p* = .724	*p* = .442	*p* = .010	*p* = .869
Log(AM)	–.2111	–.1521	.1204		.8237	–.2845	.3905
	n = 11	*n* = 11	*n* = 11		*n* = 11	*n* = 10	*n* = 8
	p = .533	*p* = .655	*p* = .724		*p* = .002	*p* = .426	*p* = .339
Log(HM)	.0556	–.0075	.2336	.8237		–.3715	.1208
	n = 13	*n* = 12	*n* = 13	*n* = 11		*n* = 12	*n* = 10
	p = .857	*p* = .982	*p* = .442	*p* = .002		*p* = .234	*p* = .740
MPN/TNC	.2946	.4112	.7070	–.2845	–.3715		–.3333
	n = 13	*n* = 11	*n* = 12	*n* = 10	*n* = 12		*n* = 10
	p = .329	*p* = .209	*p* = .010	*p* = .426	*p* = .234		*p* = .347

Variable	Variable						
	Log(SRB)	Log(AA)	Log(HA)	Log(AM)	Log(HM)	MPN/TNC	E_h Chemmac
Eh Chemmac	–.2632	–.4394	–.0599	.3905	.1208	–.3333	
	n = 11	*n* = 9	*n* = 10	*n* = 8	*n* = 10	*n* = 10	
	p = .434	*p* = .237	*p* = .869	*p* = .339	*p* = .740	*p* = .347	
Log(SO_4^{2-})	–.3004	–.4838	–.1861	.2786	.2907	.1280	.6789
	n = 14	*n* = 12	*n* = 13	*n* = 11	*n* = 13	*n* = 13	*n* = 11
	p = .297	*p* = .111	*p* = .543	*p* = .407	*p* = .335	*p* = .677	*p* = .022
Log(Fe^{2+})	.6133	.2753	.3126	.1239	.1406	–.0985	.4597
	n = 14	*n* = 12	*n* = 13	*n* = 11	*n* = 13	*n* = 13	*n* = 11
	p = .020	*p* = .386	*p* = .298	*p* = .717	*p* = .647	*p* = .749	*p* = .155
Fe^{2+}(mg L^{-1})	.4210	.4466	.3910	–.0312	–.0079	–.1598	.5728
	n = 14	*n* = 12	*n* = 13	*n* = 11	*n* = 13	*n* = 13	*n* = 11
	p = .134	*p* = .146	*p* = .187	*p* = .927	*p* = .980	*p* = .602	*p* = .065
Mn^{2+} (mg L^{-1})	.1776	–.3113	.1646	.0931	–.0544	–.0009	.7990
	n = 14	*n* = 12	*n* = 13	*n* = 11	*n* = 13	*n* = 13	*n* = 11
	p = .544	*p* = .325	*p* = .591	*p* = .786	*p* = .860	*p* = .998	*p* = .003
Log(Mn^{2+})	.1282	–.3218	.1274	.3175	.1085	–.0840	.8583
	n = 14	*n* = 12	*n* = 13	*n* = 11	*n* = 13	*n* = 13	*n* = 11
	p = .662	*p* = .308	*p* = .678	*p* = .341	*p* = .724	*p* = .785	*p* = .001
S^{2-} (mg L^{-1})	–.2938	–.0192	–.5194	–.0752	–.1031	–.2542	–.0219
	n = 13	*n* = 11	*n* = 12	*n* = 11	*n* = 12	*n* = 12	*n* = 10
	p = .330	*p* = .955	*p* = .084	*p* = .826	*p* = .750	*p* = .425	*p* = .952
Log(S^{2-})	–.0862	.1610	–.3177	–.0409	–.0842	–.2022	.2248
	n = 13	*n* = 11	*n* = 12	*n* = 11	*n* = 12	*n* = 12	*n* = 10
	p = .780	*p* = .636	*p* = .314	*p* = .905	*p* = .795	*p* = .529	*p* = .532
DOC	–.1889	–.0237	.0710	.4977	.5061	–.1380	–.4345
	n = 13	*n* = 11	*n* = 12	*n* = 10	*n* = 12	*n* = 12	*n* = 10
	p = .537	*p* = .945	*p* = .826	*p* = .143	*p* = .093	*p* = .669	*p* = .210
Log(DOC)	–.1058	.0442	.1204	.4379	.4924	–.1472	–.2658
	n = 11	*n* = 10	*n* = 10	*n* = 10	*n* = 10	*n* = 10	*n* = 8
	p = .757	*p* = .904	*p* = .740	*p* = .206	*p* = .148	*p* = .685	*p* = .525
DWR (%)	–.1604	–.1375	.3210	–.1313	–.0792	.5476	.5195
	n = 11	*n* = 11	*n* = 11	*n* = 11	*n* = 11	*n* = 10	*n* = 8
	p = .637	*p* = .687	*p* = .336	*p* = .700	*p* = .817	*p* = .101	*p* = .187
Log(Fe^{2+})/S^{2-}	.3797	.2109	.0110	.2039	.1773	–.2933	.4774
	n = 13	*n* = 11	*n* = 12	*n* = 11	*n* = 12	*n* = 12	*n* = 10
	p = .201	*p* = .534	*p* = .973	*p* = .548	*p* = .581	*p* = .355	*p* = .163
Stacked log(MPN)	.9336	.5794	.7101	–.5724	–.0523	.4398	–.4025
	n = 7	*n* = 7	*n* = 7	*n* = 7	*n* = 7	*n* = 7	*n* = 6
	p = .002	*p* = .173	*p* = .074	*p* = .179	*p* = .911	*p* = .323	*p* = .429

Variable	Variables					
	Log(SO_4^{2-})	Log(Fe^{2+})	Fe^{2+}(mg L^{-1})	Mn^{2+} (mg L^{-1})	Log(Mn^{2+})	S^{2-} (mg L^{-1})
(m)	–.6464	.4235	.3223	.1550	.3005	–.6301
	n = 14	*n* = 14	*n* = 14	*n* = 14	*n* = 14	*n* = 13
	p = .012	*p* = .131	*p* = .261	*p* = .597	*p* = .297	*p* = .021
Log(TNC)	–.3337	.6251	.6079	.4008	.3614	–.1920
	n = 13	*n* = 13	*n* = 13	*n* = 13	*n* = 13	*n* = 12
	p = .265	*p* = .022	*p* = .028	*p* = .175	*p* = .225	*p* = .550
Log(ATP)	–.5805	.5207	.2144	–.1897	–.1363	–.2592
	n = 9	*n* = 9	*n* = 9	*n* = 9	*n* = 9	*n* = 9
	p = .101	*p* = .151	*p* = .580	*p* = .625	*p* = .727	*p* = .501
Log(CHAB)	.5777	.0821	.0467	.7031	.3941	–.3032
	n = 7	*n* = 7	*n* = 7	*n* = 7	*n* = 7	*n* = 7
	p = .174	*p* = .861	*p* = .921	*p* = .078	*p* = .382	*p* = .509
Log(NRB)	.7425	.3700	.5628	.6985	.5450	.1810
	n = 7	*n* = 7	*n* = 7	*n* = 7	*n* = 7	*n* = 7
	p = .056	*p* = .414	*p* = .188	*p* = .081	*p* = .206	*p* = .698
Log(IRB)	–.3158	.1781	–.0612	–.1898	–.1762	–.3293
	n = 14	*n* = 14	*n* = 14	*n* = 14	*n* = 14	*n* = 13
	p = .271	*p* = .542	*p* = .835	*p* = .516	*p* = .547	*p* = .272
Log(MRB)	–.0048	.3399	.2364	.3662	.1493	–.1850
	n = 11	*n* = 11	*n* = 11	*n* = 11	*n* = 11	*n* = 11
	p = .989	*p* = .306	*p* = .484	*p* = .268	*p* = .661	*p* = .586
Log(SRB)	–.3004	.6133	.4210	.1776	.1282	–.2938
	n = 14	*n* = 14	*n* = 14	*n* = 14	*n* = 14	*n* = 13
	p = .297	*p* = .020	*p* = .134	*p* = .544	*p* = .662	*p* = .330
Log(AA)	–.4838	.2753	.4466	–.3113	–.3218	–.0192
	n = 12	*n* = 12	*n* = 12	*n* = 12	*n* = 12	*n* = 11
	p = .111	*p* = .386	*p* = .146	*p* = .325	*p* = .308	*p* = .955
Log(HA)	–.1861	.3126	.3910	.1646	.1274	–.5194
	n = 13	*n* = 13	*n* = 13	*n* = 13	*n* = 13	*n* = 12
	p = .543	*p* = .298	*p* = .187	*p* = .591	*p* = .678	*p* = .084
Log(AM)	.2786	.1239	–.0312	.0931	.3175	–.0752
	n = 11	*n* = 11	*n* = 11	*n* = 11	*n* = 11	*n* = 11
	p = .407	*p* = .717	*p* = .927	*p* = .786	*p* = .341	*p* = .826
Log(HM)	.2907	.1406	–.0079	–.0544	.1085	–.1031
	n = 13	*n* = 13	*n* = 13	*n* = 13	*n* = 13	*n* = 12
	p = .335	*p* = .647	*p* = .980	*p* = .860	*p* = .724	*p* = .750
MPN/TNC	.1280	–.0985	–.1598	–.0009	–.0840	–.2542
	n = 13	*n* = 13	*n* = 13	*n* = 13	*n* = 13	*n* = 12
	p = .677	*p* = .749	*p* = .602	*p* = .998	*p* = .785	*p* = .425

Variable	Variables					
	Log(SO_4^{2-})	Log(Fe^{2+})	Fe^{2+}(mg L^{-1})	Mn^{2+} (mg L^{-1})	Log(Mn^{2+})	S^{2-} (mg L^{-1})
E_h Chemmac	.6789	.4597	.5728	.7990	.8583	–.0219
	n = 11	*n* = 11	*n* = 11	*n* = 11	*n* = 11	*n* = 10
	p = .022	*p* = .155	*p* = .065	*p* = .003	*p* = .001	*p* = .952
Log(SO_4^{2-})		–.1824	–.1079	.3223	.3231	.4095
		n = 14	*n* = 14	*n* = 14	*n* = 14	*n* = 13
		p = .532	*p* = .713	*p* = .261	*p* = .260	*p* = .165
Log(Fe^{2+})	–.1824		.7841	.5406	.6606	–.4611
	n = 14		*n* = 14	*n* = 14	*n* = 14	*n* = 13
	p = .532		*p* = .001	*p* = .046	*p* = .010	*p* = .113
Fe^{2+}(mg L^{-1})	–.1079	.7841		.6614	.6701	–.1758
	n = 14	*n* = 14		*n* = 14	*n* = 14	*n* = 13
	p = .713	*p* = .001		*p* = .010	*p* = .009	*p* = .566
Mn^{2+} (mg L^{-1})	.3223	.5406	.6614		.9166	–.2703
	n = 14	*n* = 14	*n* = 14		*n* = 14	*n* = 13
	p = .261	*p* = .046	*p* = .010		*p* = .000	*p* = .372
Log(Mn^{2+})	.3231	.6606	.6701	.9166		–.3886
	n = 14	*n* = 14	*n* = 14	*n* = 14		*n* = 13
	p = .260	*p* = .010	*p* = .009	*p* = .000		*p* = .189
S^{2-} (mg L^{-1})	.4095	–.4611	–.1758	–.2703	–.3886	
	n = 13	*n* = 13	*n* = 13	*n* = 13	*n* = 13	
	p = .165	*p* = .113	*p* = .566	*p* = .372	*p* = .189	
Log(S^{2-})	.4025	–.1409	.1077	–.0842	–.0899	.8756
	n = 13	*n* = 13	*n* = 13	*n* = 13	*n* = 13	*n* = 13
	p = .173	*p* = .646	*p* = .726	*p* = .784	*p* = .770	*p* = .000
DOC	–.3194	–.0241	–.3628	–.5197	–.3640	–.2875
	n = 13	*n* = 13	*n* = 13	*n* = 13	*n* = 13	*n* = 12
	p = .287	*p* = .938	*p* = .223	*p* = .069	*p* = .221	*p* = .365
Log(DOC)	–.4165	.0501	–.4063	–.5848	–.3526	–.3943
	n = 11	*n* = 11	*n* = 11	*n* = 11	*n* = 11	*n* = 11
	p = .203	*p* = .884	*p* = .215	*p* = .059	*p* = .287	*p* = .230
DWR (%)	.3283	–.1152	.1204	.3526	.3746	–.3560
	n = 11	*n* = 11	*n* = 11	*n* = 11	*n* = 11	*n* = 11
	p = .324	*p* = .736	*p* = .724	*p* = .288	*p* = .256	*p* = .283
Log(Fe^{2+})/S^{2-}	.3043	.6499	.6102	.4462	.5065	.2885
	n = 13	*n* = 13	*n* = 13	*n* = 13	*n* = 13	*n* = 13
	p = .312	*p* = .016	*p* = .027	*p* = .126	*p* = .077	*p* = .339
Stacked log(MPN)	.0716	.5444	.3691	.3154	.0199	.1378
	n = 7	*n* = 7	*n* = 7	*n* = 7	*n* = 7	*n* = 7
	p = .879	*p* = .206	*p* = .415	*p* = .491	*p* = .966	*p* = .768

Variable	Variables					
	Log(S^{2-})	DOC	Log(DOC)	DWR (%)	Log(Fe^{2+})/S^{2-}	Stacked log(MPN)
(m)	–.4666	.3305	.3089	–.1699	–.0957	–.4586
	n = 13	*n* = 13	*n* = 11	*n* = 11	*n* = 13	*n* = 7
	p = .108	*p* = .270	*p* = .355	*p* = .618	*p* = .756	*p* = .301
Log(TNC)	–.0804	.0921	.0801	–.3396	.3507	.7272
	n = 12	*n* = 12	*n* = 10	*n* = 10	*n* = 12	*n* = 7
	p = .804	*p* = .776	*p* = .826	*p* = .337	*p* = .264	*p* = .064
Log(ATP)	–.2329	.4824	.6126	–.6552	.2427	.9860
	n = 9	*n* = 8	*n* = 8	*n* = 9	*n* = 9	*n* = 5
	p = .546	*p* = .226	*p* = .106	*p* = .055	*p* = .529	*p* = .002
Log(CHAB)	–.1784	–.6170	–.6882	.2400	.0345	.6817
	n = 7	*n* = 6	*n* = 6	*n* = 7	*n* = 7	*n* = 6
	p = .702	*p* = .192	*p* = .131	*p* = .604	*p* = .942	*p* = .136
Log(NRB)	.3095	–.8732	–.8612	.3858	.3422	.5919
	n = 7	*n* = 6	*n* = 6	*n* = 7	*n* = 7	*n* = 7
	p = .499	*p* = .023	*p* = .028	*p* = .393	*p* = .452	*p* = .162
Log(IRB)	–.1987	–.0686	.0214	.2285	–.1267	.8977
	n = 13	*n* = 13	*n* = 11	*n* = 11	*n* = 13	*n* = 7
	p = .515	*p* = .824	*p* = .950	*p* = .499	*p* = .680	*p* = .006
Log(MRB)	–.0314	–.1753	–.1604	–.1099	.1922	.9131
	n = 11	*n* = 10	*n* = 10	*n* = 11	*n* = 11	*n* = 7
	p = .927	*p* = .628	*p* = .658	*p* = .748	*p* = .571	*p* = .004
Log(SRB)	–.0862	–.1889	–.1058	–.1604	.3797	.9336
	n = 13	*n* = 13	*n* = 11	*n* = 11	*n* = 13	*n* = 7
	p = .780	*p* = .537	*p* = .757	*p* = .637	*p* = .201	*p* = .002
Log(AA)	.1610	–.0237	.0442	–.1375	.2109	.5794
	n = 11	*n* = 11	*n* = 10	*n* = 11	*n* = 11	*n* = 7
	p = .636	*p* = .945	*p* = .904	*p* = .687	*p* = .534	*p* = .173
Log(HA)	–.3177	.0710	.1204	.3210	.0110	.7101
	n = 12	*n* = 12	*n* = 10	*n* = 11	*n* = 12	*n* = 7
	p = .314	*p* = .826	*p* = .740	*p* = .336	*p* = .973	*p* = .074
Log(AM)	–.0409	.4977	.4379	–.1313	.2039	–.5724
	n = 11	*n* = 10	*n* = 10	*n* = 11	*n* = 11	*n* = 7
	p = .905	*p* = .143	*p* = .206	*p* = .700	*p* = .548	*p* = .179
Log(HM)	–.0842	.5061	.4924	–.0792	.1773	–.0523
	n = 12	*n* = 12	*n* = 10	*n* = 11	*n* = 12	*n* = 7
	p = .795	*p* = .093	*p* = .148	*p* = .817	*p* = .581	*p* = .911
MPN/TNC	–.2022	–.1380	–.1472	.5476	–.2933	.4398
	n = 12	*n* = 12	*n* = 10	*n* = 10	*n* = 12	*n* = 7
	p = .529	*p* = .669	*p* = .685	*p* = .101	*p* = .355	*p* = .323
Eh Chemmac	.2248	–.4345	–.2658	.5195	.4774	–.4025
	n = 10	*n* = 10	*n* = 8	*n* = 8	*n* = 10	*n* = 6
	p = .532	*p* = .210	*p* = .525	*p* = .187	*p* = .163	*p* = .429
Log(SO_4^{2-})	.4025	–.3194	–.4165	.3283	.3043	.0716
	n = 13	*n* = 13	*n* = 11	*n* = 11	*n* = 13	*n* = 7
	p = .173	*p* = .287	*p* = .203	*p* = .324	*p* = .312	*p* = .879
Log(Fe^{2+})	–.1409	–.0241	.0501	–.1152	.6499	.5444
	n = 13	*n* = 13	*n* = 11	*n* = 11	*n* = 13	*n* = 7
	p = .646	*p* = .938	*p* = .884	*p* = .736	*p* = .016	*p* = .206

Variable	Variables					
	Log(S^{2-})	DOC	Log(DOC)	DWR (%)	Log(Fe^{2+})/S^{2-}	Stacked log(MPN)
Fe^{2+}(mg L^{-1})	.1077	–.3628	–.4063	.1204	.6102	.3691
	n = 13	*n* = 13	*n* = 11	*n* = 11	*n* = 13	*n* = 7
	p = .726	*p* = .223	*p* = .215	*p* = .724	*p* = .027	*p* = .415
Mn^{2+} (mg L^{-1})	–.0842	–.5197	–.5848	.3526	.4462	.3154
	n = 13	*n* = 13	*n* = 11	*n* = 11	*n* = 13	*n* = 7
	p = .784	*p* = .069	*p* = .059	*p* = .288	*p* = .126	*p* = .491
Log(Mn^{2+})	–.0899	–.3640	–.3526	.3746	.5065	.0199
	n = 13	*n* = 13	*n* = 11	*n* = 11	*n* = 13	*n* = 7
	p = .770	*p* = .221	*p* = .287	*p* = .256	*p* = .077	*p* = .966
S^{2-} (mg L^{-1})	.8756	–.2875	–.3943	–.3560	.2885	.1378
	n = 13	*n* = 12	*n* = 11	*n* = 11	*n* = 13	*n* = 7
	p = .000	*p* = .365	*p* = .230	*p* = .283	*p* = .339	*p* = .768
Log(S^{2-})		–.4871	–.4911	–.2472	.5211	.1156
		n = 12	*n* = 11	*n* = 11	*n* = 13	*n* = 7
		p = .108	*p* = .125	*p* = .464	*p* = .068	*p* = .805
DOC	–.4871		.9060	–.4014	–.2955	–.2678
	n = 12		*n* = 11	*n* = 10	*n* = 12	*n* = 6
	p = .108		*p* = .000	*p* = .250	*p* = .351	*p* = .608
Log(DOC)	–.4911	.9060		–.2852	–.3636	–.3630
	n = 11	*n* = 11		*n* = 10	*n* = 11	*n* = 6
	p = .125	*p* = .000		*p* = .424	*p* = .272	*p* = .479
DWR (%)	–.2472	–.4014	–.2852		–.3561	–.3776
	n = 11	*n* = 10	*n* = 10		*n* = 11	*n* = 7
	p = .464	*p* = .250	*p* = .424		*p* = .282	*p* = .404
Log(Fe^{2+})/S^{2-}	.5211	–.2955	–.3636	–.3561		.4375
	n = 13	*n* = 12	*n* = 11	*n* = 11		*n* = 7
	p = .068	*p* = .351	*p* = .272	*p* = .282		*p* = .326
Stacked log(MPN)	.1156	–.2678	–.3630	–.3776	.4375	
	n = 7	*n* = 6	*n* = 6	*n* = 7	*n* = 7	
	p = .805	*p* = .608	*p* = .479	*p* = .404	*p* = .326	

As described in section 1.2, microbial metabolic processes will lower the redox potential (Eh) in the environment. Figure 1-24 shows the measured Eh (Chemmac) in groundwater from the different depths in the 13 boreholes studied. The values did not indicate a significant correlation with depth (p = 0.728, Table 1-6). The measured Eh was generally low in Laxemar compared with the values measured in Forsmark. In Laxemar, the lowest Eh value observed was –303 mV at 548 m in borehole KLX17A and the highest was –210 mV at 242 m in KSH01A. The measured Eh did not relate to depth (Figure 1-24). Significantly correlated with the measured Eh values were ^{10}Log(SO_4^{2-}) at p = 0.02 and both the concentration of manganese and the ^{10}Log of manganese at p = 0.003 and 0.001, respectively. At first sight, measured Eh was not significantly correlated with any of the microbiology variables (Table 1-6). Since measured Eh was significantly correlated with the ^{10}Log of the SRB in Forsmark /Laaksoharju 2008/, these data were evaluated more thoroughly. In this dataset, the data from boreholes KLX03 at 171 m depth, KLX08 at 150 m and KLX13A at 408 m were removed. The SRB values from these sections were the lowest found in the site investigation in both Forsmark and Laxemar, as can be seen in Figure 1-24. Figure 1-25 shows the correlation between the measured Eh and all SRB data, and Figure 1-26 shows that the correlation between Eh and a modified set of SRB data was significant at p = 0.006. This variable only displayed a significant correlation with manganese, ferrous iron, and sulphate. Possibly, Chemmac Eh data do relate to microbial processes as will be discussed later, but not with calculated Eh.

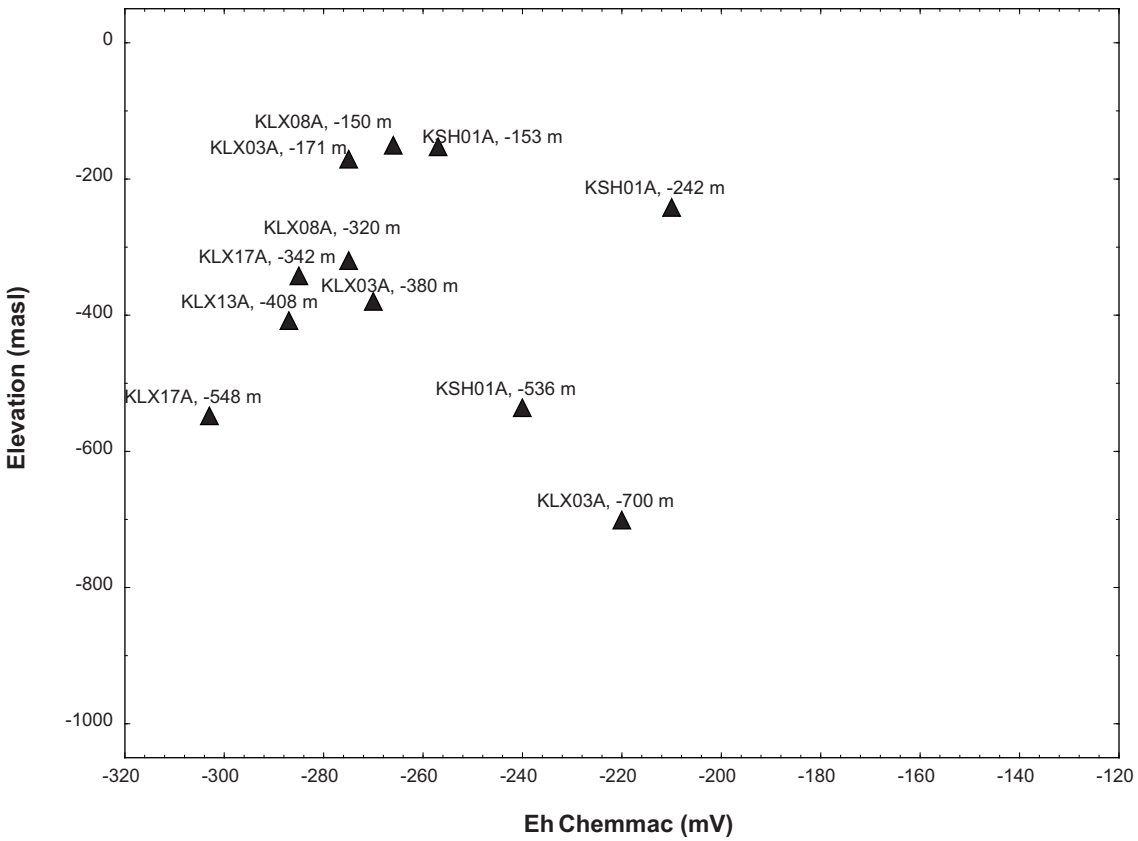

Figure 1-24. *Measured Eh versus depth in the Laxemar area. Data from extended freeze 2.3 (November 30, 2007).*

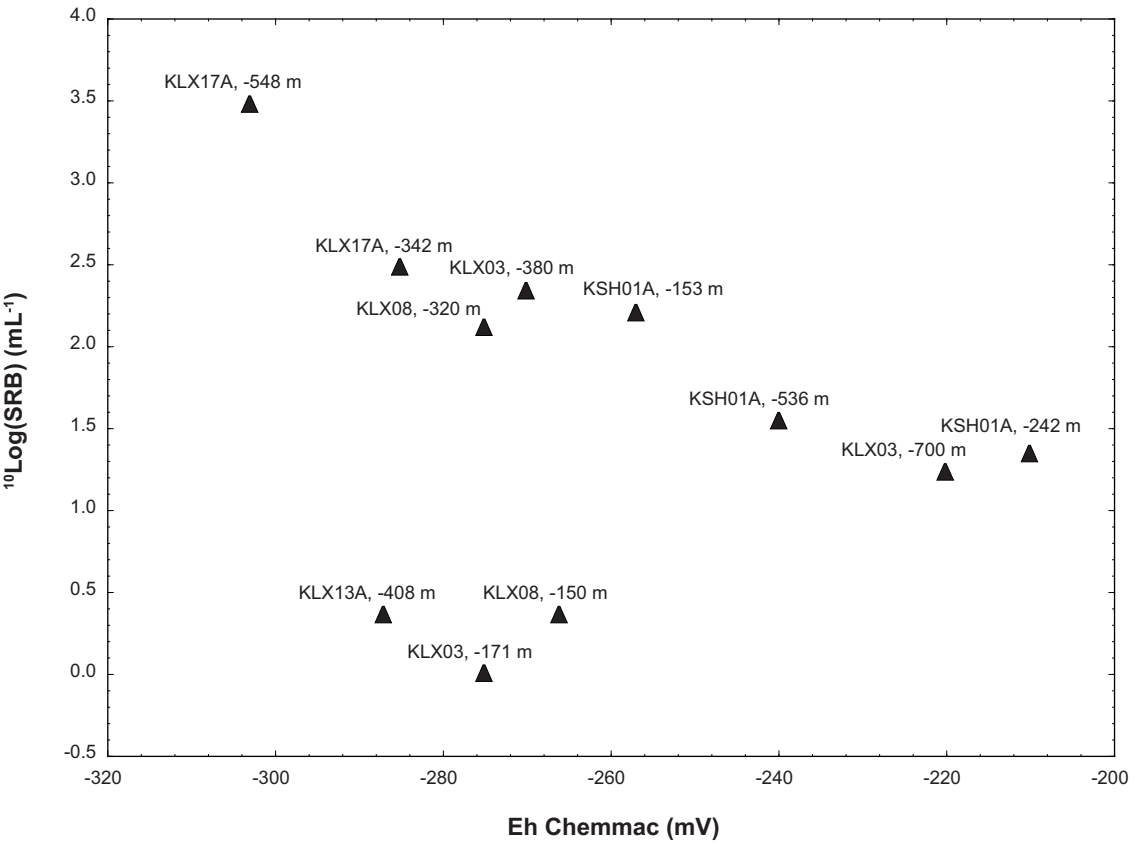

Figure 1-25. *The relationship between the number of sulphate-reducing bacteria and the Eh analysed using the Cemmach system. Data from extended freeze 2.3 (November 30, 2007).*

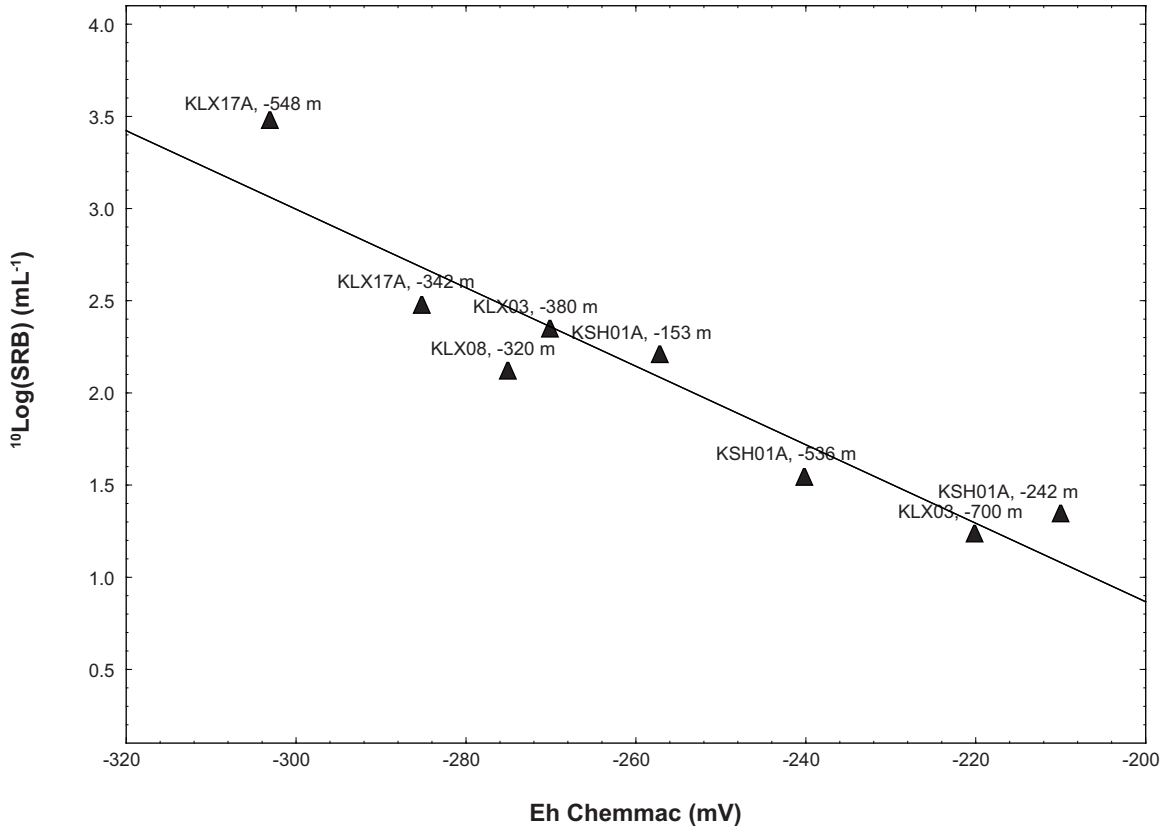

Figure 1-26. *The relationship between the number of sulphate-reducing bacteria with some data excluded (see Figure 1-25) and the Eh analysed using the Cemmach system. Statistics:* $^{10}Log(SRB) = –171 – 41 \times Eh$, $r = –0.94$, *significant at* $p = 0.0006$, $n = 8$. *Data from extended freeze 2.3 (November 30, 2007).*

Many microorganisms use organic carbon as their energy source and electron donor (see section 1.2). Dissolved organic carbon is therefore a factor that could influence Eh. However, a significant correlation was not present for the organic carbon variables TOC, log(DOC) (Table 1-6), or DOC (not shown).

1.14 Discussion: the microbial model

1.14.1 A theoretical model of microbial reactions in a crystalline groundwater environment

Figure 1-27 shows a theoretical model of microbial reactions in a crystalline groundwater environment. The reactions depicted are metabolic redox reactions involving many different physiological groups of microorganisms. Which of the groups is active is determined by the available energy, carbon sources, and electron donors. The activities of the different groups are described in Table 1-1. This model proposes a depth-related diversification of the microbial populations comparable to that found in a shallow aquatic sediment environment; the latter can be modelled as a biosphere involving oxygenic photosynthesis that creates a chemical potential. Mineralisation is restored via several redox processes carried out by a variety of organisms /Fenchel et al. 1998/. The greatest difference between the two systems is the depth scale: the shallow aquatic sediment environment extends over a depth range of centimetres, while the deep groundwater system extends to a depth of at least 1,000 m.

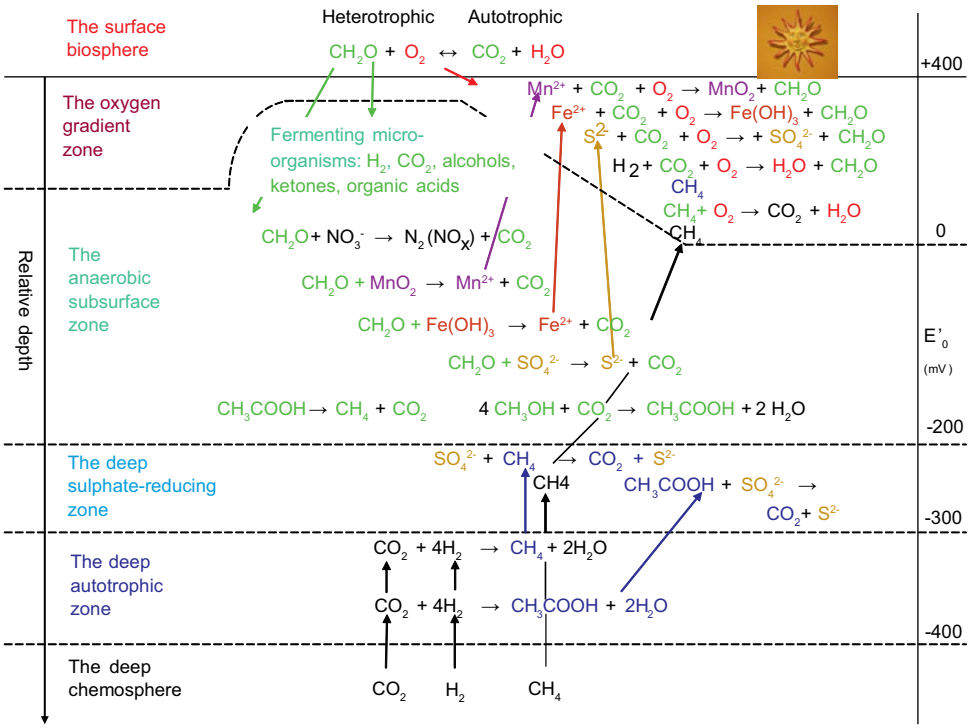

Figure 1-27. *Theoretical model of microbial reactions in a crystalline groundwater environment from /SKB 2006/.*

Figure 1-28 shows the stacked ^{10}log values of MPN for all sampled sections, sorted by depth. The highest numbers of microorganisms are found in the depth range from 300 to 600 m. The reason for this is unknown, though it could be due to intersection with other water-bearing fractures that allowed different groundwater types to mix. Interestingly, both IRB and SRB were high in these sections, supporting the idea that different groundwaters may have been mixing. In general, it can be seen that acetogenic bacteria are present in all sampled sections, even comprising the dominant group in some sections. There is no obvious explanation for this, but presumably there was mixing of different groundwaters in these sections, creating a suitable environment for iron and sulphate reducers. Another possibility is that the sampling of groundwater from a large volume of rock, if the flow in the sampled fracture or fractures is low but large volumes of water must be pumped out before sampling, could cause the mixing of groundwater from several different groundwater environments. Whether the mixing that occurred in the sampled boreholes represents natural mixing or was induced by drilling and pumping in the area needs to be further investigated. The sections with high stacked MPN numbers also have lower Eh values than do sections with lower stacked MPN's (see Figure 1-24 and Figure 1-28). In comparison, in the Olkiluoto area in Finland, such high numbers of stacked MPN are rarely seen and only found in very shallow water /Pedersen 2008/.

In Table 1-6 it can be seen that there is a significant correlation between the stacked ^{10}log values and the ATP values, with significance at $p = 0.002$. From this it can be concluded that the different groups were all active at the time of sampling, since ATP is the energy transport molecule and present only in living cells and the MPN measurements reflect the microbial processes in the sampled groundwater.

Figure 1-29 presents the theoretical model of the microbial system in Laxemar, as can be interpreted from the site investigation results, which pertain to samples from 150 m down to 922 m. The microbial reactions noted in black are those that we have confirmed to be ongoing; those noted in grey must still be verified.

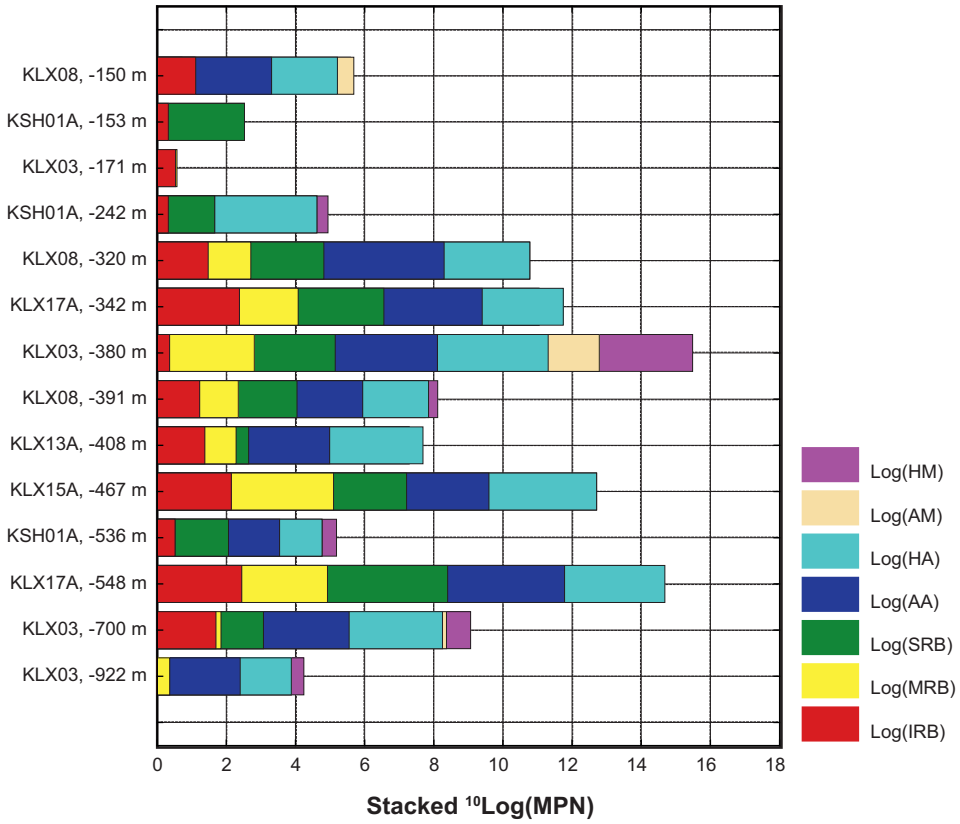

Figure 1-28. *Stacked log[10] MPN values for samples from Laxemar sorted by depth.*

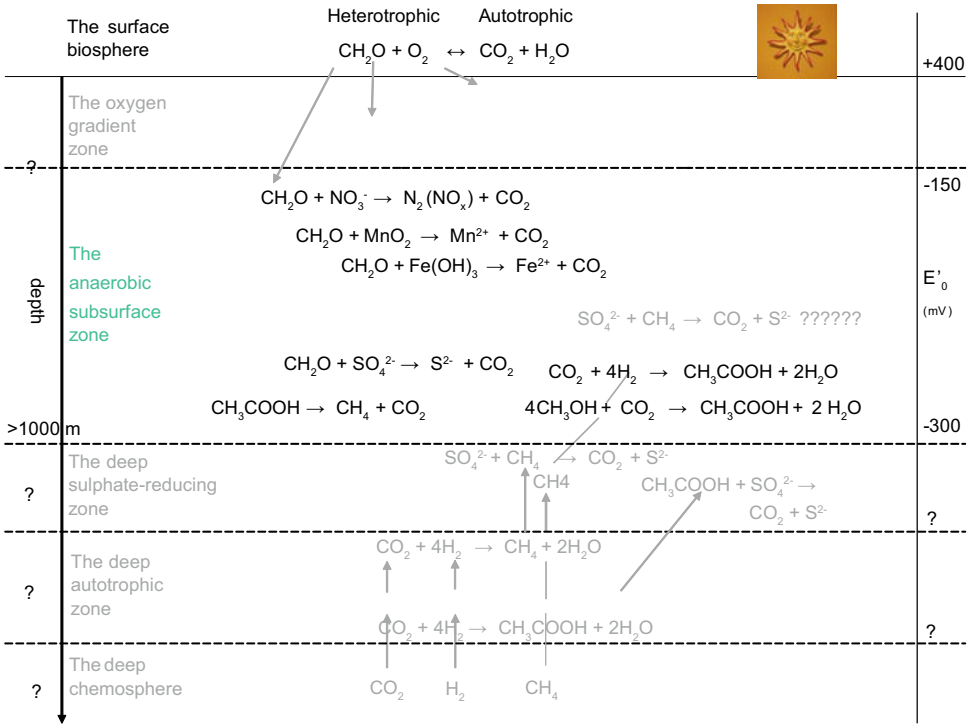

Figure 1-29. *The theoretical model of the microbial system in Laxemar: those reactions in black have been confirmed in the groundwaters, whereas those in grey require verification.*
? = depths and redox values have not yet been confirmed.

Anaerobic respiration

Nitrate- iron-, manganese-, and sulphate-reducing bacteria are the groups of anaerobic respiring organisms that have been analyzed during the site investigation. In Figure 1-28, the nitrate reducers are omitted, since this group was not included in the first six boreholes investigated (see Table 1-2). There is no special trend or pattern in the presence of anaerobic organisms; these organisms instead follow the overall pattern that if the total MPN values are high, so are the numbers of anaerobic organisms. It was only the deepest section of borehole KLX03, the 922 m depth interval, that contained low numbers of this group and then only manganese reducers.

Acetogens and methanogens

In all sampled sections where the MPN's of acetogens and methanogens were determined, acetogens were found to be dominant. Methanogens were barely present in the Laxemar area, a finding supported by the low concentrations of methane measured in the area (see Figure 1-28 and Chapter 3, "Gases", in this report). Only in borehole KLX03 at 380 m depth were there relatively high methanogen numbers. The acetogens, a group of organisms that can live on hydrogen gas and organic one-carbon compounds and/or carbon dioxide, seem to create a background level of organic carbon in granitic groundwater /Pedersen 2001, Lin et al. 2005/. The source of energy for the formation of this background level of organic carbon can be either the sun in a surface system or radio- or thermocatalytically derived hydrogen gas in deep, subsurface systems /Lin et al. 2005/.

Groundwater chemistry is of course a combination of microbially mediated and chemical processes. The following are the reactions involved in determining the final sulphide concentration in groundwater; the reactions are categorised as either microbial or inorganic.

Microbial processes

As discussed above, one basic source of energy for microbial growth in granitic groundwater is hydrogen. In the Laxemar groundwater, acetogens are the group that uses hydrogen in producing acetate (Eq. 1-1). The acetate can then be used by anaerobic organisms, which in Laxemar consist of iron and manganese reducers in the shallow groundwater. Since manganese does not easily form sulphide compounds in groundwater, the focus here is on iron reduction (Eq. 1-2). In the deeper groundwaters, sulphate reducers use the acetate in their respiration, with or without hydrogen gas (Eq. 1-3). The sulphate reducers can also use other carbon sources in reducing sulphate (Eq. 1-4). One microbial sulphate reduction process has not been detected in the Laxemar-Simpevarp area, namely, anaerobic sulphate reduction with methane (Eq. 1-5).

AA: $H_2 + CO_2 \Rightarrow$ acetate (Eq. 1-1)

IRB: acetate + $Fe^{3+} \Rightarrow Fe^{2+} + CO_2$ (Eq. 1-2)

SRB: acetate + SO_4^{2-} (+ H_2) $\Rightarrow H_2S + CO_2$ (Eq. 1-3)

SRB: DOC + $SO_4^{2-} \Rightarrow H_2S + CO_2$ (Eq. 1-4)

AM + SRB: $CH_4 + SO_4^{2-} \Rightarrow H_2 + CO_2 + SO_4^{2-} \Rightarrow H_2S + CO_2$ (Eq. 1-5)

Inorganic processes (pH > 6.5)

The sulphide produced via Eqs. 1-3 and 1-4 will react with compounds in the groundwater environment. It can reduce ferric iron present in fracture-filling materials and in minerals, producing ferrous iron, elemental sulphur, and hydroxide ions (see Eq. 1-6). It can either precipitate or form colloids with ferrous ions, forming iron sulphide (Eq. 1-7). The iron sulphide can react with elemental sulphur to produce Fe_3S_4. The precipitation reactions all reduce the amount of soluble sulphide in the water, which explains the low sulphide levels in groundwater in Laxemar. It also explains the good correlation between sulphide and the iron sulphide ratio displayed in Figure 1-30. It is only in a groundwater environment containing small amounts of iron that the sulphide concentration can increase. This description does not include all sulphur species that can be present, for example, sulphite and thiosulphate.

$$H_2S + 2FeOOH \Rightarrow S^0 + 2Fe^{2+} + 4OH^- \quad \text{(Eq. 1-6)}$$

$$H_2S + Fe^{2+} \Rightarrow FeS + 2H^+ \quad \text{(Eq. 1-7)}$$

$$3FeS + 3S^0 \Rightarrow Fe_3S_4 + 2S^0 \Rightarrow 3FeS_2 \quad \text{(Eq. 1-8)}$$

1.14.2 Limitations of microbial processes

Nitrogen and phosphorous can be limiting in microbial systems that have unlimited supplies of energy. It had formerly been suggested that the subsurface environment should be limited by nutrients such as nitrogen and phosphorous. The subsurface environment is, however, an environment that is most likely limited in its energy supply, so it is unlikely for nutrients to limit microbial growth and/or metabolic activity. There are sources of both nitrogen and phosphorous in granitic groundwater, as discussed below.

Nitrogen

All living cells need reduced nitrogen with which to synthesize amino acids and the nitrogen bases of the nucleotides. The soluble sources of this are ammonium and nitrate, which are found in limited amounts in deep groundwater. Microorganisms have another option when it comes to incorporating nitrogen into the cell, namely, nitrogen fixation. This ability is widespread in microbial groundwater populations, so nitrogen availability will rarely limit growth.

Phosphorous

Microorganisms use phosphorous in the form of phosphate, which is found in low amounts soluble in groundwater. It has been demonstrated that microbes can weather phosphate from phosphate-rich minerals, such as apatite, in rock /Bennett et al. 2001/. Microorganisms also recycle the phosphate available in the microbial community through the succession of different populations.

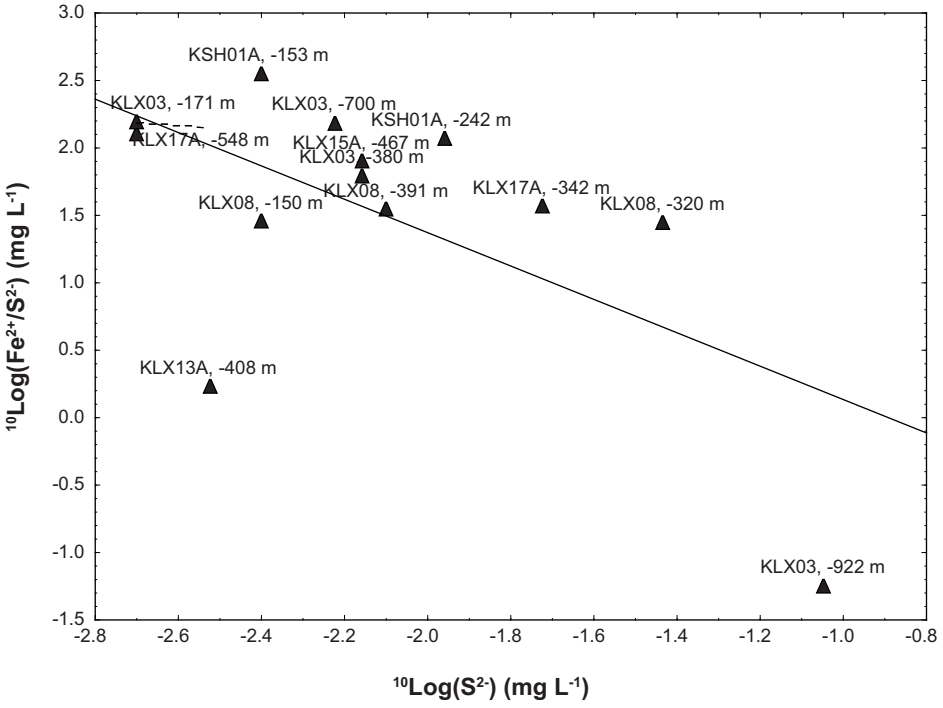

Figure 1-30. *The relationship between the concentration of sulphide and the Fe^{2+}/S^{2-} ratio. Statistics: $^{10}Log(Fe^{2+}/S^{2-}) = -1.1 - 1.2 \times {}^{10}Log(S^{2-})$, r = 0.9 , significant at p = 0.03, n = 12. Data from extended freeze 2.3 (November 30, 2007).*

1.15 Conclusions

- The data on total number of cells (TNC) were in the range of the cell numbers earlier found in other boreholes in other Fennoscandian shield groundwater sites.
- Measured ATP (energy carrier molecule) was significantly correlated with total number of cells and with the stacked most probable numbers (MPN) of different physiological groups of microorganisms. This indicates that MPN reflects the active population in groundwater, since ATP is only present in living cells.
- The results of fractionation filtration indicated that most of the organic material was smaller than 1,000 D in size and that only a minor part was in the > 5,000 D fraction.
- The relatively high numbers of IRB imply that they are important for the geochemistry in the Laxemar area. Since most IRB use partially oxidized organic matter, such as short-chain organic acids, as their sources of energy, electron, and carbon, they participate in the degradation of organic matter originating from the ground surface.
- A good correlation was found between IRB and MRB. These organisms can toggle between the electron acceptors ferric iron and manganese(IV) depending on availability. This correlation also attests to the stability and reproducibility between the different physiological MPN groups applied.
- The highest most probable numbers of microorganisms were found in the depth interval of 300–600 m.
- Acetogens were the dominant microorganisms in the sections studied; there were often one or two orders of magnitude more acetogens than the second most common organism type, which were iron- and/or sulphate-reducing bacteria. Acetogenic activity produces acetate, which is used by most physiological groups of microorganisms.
- The sulphide concentration in groundwater in Laxemar appears to be controlled by the presence of ferrous iron. The low observed values could also relate to heavy pumping before sampling.
- Cross correlations between the different cultivation and biomass results were generally good.
- The drill water residual (DWR) was not found to correlate with any of the included variables.
- The Eh as determined using the Chemmac electrodes was well correlated with the most probable number of sulphate-reducing bacteria; this is reasonable, because this group of microbes produces sulphide, which reacts with the electrodes used to measure Eh.

2 Colloids

2.1 Introduction

Particles in the size range from 1 to 1×10^{-3} µm are regarded as colloids /Stumm and Morgan 1996/. Their small size inhibits them from settling, which gives them the potential to transport radionuclides in groundwater. The aim of the study of colloids in the site investigation was to quantify and determine the composition of colloids in groundwater samples from the boreholes.

Radionuclides can sorb (adhere) to colloidal particles or be incorporated within them and be transported with them. It is therefore important to estimate the extent to which such colloids can occur or be formed in the groundwater and for what time periods these colloids can remain stable. A summary of the reasons for analysing colloids can be found in /SKB 2006b/ (section 5.9). In summary, SR-CAN concluded that "Radionuclides in the groundwater can occur sorbed on colloids, and that the possibility that a small fraction will be bound irreversibly to mobile natural colloidal particles cannot be entirely excluded. However, as long as dose calculations are dominated by weakly or non-sorbing radionuclides, the overall consequence of colloid enhanced transport for the safety of the repository is negligible". In any case, the presence and nature of colloids need to be investigated in a site investigation.

There are both inorganic and organic colloids, and the site investigation measured both types. Microorganisms must also be considered colloids, as there are many groundwater microorganisms ≤ 1 µm in size. The results of the organic colloid analyses are presented in Section 1 of this report, "Microbiology and microbial model". In addition, a recent study of groundwater in the Äspö tunnel has found a variety of viruses in the water; these are protein particles, approximately 200 nm in diameter, that infect microbial cells.

2.2 Methods

Details about the methods and procedures for each borehole can be found in the respective hydrogeochemical progress reports ("P reports", see www.skb.se/publications). Two different methods were used in analysing colloids. The first included filtering the groundwater through a series of connected filters in a closed system under pressurized argon. The final filters had pore sizes of 0.2 and 0.05 µm, and were installed after a 0.4-µm pre-filter. The samples from boreholes KLX13A, KLX15A, and KLX17A were filtered through a 2.0-µm filter before the 0.4-µm filter. The mineral composition of the colloids collected on the filters was determined using inductively coupled plasma spectroscopy (ICP), and the quantities of the analysed elements were recalculated in µg L^{-1} (ppb), taking account of the registered water flow (mL h^{-1}) through the filters and the filtration time. The elements analysed were calcium (Ca), iron (Fe), sulphur (S), manganese (Mn), aluminium (Al), and silicon (Si). The second method was fractionation using a defined cut-off membrane filter (i.e. of a particular pore size), concomitant with the analysis of organic colloids; two different filter pore sizes were used, 1,000 D and 5,000 D. The elements Fe, Si, Al, S, U, and Mg were reported to the Sicada database. The sample descriptions and colloid filtering data are compiled in Table 2-2.

Two other analysis methods were used for some samples during the last sampling campaign in Laxemar, namely, laser-induced breakdown colloid detection (LIBD) /Berg et al. 2006/ and colloid analysis by means of submicron filtration plus scanning electron microscopy and energy-dispersive spectroscopy (SEM/EDS) /Nilsson and Degueldre 2007/. The results of these investigations are presented in sections 2.9 and 2.10.

Table 2-1. Element analyses of the 0.05- and 0.2-µm colloid fractions and the 0.4-µm precipitation fraction from borehole KSH01A, Simpevarp subarea.

Colloid phase	Borehole and filter pore size								
	KSH01A, 161.75 m depth Filter pore size (µm)			KSH01A, 253.3 m depth Filter pore size (µm)			KSH01A, 556.5 m depth Filter pore size (µm)		
	0.05	0.2	0.4	0.05	0.2	0.4	0.05	0.2	0.4
Colloid phase (µg L⁻¹)									
Ca as calcite, $CaCO_3$	267.2	199.2	244.75	385.2	d.m.[2]	262.6	448.5	436.2	703
Fe as $Fe(OH)_3$	3.82	8.02	389.5	0.764	d.m.	150.2	3.44	5.73	10.7
S as sulphur	b.d.[1]	b.d.	1.4	16.4	d.m.	5.2	7.8	7.7	15.6
Mn as $Mn(OH)_2$	0.168	0.162	1.70	0.162	d.m.	1.05	0	0	0.162
Al as K-Mg-illite clay: $K_{0.6}Mg_{0.25}Al_{2.3}Si_{3.5}O_{10}(OH)_2$	3.09	3.71	92.7	2.47	d.m.	82.2	1.236	2.47	4.9
Si as SiO_2	b.d.	b.d.	b.d.	b.d.	d.m.	26.6	b.d.	b.d.	18.08
Total (ppb, µg L^{-1})	274.3	211.1	730.0	405.0	–	527.8	461.0	452.1	752.4
Total, omitting calcite	7.08	11.9	485.3	19.8	–	265.25	12.5	15.9	49.4
Total, omitting calcite and sulphur	7.08	11.9	483.9	3.4	–	260.0	4.7	8.2	33.8

[1] b.d. = below detection limit; [2] d.m. = data missing due to broken filter.

Table 2-2a. Element analyses of the 0.05- and 0.2-µm colloid fractions and the 0.4-µm precipitation fraction from borehole KLX03, Laxemar subarea.

Colloid phase	Borehole and filter pore size											
	KLX03, 171 m Filter pore size (µm)			KLX03, 380 m Filter pore size (µm)			KLX03, 700 m Filter pore size (µm)			KLX03, 922 m* Filter pore size (µm)		
	0.05	**0.2**	**0.4**	**0.05**	**0.2**	**0.4**	**0.05**	**0.2**	**0.4**	**0.05**	**0.2**	**0.4**
Colloid phase (µg L⁻¹)												
Ca as calcite, $CaCO_3$	b.d.[1]	b.d.	b.d.	b.d.	b.d.	b.d.	b.d.	b.d.	b.d.	1,529	147.3	926.1
Fe as $Fe(OH)_3$	10.7	16.8	9.45	0.9	1.0	11.95	1.05	3.3	3.1	1.2	2.7	4.4
S as sulphur	b.d.	b.d.	b.d.	b.d.	b.d.	b.d.	b.d.	b.d.	b.d.	35.8	b.d.	16.2
Mn as $Mn(OH)_2$	b.d.	b.d.	b.d.	b.d.	b.d.	0.2	b.d.	b.d.	b.d.	b.d.	b.d.	b.d.
Al as K-Mg-illite clay: $K_{0.6}Mg_{0.25}Al_{2.3}Si_{3.5}O_{10}(OH)_2$	0.5	1.3	2.2	0.3	0.4	13.3	0.3	0.4	0.7	0.95	1.9	2.7
Si as SiO_2	b.d.	b.d.	b.d.	b.d.	b.d.	b.d.	37.4	b.d.	b.d.	35.6	b.d.	b.d.
Total (ppb, µg L^{-1})	11.2	18.1	11.6	1.2	1.4	25.2	1.35	3.7	10.1	1,567	152	981.2
Total, omitting calcite	11.2	18.1	11.6	1.2	1.4	25.2	1.35	3.7	10.1	38	4.7	52.1
Total, omitting calcite and sulphur	11.2	18.1	11.6	1.2	1.4	25.2	1.35	3.7	10.1	2.2	4.7	35.9

* Pressure was increased during filtration; [1] b.d. = below detection limit.

Table 2-2b. Element analyses of the 0.05- and 0.2-µm colloid fractions and the 0.4-µm precipitation fraction from borehole KLX08, Laxemar subarea.

Colloid phase	Borehole and filter pore size								
	KLX08, 320 m Filter pore size (µm)			KLX08, 390 m Filter pore size (µm)			KLX08, 504 m Filter pore size (µm)		
	0.05	0.2	0.4	0.05	0.2	0.4	0.05	0.2	0.4
Colloid phase (µg L^{-1})									
Ca as calcite, $CaCO_3$	0	0	0	0	0	0	0	0	0
Fe as $Fe(OH)_3$	7.6	8.8	7.6	6.8	3.6	18.4	0.15	0.10	0.15
S as sulphur	0	0	0	0	0	0	0	0	0
Mn as $Mn(OH)_2$	0	0	0.05	0	0	0	0	0	0
Al as K-Mg-illite clay: $K_{0.6}Mg_{0.25}Al_{2.3}Si_{3.5}O_{10}(OH)_2$	0	28.2	20.8	3.8	1.7	12.8	0	0.8	5.4
Si as SiO_2	0	0	0	0	0	0	0	0	0
Total (ppb, µg L^{-1})	7.6	37.6	28.4	7.6	5.3	31.2	0.15	0.9	5.6
Total, omitting calcite	7.6	37.6	28.4	7.6	5.3	31.2	0.15	0.9	5.6
Total, omitting calcite and sulphur	7.6	37.6	28.4	7.6	5.3	31.2	0.15	0.9	5.6

Table 2-2c. Element analyses of the 0.05- and 0.2-µm colloid fractions and the 0.4-µm precipitation fraction from Laxemar subarea.

Colloid phase	Borehole and filter pore size								
	KLX13A, 408 m Filter pore size (µm)			KLX15A, 467 m Filter pore size (µm)			KLX17A, 342 m Filter pore size (µm)		
	0.05	0.2	0.4	0.05	0.2	0.4	0.05	0.2	0.4
Pore size (µm)	0.05	0.2	0.4	0.05	0.2	0.4	0.05	0.2	0.4
Chloride (mg L^{-1})	744	744	744	5,890	5,890	5,890	18	18	18
Iron (mg L^{-1})	< 0.006	< 0.006	< 0.006	0.5	0.5	0.5	1.0	1.0	1.0
Colloid phase (µg L^{-1})									
Ca as calcite, $CaCO_3$	b.d.[1]	b.d.	b.d.	190	640	b.d.	b.d.	b.d.	b.d.
Fe as $Fe(OH)_3$	0.05	3.8	10	2.5	2.7	2.0	22	30.3	n.a.
S as sulphur	b.d.	b.d.	b.d.	74	111	47	b.d.	b.d.	b.d.
Mn as $Mn(OH)_2$	b.d.	b.d.	b.d.	0.12	0.34	b.d.	0.1.	0.26.	b.d.
Al as K-Mg-illite clay: $K_{0.6}Mg_{0.25}Al_{2.3}Si_{3.5}O_{10}(OH)_2$	1.0	2.6.	36	0.3	0.4	13.3	0.3	0.4	0.7
Si as SiO_2	b.d.	b.d.	38.5.	2,541	2,699	2,817	37.4	b.d.	b.d.
Total (ppb, µg L^{-1})	1.05	6.4	84.5	2,808	3,453	2,879	59.8	31	< 0.7
Total, omitting calcite	1.05	6.4	84.5	2,618	2,813	2,879	59.8	31	< 0.7
Total, omitting calcite and sulphur	1.05	6.4	84.5	2,544	2,702	2,832	59.8	31	< 0.7

2.3 Databases

The colloid filtration and colloid fractionation data in the Sicada database were compiled by Maria Gimeno and distributed to the author via the Chemnet website. The LIBD and SEM/EDS data were taken from unpublished reports provided by the Laxemar-Simpevarp site investigation staff.

2.4 Evaluation of colloid data obtained using the filtration method

When evaluating the primary data, we excluded from the analyses data obtained using colloid filtration for borehole KLX15A, 467 m depth, because they were extremely likely due to debris from drilling, since the silicon and sulphur values are extremely high. The LIBD data display the same pattern (see section 2.9) but the fractionation data do not. On the other hand, using the LIBD method on the sample from borehole KLX17A, 548 m depth, indicated too many particles. The groundwater from this section was also analyzed by fractionation, which indicated a high aluminium content, but no filtration had been done. The high numbers of colloids found in this sample were also most likely due to sampling artefacts. All other available data were used in the evaluation.

/Laaksoharju et al. 1995/ calculated calcium values as calcite and sulphur values as pyrite and subtracted both from the total amount of colloids. Here, the calcite values were subtracted from the total amount of colloids. The sulphur values, however, were not recalculated as pyrite because the presence of this compound could not be confirmed. Sulphur was therefore represented as given in Sicada without recalculation to any mineral phase. Calcium and sulphur colloids are commonly regarded as pressure drop related, and their actual concentrations in the sampled groundwater cannot be safely inferred from the data.

2.4.1 Colloids versus depth

In evaluating the background levels of colloids in groundwater, colloid concentration versus depth was examined. It can be seen in Figure 2-1 that the colloid concentration was highest at a depth of 320 m in borehole KLX08 and 342 m in KLX17A at 45 and 90 µg L^{-1}, respectively. The shallowest depth, i.e. 153 m in KSH01A, had a colloid concentration of 19 µg L^{-1}. The average colloid concentration found in this study was 23.6 SD ± 26.8 µg L^{-1}, a finding in agreement with the results of studies of colloids in crystalline rock in Switzerland (30 ± 10 and 10 ± 5 µg L^{-1}) /Degueldre et al. 1996/ and Canada (300 ± 300 µg L^{-1}) /Vilks et al. 1991/ that used the same approach as was used here.

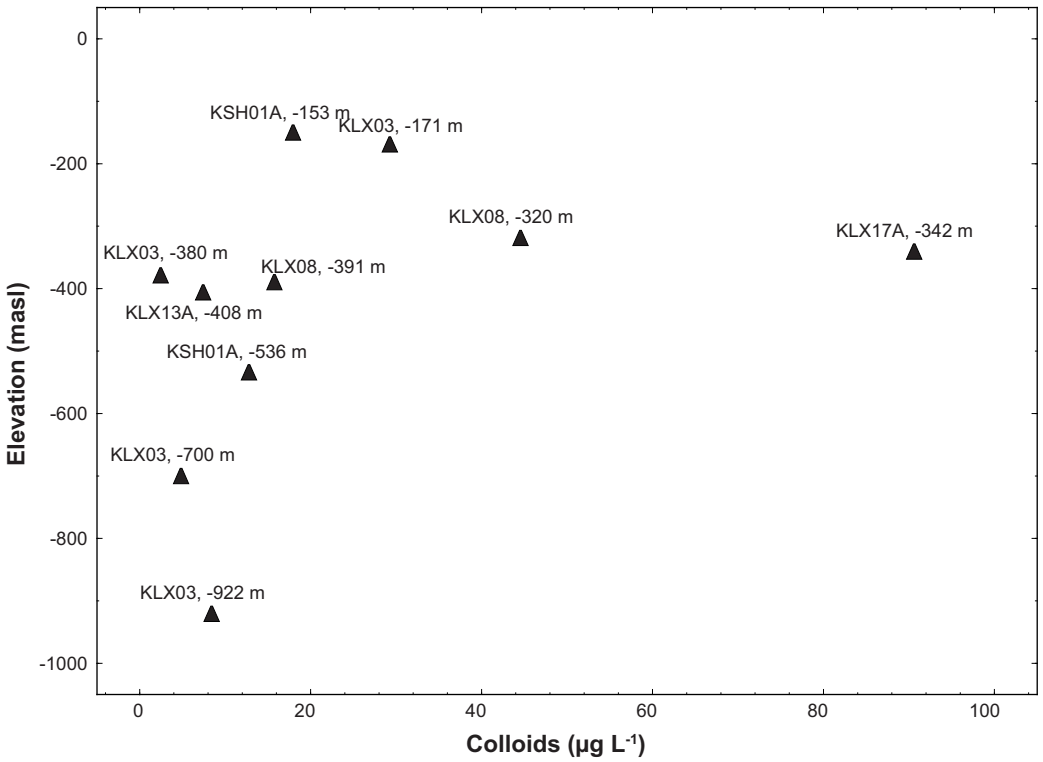

Figure 2-1. *Colloid concentration (µg L^{-1}) versus depth in the Laxemar–Simpevarp area. Data from data freeze 2.3. Data from KLX15A, –467 m, are excluded (see text).*

2.5 Colloids and chloride

Figure 2-2 shows the amount of colloids versus chloride. In groundwater with a high chloride concentration the amount of colloids usually decreases, because the higher ion strength increases the precipitation of various solid particles. The chloride concentrations in this dataset ranged from 18 to 10,500 mg L^{-1}. The highest amount of colloids was found in borehole KLX17A at a depth of 342 m, where the chloride concentration was 576 mg L^{-1}; the lowest amounts were found in borehole KLX03 at 380 m depth.

2.6 Colloids and iron

High ferric iron concentrations in groundwater force the precipitation of other compounds due to the ability of iron to co-precipitate, producing larger particles; thus, the amount of colloids should decrease with increasing iron concentration. Figure 2-3 shows colloid concentration versus iron content in groundwater in Laxemar. The data correspond relatively well with the theory, although with some exceptions. The sample from a depth of 342 m in borehole KLX17A contained especially high amounts of both colloids and iron. The iron data capture total iron, and in deep groundwater most of the iron is ferrous. Many of the samples from the Laxemar-Simpevarp area contained an iron colloid fraction (Figure 2-4), in particular, the larger 0.2-µm fraction.

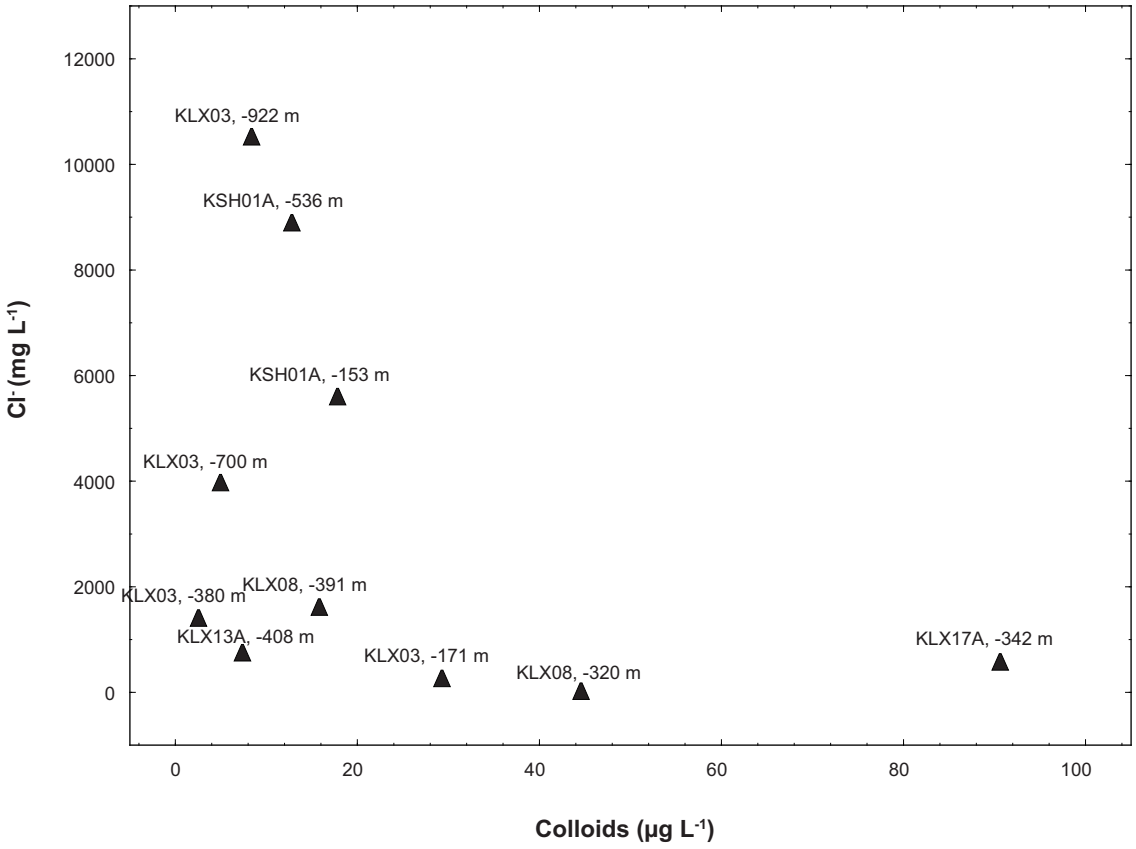

Figure 2-2. *Colloid concentration (µg L^{-1}) versus amount of chloride in the groundwater in the Laxemar–Simpevarp area. Data from extended data freeze 2.3 (November 30, 2007).*

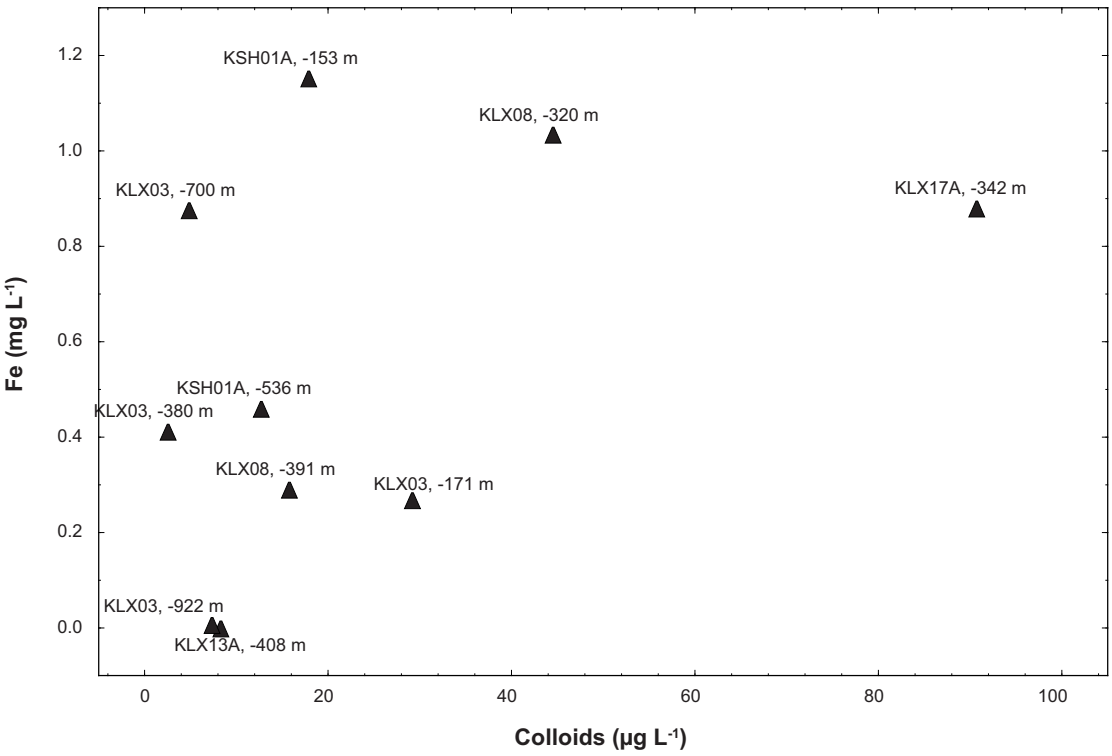

Figure 2-3. *Colloid concentration (µg L^{-1}) versus iron concentration in the groundwater in the Laxemar–Simpevarp area. Data from extended data freeze 2.3 (November 30, 2007).*

2.7 Composition of colloids: size distribution

To understand the size distributions of the various colloidal minerals, the stacked amounts of these minerals were plotted for the two pore sizes, 0.05 and 0.2 µm (Figure 2-4, a and b). The data were obtained using the colloid filtration method. In this figure it can be seen that in the smallest fraction, the 0.05-µm fraction, most of the colloids were either sulphur or iron. Some samples had high values for silicon, which probably comprises debris from the drilling. The silicon could have come from natural clay fracture contents, but the large amount of silicon suggests that it more likely came from the drilling. The larger fraction consisted mostly of iron and aluminium. The question that arises is whether these were "real" colloids or simply sampling artefacts (i.e. sulphur colloids formed because of pressure release and iron colloids because of oxidation). The filtration method indicated higher amounts of colloids than did the fractionation method, as can be seen in next section.

2.8 Inorganic colloids: fractionation

Fractionation filtration was performed on groundwater sampled from 11 sections of five boreholes (Table 2-3); when using this method, the 1,000–5,000 D fraction was considered the colloid fraction.

Measurable amounts of colloids were obtained in 6 of 11 samples. Of these, boreholes KLX03 at 171 m depth, KLX08 at 320 m, and KLX17A at 342 m are the ones that also were sampled using the filtration method. In groundwater from KLX03 at 171 m dept, both methods indicated iron content. The fractionation sample from KLX08, 320 m, had a high aluminium content, which was found also in the 0.2-µm filtration sample. The fraction sample from KLX17A at 342 m depth, had an extremely high sulphur content, which was not found in the filtration samples. The filtration results indicated high amounts of iron and silicon.

This comparison of the results of the filtration and fractionation methods indicates that they produced very different results. To compare these methods more thoroughly, a well-designed experiment is needed in which the samples are taken at the same time and from the same groundwater.

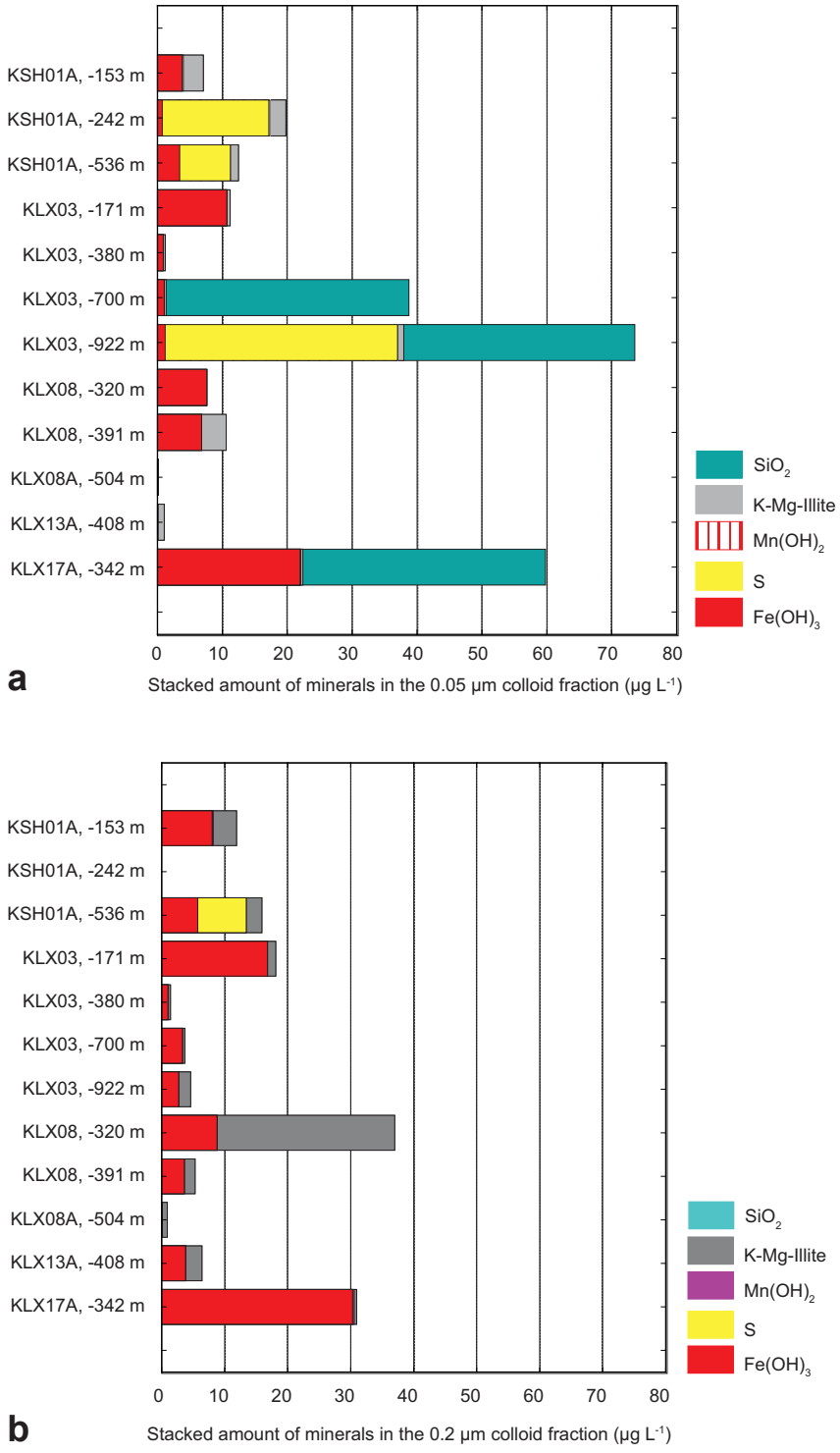

Figure 2-4. *Colloid composition in groundwater in Laxemar–Simpevarp area. Stacked amounts of minerals in two colloid fractions from colloid filtrations: a) colloids ≤ 0.05 µm and b) colloids ≤ 0.2 µm.*

Table 2-3. Boreholes and section depths from which colloid fractionation samples were taken in Simpevarp and Laxemar.

Borehole and depth section	Al as K-Mg-Illite clay: $K_{0.6}Mg_{0.25}Al_{2.3}Si_{3.5}O_{10}(OH)_2$ (μg L^{-1})	Ca as calcite $CaCO_3$ (μg L^{-1})	Fe as $Fe(OH)_3$ (μg L^{-1})	Mn as $Mn(OH)_2$ (μg L^{-1})	Si as SiO_2 (μg L^{-1})	S as sulphur (μg L^{-1})
KSH01A, 153 m	n.d	n.d	n.d	n.d	n.d	n.d
KSH01A, 536 m	n.d	n.d	n.d	n.d	n.d	n.d
KLX03, 171 m	n.d	**3.7**	**0.2**	**5.0**	n.d	n.d
KLX03, 380 m	n.d	n.d	n.d	n.d	n.d	n.d
KLX03, 504 m	n.d	n.d	n.d	n.d	n.d	n.d
KLX08, 150 m	**6.6**	**1.5**	**0.02**	n.d	n.d	n.d
KLX08, 320 m	**21.6**	n.d	n.d	n.d	n.d	n.d
KLX08, 391 m	n.d	n.d	n.d	n.d	n.d	n.d
KLX15A, 467 m	n.d	n.d	n.d	n.d	n.d	**5.2**
KLX17A, 342 m	n.d	n.d	n.d	n.d	n.d	**600**
KLX17A, 548 m	**8.3**	n.d	n.d	n.d	n.d	n.d

2.9 Laser-induced breakdown colloid detection

Laser-induced breakdown colloid detection (LIBD) was used to analyse groundwater samples from boreholes KLX13A, KLX15A, and KLX17A in Laxemar. The sampling procedure and method is described in the progress report ("P-report", see www.skb.se/publications) on borehole KFM06A as part of the Forsmark site investigation /Berg et al. 2006/. Table 2-4 presents the most important results. In the samples from boreholes KLX13A and KLX15A, it was possible to distinguish two main average colloid fractions from the measurement results. One fraction had colloids with average diameters of 60–110 nm and the second fraction average diameters of 1,100 to 1,400 nm. The results represent the means of several measurements and are presented together with the standard deviation, ± SD.

The smaller fraction (60–110 nm) contained 2.3×10^6 particles per millilitre and the larger (1,100–1,400 nm) between 1.2×10^6 and 9.3×10^6 particles per millilitre (see Table 2-4). The second fraction contained more than 99% of the total particle mass, whereas the total colloid

Table 2-4. Results of LIBD analyses of groundwater samples from Laxemar. Data from data freeze 2.3.

Borehole and depth section	Number of colloids, 60–110-nm fraction (mL^{-1})	Number of colloids, 1,100–1,400-nm fraction (mL^{-1})	Colloid mass concentration, 60–110-nm fraction (μg L^{-1})	Colloid mass concentration, 1,100–1,400-nm fraction (μg L^{-1})
KLX13A, 408 m				
SKB PVB 203, *n* = 5	$3.7 \times 10^6 \pm 2.1 \times 10^6$	$3.3 \times 10^5 \pm 5.8 \times 10^5$	10.4 ± 16.6	999 ± 265
SKB PVB 025, *n* = 3	$2.3 \times 10^6 \pm 1.1 \times 10^6$	$9.3 \times 10^5 \pm 7.3 \times 10^5$	2.0 ± 0	565 ± 107
KFM15A, 467 m				
SKB PVB 220*, *n* = 5	$4.3 \times 10^6 \pm 4.0 \times 10^6$	$1.2 \times 10^5 \pm 2.7 \times 10^4$	2.16 ± 2.1	780 ± 113
SKB PVB 9506-6, *n* = 5	$7.9 \times 10^6 \pm 1.0 \times 10^7$	$1.2 \times 10^5 \pm 5.5 \times 10^3$	61.8 ± 62.6	566 ± 90.3
KLX17A, 342 m				
SKB PVB 024, one fraction only	$2.6 \times 10^6 \pm 4.5 \times 10^5$	–	208 ± 93	–
SKB PVB 9506-4, one fraction only	$2.8 \times 10^6 \pm 5.6 \times 10^5$	–	108 ±20	–
KLX17A, 548 m	**	**	**	**

* PVB sampler number; ** Too many colloids for LIBD to function properly.

number density is determined by the smaller fraction. The mean size of the colloid particles in the smaller fraction from boreholes KLX13A and KLX15A was 92 ± SD 80 nm. The sample from KLX17A had a mean size of 355 ± SD 75 nm. These high values possibly come from some kind of sampling artefact, as the SEM images of the same sample suggest that the large particles were agglomerates of small colloids. EDX (energy-dispersive X-ray spectroscopy) analyses indicated that the colloids mostly consisted of aluminium, silica, iron, and calcium.

2.10 Colloid analyses by means of micro-filtration plus scanning electron microscopy and energy-dispersive spectroscopy

One sample from a depth of 391 m in borehole KLX17A was examined using micro-filtration plus scanning electron microscopy and energy-dispersive spectroscopy (SEM/EDS). The sampling, analysis, and data handling are described by /Nilsson et al. 2008/. The colloid concentration was determined to be approximately 40 µg L^{-1} for colloid sizes of 50–200 nm, while the number of colloids in the same size range was approximately 47×10^9 mL^{-1}. Most of the colloids (39×10^9) were smaller than 50 nm. The colloids were assumed to be clay, based on the chemical composition of those with an average size of less than 200 nm. No measurements of the mass of separate elements were made in this investigation, so the contribution of the different elements to the total mass of colloids is unknown. Another explanation could be that most of the material is debris from the drilling, as discussed in section 2.7.

2.11 Microbes and viruses as possible colloids

Microorganisms vary considerably in size. In groundwater, many of them are $\leq 10^{-3}$ mm and should be considered colloids /Laaksoharju and Wold 2005/. In addition, many microorganisms have negatively charged groups, such as hydroxyl and carboxyl groups, on their surfaces; this allows positively charged ions and compounds in groundwater to bind easily to free-living microbes.

A recent study of groundwater in the Äspö HRL tunnel has revealed the presence of many different types of microbial viruses /Kyle et al. 2008/. Figure 2-5 shows some of the different types of viruses found in the Äspö groundwater; on average, the viruses were approximately 200 nm in diameter.

The study has also found approximately ten times more viruses than microbial cells in groundwater in the Äspö HRL tunnel (see Figure 2-6), the same as the ratio between colloids and cells in Laxemar. There was a strong negative correlation between salinity and the number of viruses, similar to that between colloids and salinity. The finding of viruses in groundwater suggests a possible biological origin for a fraction of the colloids.

2.12 Conclusions

- The apparent mass concentration of the colloids differs considerably depending on the detection method used: the highest values were obtained using the filtration method, while fractionation gave very low values. However, filtration values are in the same order of magnitude as the LIBD values, and most of the samples were found to contain below 100 µg L^{-1} of colloids.
- The number of colloids found in Laxemar-Simpevarp groundwater was in the order of 10^6 mL^{-1}.
- The filtration and fractionation method indicated that the colloids were composed mostly of iron and sulphur. LIBD with EDX, on the other hand, indicated that the colloids were composed mostly of aluminium, silica, and iron.
- Some samples were probably heavily contaminated with drilling debris.
- Viruses have been found in groundwater in the Äspö HRL tunnel, in numbers close to the measured numbers of colloids. This, together with the fact that microbes are present in numbers close to the numbers of colloids, indicates that many of the colloids are probably of biological origin. The presence of viruses in groundwater in Laxemar needs to be investigated.

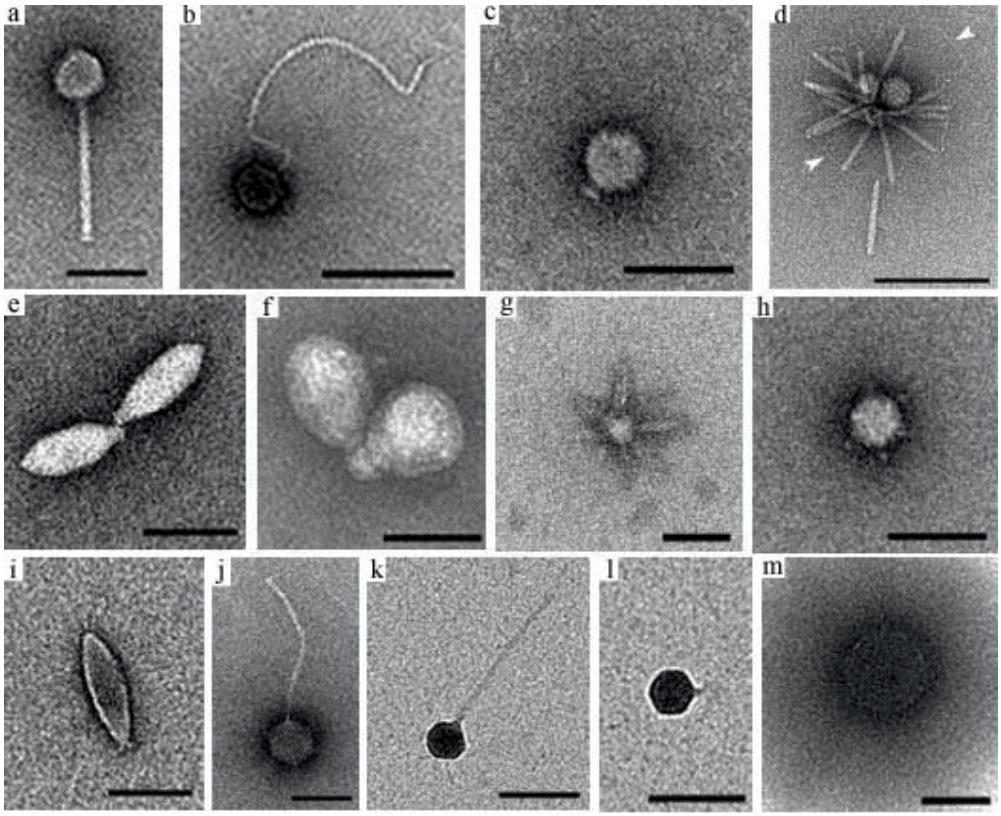

Figure 2-5. *Transmission electron micrographs of viruses from Äspö groundwater. Scale bar indicates 125 nm, except in a and d where it indicates 250 nm.*

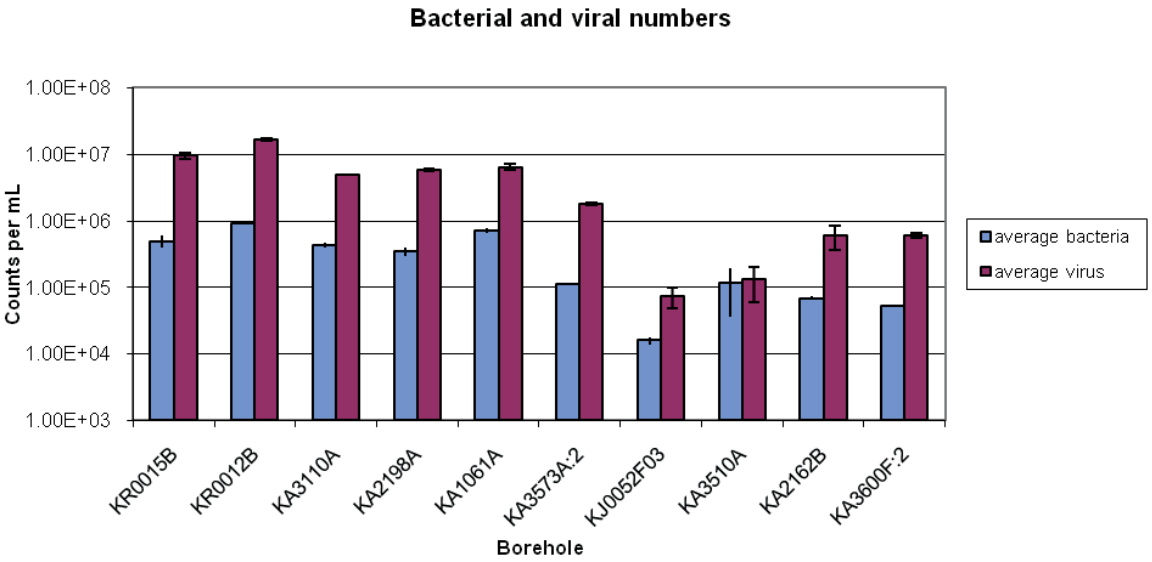

Figure 2-6. *Numbers of microbial cells and viruses in Äspö groundwater.*

3 Gases

3.1 Introduction

Dissolved gases in groundwater contribute to the mass of dissolved species. The gases can be defined as chemically active or inactive. Biological processes are included in the term "chemically active". Chemically active species are oxygen, hydrogen sulphide (with its anionic dissociation products, HS^- and S^{2-}), carbon dioxide (with carbonic acid and its anionic dissociation products, HCO_3^- and CO_3^{2-}), methane, and hydrogen. Chemically inactive, inert gases are the noble gases and, to some extent, nitrogen. Nitrogen fixation and denitrification by microorganisms may possibly influence the pool of nitrogen gas in groundwater, making nitrogen a gas difficult to define as purely (bio)chemically active or inactive. Finally gases such as ethane and propane and their reduced forms can be found in deep groundwater.

The distribution and composition of dissolved gases in deep groundwater must be understood when assessing the safety of a deep geological nuclear waste repository, for the following main reasons:

- Microbubbles of gas may potentially transport radionuclides from the repository to the surface. This would be important in cases in which the total amount of dissolved gas approaches the saturation limit in groundwater.
- The chemically active gases oxygen, hydrogen, sulphide, and carbon dioxide are parts of fundamental redox couples that participate in several solid–aqueous phase transformations, such as the precipitation of ferric iron oxides, iron sulphide, and calcite. Without information on these gases, the redox system at a site cannot be fully understood.
- The (bio)chemically active gases methane and hydrogen may serve as sources of energy for various microbiological processes as well as being produced by microbial processes.
- The chemically inert noble gases can function as conservative tracers in evaluating groundwater systems.

The above items are briefly reviewed below.

3.1.1 Observations of gas in Fennoscandian Shield groundwater

Earlier studies of groundwater in the Fennoscandian Shield have reported high amounts of dissolved gases at some locations. The upwelling of large volumes of gas through major fault zones has been reported from the Åland Sea, northern Baltic Proper /Söderberg 1993/. The groundwater of Olkiluoto contains more than 1,000 mL of dissolved gases L^{-1} when the depth approaches 800 m /Pitkänen and Partameis 2007/. In general, western Finland groundwater contains high volumes, i.e. 100–500 mL of dissolved gases L^{-1}, over a depth range of 100–500 m /Pedersen 2001, Sherwood Lollar et al. 1993a/. Groundwater in the Äspö HRL contains smaller volumes, typically 20–60 mL dissolved gases L^{-1}; however, this dataset is still somewhat limited /Pedersen 2001, 2005ab/.

3.1.2 Microbubbles of gas

The occurrence of gas bubbles small enough to travel upwards in fractured rock has been proposed /Goodfield and Rodwell 1998/. It was suggested that the gas/water interface of such bubbles can adsorb particles of various types in the groundwater. Radionuclides can attach to colloids, such as dispersed bentonite. If colloid–radionuclide particles sorb in the gas/water interface of microbubbles in groundwater, rapid upwards transport may occur, as has been suggested for various trace metals /Malmqvist and Kristiansson 1984/. The bubbles could move rapidly upwards in the groundwater and can cause dispersion of radionuclides over large areas. The mechanisms

of origin of gas bubbles can be several. During the transport of groundwater to the surface, the pressure decreases and the solubility of the various gases contained in the water also decreases; if the pressure decreases, perhaps due to a tectonic event, gas bubbles may form /Goodfield and Rodwell 1998/. Therefore, it is important to analyse the total amount of gas in groundwater. Groundwater containing total amounts of dissolved gas approaching saturation will be prone to gas bubble formation with even a small pressure drop. When gas is produced in the repository by the anaerobic corrosion of metals, the total volume of background groundwater gas and corrosion gases will indicate when bubbles may form. In addition, it has been suggested that alpha particles generated by radioactive decay, mainly of uranium and thorium, could induce bubble formation at depth /Goodfield and Rodwell 1998/. In a site investigation, it is therefore very important to evaluate the presence of gas in groundwater and include these data in hydro-geochemical models. A special case may occur if migrating radionuclides reach a major fault with upwelling gas of the types described by /Söderberg 1993, Söderberg and Flodén 1991, Flodén and Söderberg 1994/. Microbubble gas transport of radionuclides could then occur in the fault, as depicted in Figure 3-1.

3.1.3 Biochemically active gases

Some gases are involved in microbiological reactions, for example, methane, carbon dioxide, and hydrogen. Methane is produced by methanogens in reduced environments and can be used as a substrate by methanotrophic bacteria. Carbon dioxide is used as a carbon source and terminal electron acceptor by autotrophic organisms and is the end product of the microbial degradation of organic carbon compounds. Consortia of methanogens and sulphate-reducing bacteria can oxidise methane anaerobically /e.g. Boetius et al. 2000/. Hydrogen is used as an energy and electron source by methanogens, acetogens, and other autotrophic microorganisms, such as sulphate reducers. It is also one of the end products of microbiological fermentation.

Analysis of stable isotopes can indicate whether gases such as methane are of biogenic or non-biogenic origin /Sherwood Lollar 1993ab/. Analyses of stable isotopes were, however, not performed in the Laxemar-Simpevarp site investigations.

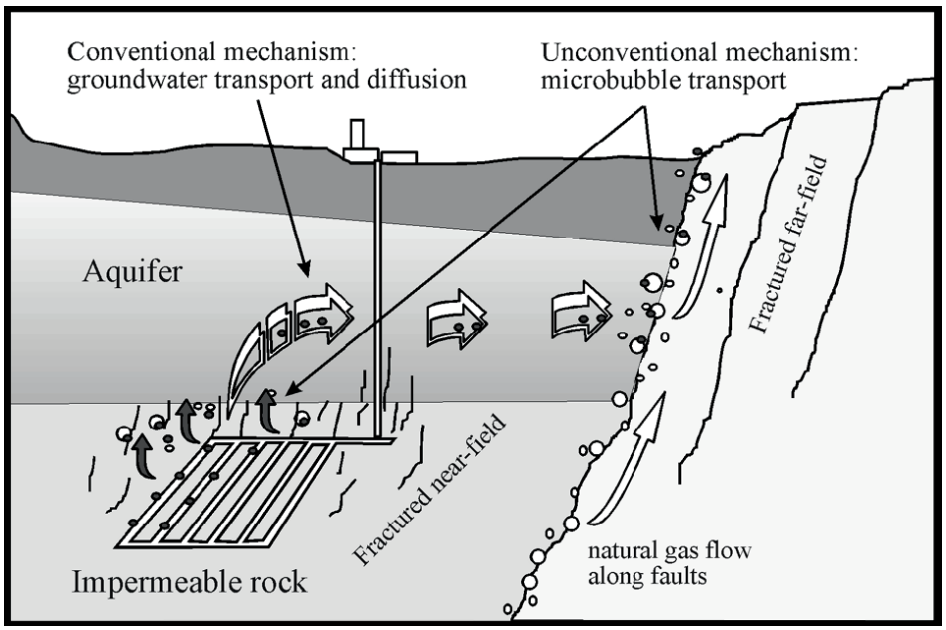

Figure 3-1. *Sketch of a possible layout of a nuclear waste repository and radionuclide migration. Currently available migration models are based on groundwater transport and diffusion. However, evidence indicates the possibility of faster nuclide transport by gas microbubbles, generated in the repository itself (near field) or naturally occurring in water-conducting faults (far field) image and text from /Etiope 1998/.*

3.1.4 Origin of gases, tracer properties

Gases in groundwater are of various origins, and gas is found in many Fennoscandian Shield groundwaters in concentrations too high to be explained by equilibria with air, implying a source from deeper in the Earth. Gases trapped in the mantle during the accretion of the planets are continuously being released /Apps and van de Kamp 1993/. Because it is so light, He leaves the atmosphere, while other, heavier gases remain longer. Nitrogen, hydrogen, helium, and carbon dioxide are continuously released from the mantle and migrate from the upper mantle to the crust, and finally to the atmosphere.

3.2 Available gas data

During the investigation of the Laxemar-Simpevarp area, up to 12 gases were analysed making up the data available in data freeze Laxemar 2.3. They were helium, argon, nitrogen, carbon dioxide, methane, carbon monoxide, oxygen, hydrogen, ethyne, ethene, ethane, and propane. The gas contents were analysed in groundwater from 14 depths of six boreholes, KSH01A, KLX03, KLX08, KLX13A, KLX15A, and KLX17A. Table 3-1 presents a summary of the boreholes, depth intervals, and available data for this report.

3.3 Data quality

The gas sampling and analysis procedures are described in SKB internal documents. According to the laboratory that performed the analyses (Paavo Ristola OY, Ramboll Finlandia), the precision of the method is 20%. The gas was sampled using the PVB sampler. This vessel has a piston that separates the groundwater sample from a lower compartment filled with argon or nitrogen gas (in Laxemar, only nitrogen gas has been used). This gas will balance the pressure of the groundwater when sampled, which reduces large shifts in pressure in the sample that would result in degassing. There have occasionally been some problems with leakage of pressure gas into the sample, which elevates the nitrogen concentration in the sample. This effect is difficult to track. One possibility is to take two samples using two samplers, one containing nitrogen and one argon in the lower compartment. This was done twice in the Forsmark Site investigation and in both cases an inverse relationship between argon and nitrogen was observed (Table 3-2). Argon was elevated in the sampler containing argon as the pressure gas relative to the sampler containing nitrogen, and vice versa when nitrogen was used. This contamination effect becomes almost impossible to compensate for in calculating gas concentrations unless two samples are taken every time (not done here), because the degree of contamination for one of the two gases will remain unknown. The best possible way, presently, is to judge a sample result in relation to several other results for samples from similar depths. A large discrepancy between a particular sample result and the average result for samples from the same depth region indicates a sampling artefact. As a result of this, all other gases in these potentially contaminated samples were diluted, so the results underestimate the actual values of all other gases. Stable isotope data concerning nitrogen (and the other gases) would have helped to confirm or reject whether nitrogen contamination from the pressure vessel was a problem.

During the extraction process, there were problems with air entering the sample, which was detected as the presence of oxygen. Data reported in Sicada are not corrected for this air leakage into the samples; the data used in this report, however, are corrected for such leakage using the dissolved content of oxygen as an indicator. The oxygen could originate either from the sampling vessel or from gas extraction and analysis in the laboratory. As deep groundwater generally contains ferrous iron and sometimes sulphide, oxygen should not be present, because these two ions are not stable in oxygenated water.

Table 3-1. Boreholes, sample ID, depth, sampling date, and gas volume and composition available in SICADA for analysis in the Laxemar model, version 2.3 SDM-Site Laxemar. All volumes are at a standard temperature (20°C) and pressure (1 atmosphere).

Borehole	ID no.	Depth, secmid (m)	Sampling date	(mL L^{-1})						(µL L^{-1})						
				Total gas	N_2	CO_2	CH_4	Ar	He	H_2	CO	C_2H_2	C_2H_4	C_2H_6	C_3H_6	C_3H_8
KSH01A	5263	–153	2003-04-22	80	75.5	0.79	0.06	1.28	2.2	0	–4.2	0.1	0.23	1	0	1.4
KSH01A	5269	–242	2003-04-24	107	104	0.8	0.09	1.1	1.5	85	–11	0	0.93	0.88	0	2.5
KSH01A	5288	–536	2003-09-15	76	67.2	0.08	0.04	1.4	7.5	81	–3.9	0.35	0.71	0.7	0	1.7
KLX03	7953	–171	2004-12-15	62	54	1.4	0.87	0.77	0.07	0	–3.1	0	0.17	0.08	0	0
KLX03	10091	–380	2005-03-22	53	49	1.8	0.62	0.73	0.72	110		0	0.07	0.1	0	–0.05
KLX03	10242	–700	2005-04-25	66	60	0.38	0.21	0.89	3.8	190	–3.3	0	0.12	0.42	0.08	0.08
KLX03	10076	–922	2005-02-14	76	67	0.01	0.06	1	8.6	0		0.57	0.62	1.1	0.28	0.28
KLX08	11228	–504	2006-07-26	62	60	0.071	0.025	1.1	1.4	0	–3.1	0	0.16	0.31	0.07	0.08
KLX08	11183	–391	2006-06-26	63	61	0.13	0.029	0.83	1.2	46	–3.2	0	0.07	0.14	0	0
KLX13A	11609	–408	2007-01-17	90	87.8	0.75	0.015	0.52	0.159	0.5	0.93	0	0	0.07	0	0
KLX15A	15008	–467	2007-08-06	87	83	0.14	0.021	0.68	2.8	0	–4.3	0.33	0.83	0.73	0.36	0.29
KLX17A	11810	–342	2007-04-18	67	65	0.71	0.07	0.77	0.18	0	–3.3	0	0.21	0.28	0.07	0.07
KLX17A	11692	–548	2007-02-26	66	64.6	1.34	0.145	0.35		0.7	1.35	0	0	0.12	0	0

* Value is 0 or below detection limit.

Table 3-2. Ratios between nitrogen and argon in samples taken with nitrogen or argon in the PVB pressure compartment from /Laaksoharju 2008/.

Borehole	Depth, secmid (m)	Sampling date	N_2	Ar	N_2/Ar
KFM02A-N_2	503	2003-09-29	77	1.1	70
KFM02A-Ar	503	2003-09-29	63	4.9	12.9
KFM10A-N_2	328	2006-10-30	65	0.76	85.5
KFM10A-Ar	328	2006-10-30	59	7.9	7.5

3.4 Total gas volumes

Figure 3-2 shows the total volumes of gas in Laxemar groundwater samples; all volume values shown are at atmospheric pressure. There was no general trend towards an increasing amount of gas with depth, as found in groundwater from Forsmark see /Laaksoharju et al 2008b/. The smallest volume of gas was found in groundwater from borehole KLX03 at 380 m depth, which contained 53 mL L^{-1}. The largest volume of gas was found in groundwater from KSH01A at 242 m depth. This can be compared with the sample from the deepest section of KLX03 at a depth of 922 m, where the groundwater contained 76 mL L^{-1} of gas. The three samples from the Simpevarp subarea all contained larger volumes of gas than did the samples from the Laxemar subarea from the same depth interval. There are two exceptions to this, groundwater samples from KLX13A at 408 m depth and KLX15A at 536 m, both of which contained approximately 90 mL L^{-1} of gas. Examining the ratios between different gases indicated that the reason for this was probably leakage of nitrogen into the sample container, as discussed below.

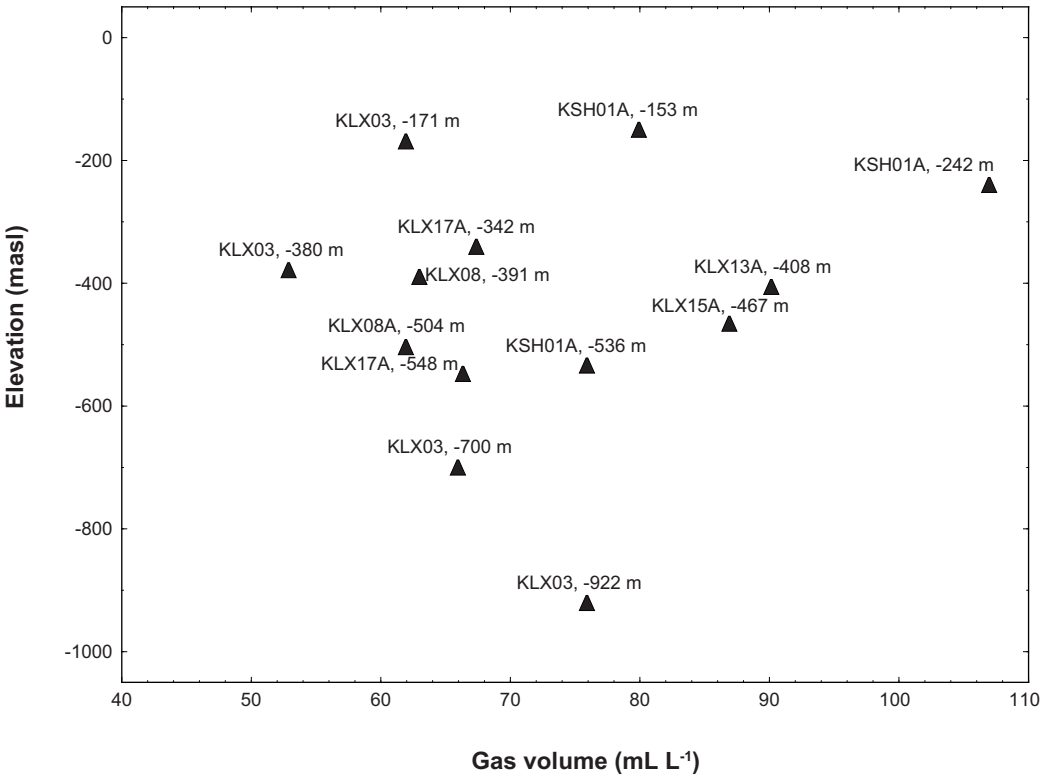

Figure 3-2. *The total volume of gas in groundwater from boreholes in Laxemar and Simpevarp. Data from extended data freeze 2.3 (November 30, 2007).*

3.4.1 Nitrogen

Figure 3-3 shows that the amount of nitrogen – the dominant gas in all samples of groundwater from the Laxemar-Simpevarp area – follows the trend of the total amount of gas, and increases with depth. This corresponds to the gas content in groundwater in Olkiluoto, Finland, which also displayed an increasing trend with depth down to 1,100 m /Pitkänen et al. 2004, Pitkänen and Partamies 2007/, and in Forsmark /Laaksoharju et al. 2008b/. The highest concentration of N_2 found in the Laxemar investigation was at a depth of 242 m in borehole KSH01A, where it reached 104 mL L^{-1} of groundwater, while the lowest was 49 mL L^{-1} at a depth of 380 m in borehole KLX03. Looking at Figure 3-3, it cannot be excluded that the samples from KLX13A, 408 m depth, and KLX15A, 467 m were contaminated with nitrogen from the PVB pressure compartment, as they contained approximately 20 mL more nitrogen L^{-1} than did other samples from the same depth. This is further supported by the discussion of the nitrogen/helium ratio in section 3.8 (see Figure 3-11).

The origin of nitrogen in groundwater is considered to be crustal degassing of the bedrock. It has earlier been suggested that the nitrogen gas in groundwater originates entirely from the atmosphere /Andrews et al. 1989; Pitkänen and Partemies 2007/. This assumption was made based on calculations of the N_2/Ar and $^{15}N/^{14}N$ ratios in the measured gas. The solubility of nitrogen gas in water at atmospheric pressure at 10°C is 0.024 g kg^{-1} /Aylward and Findley 2002/, which corresponds to 0.9 mmol L^{-1} or 21 mL L^{-1}. The most nitrogen gas found in Laxemar during the site investigation was 104 mL L^{-1} in a total gas volume of 107 mL L^{-1} at a pressure of one atmosphere. This corresponds to 4.6 mmol L^{-1} or 0.130 g nitrogen L^{-1} of groundwater and is close to 5.4 times more nitrogen in the groundwater than solubility permits at atmospheric pressure. In reality, the amount of nitrogen is even higher than 6.3 times, because other shallow groundwater gases, in particular, carbon dioxide and oxygen, will reduce the solubility of nitrogen during the entrapment of atmospheric nitrogen. The numbers used here are thus conservative. It is deemed very unlikely that the observed excess of dissolved nitrogen in the deep Laxemar groundwater originates from atmospheric entrapment during groundwater recharge. Most dissolved nitrogen must instead originate from deep crustal sources.

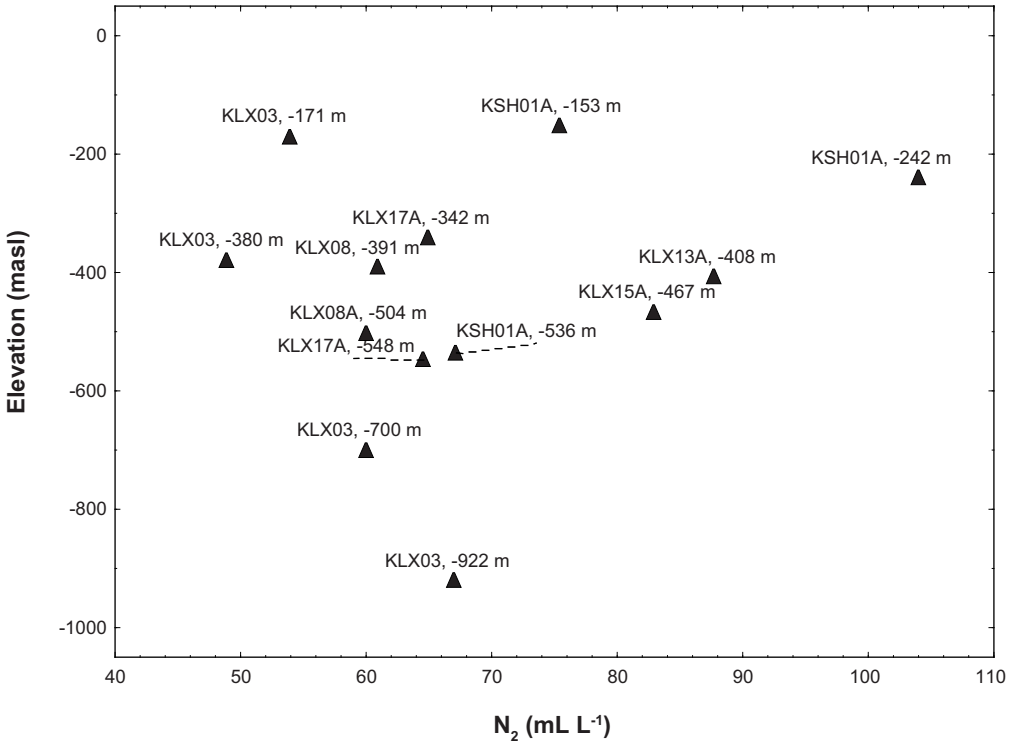

Figure 3-3. *Nitrogen concentration versus depth in samples from boreholes in the Laxemar–Simpevarp area.*

The increase in nitrogen concentration over depth suggests that most of the nitrogen comes from deep crustal sources. Actually, none of the analysed groundwater samples have nitrogen concentrations at or below the solubility limit (21 mL L^{-1}) at atmospheric pressure; the absolute majority of the gas samples had nitrogen concentrations above this limit, supporting the suggested deep crustal origin.

Using data from /Chapoy et al. 2004/, the saturation concentration of nitrogen in a water–nitrogen system can be calculated. This calculation indicates that at a pressure of 7 MPa, which corresponds to a depth of 700 m, 1,200 mL of nitrogen gas can be dissolved in 1 kg of water at 10°C. All samples in Laxemar and Simpevarp had total gas volumes below 107 mL L^{-1} of water. Although the concentration of gas generally increases with depth, the gases are not oversaturated at the depths at which they were sampled.

3.4.2 Helium

The amount of helium in groundwater from the Laxemar-Simpevarp area increases with depth (see Figure 3-4 and Table 3-1). The lowest values of helium were found in groundwater from boreholes KLX03 at 171 m depth, KLX13A at 408 m, and KLX17A at 342 m. These values might be too low because of the leakage of the sampling containers and the ensuing contamination with nitrogen from the pressure gas (see section 3.5). The results are consistent with the helium content in groundwaters from other Fennoscandian Shield sites, such as Olkiluoto in Finland and the Äspö HRL tunnel. The higher concentrations with depth depend on the origin of the helium being deep sources in the Earth. There are four helium reservoirs on earth, namely, the atmosphere, crust, and upper and lower mantle /Apps and Van de Kamp 1993/. Since helium is not retained in the atmosphere, its concentration in air is very low (5.24 ppm by volume). The helium in the air comes from the outgassing of the continental crust and the degassing of the mantle. Helium is present as a mixture of two stable isotopes, helium-3 and helium-4, in relative abundances of 1.38×10^{-4} % and 99.999862%, respectively; helium-3 is mainly of primordial origin, but is also produced by the beta decay of tritium to helium-3, though this reaction is rare, while helium-4 is produced by the radioactive decay of uranium- and thorium-series radionuclides. Helium is constantly produced in the crust and the mantle by these reactions /Marshall and Fairbridge 1999/.

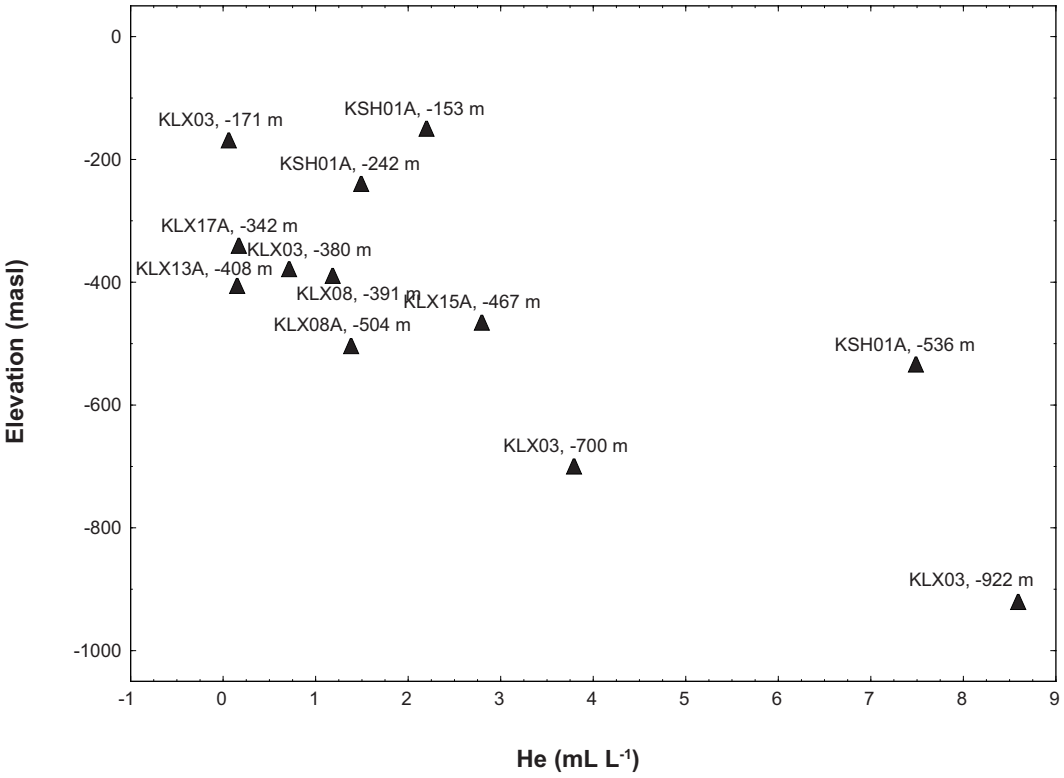

Figure 3-4. *Helium concentration versus depth in samples from boreholes in the Laxemar-Simpevarp area.*

3.4.3 Carbon dioxide

Carbon dioxide in groundwater is a dissociation product of dissolved carbonates from fractures in the bedrock and from the biological degradation of organic material in the soil and shallow bedrock. It functions as a carbon source and electron acceptor for autotrophic methanogens and acetogens. The carbon dioxide concentrations in samples from the Laxemar-Simpevarp area displayed a slight decreasing trend with depth (see Figure 3-5). At a depth of 922 m, the carbon dioxide concentration was very low, i.e. 0.01 mL L^{-1}. This pattern has also been observed for carbon dioxide concentrations in groundwater from the Forsmark site investigation /Laaksoharju et al. in manuscript/ and from the Olkiluoto site in Finland /Pitkänen et al. 2004, Pitkänen and Partamies 2007/. The carbon dioxide in the shallower groundwater comes from the degradation of organic material at the ground surface. At greater depths, the amount of organic material is less than at surface. The carbon dioxide may also be consumed by autotrophic microorganisms, such as methanogens and acetogens.

3.4.4 Methane and higher hydrocarbons

In the case of methane, there was no obvious trend with depth, except for the four sections in KLX03, which displayed a clear decreasing trend with depth. The amounts found were very low, between 20 and 100 µL L^{-1} (see Table 3-2 and Figure 3-6). The highest volume found was 870 µL L^{-1} in borehole KLX03, at a depth of 171 m.

Methane in groundwater can be either biotic or abiotic in origin. Biotic methane is produced by methanogenic *Archaea*, a group of prokaryotic organisms. They can use either C1 compounds or acetate (Equation 3-1). They can also fix carbon dioxide, using hydrogen gas as an energy and electron source (Equation 3-2). Their substrate can be biodegraded organic matter, as in sea and lake sediments or composts, or carbon dioxide and hydrogen originating in the mantle /Apps and Van de Kamp 1993/.

$$CH_3COOH \rightarrow CH_4 + CO_2 \qquad \text{(Eq. 3-1)}$$

$$CO_2 + 4H_2 \rightarrow CH_4 + 2H_2O \qquad \text{(Eq. 3-2)}$$

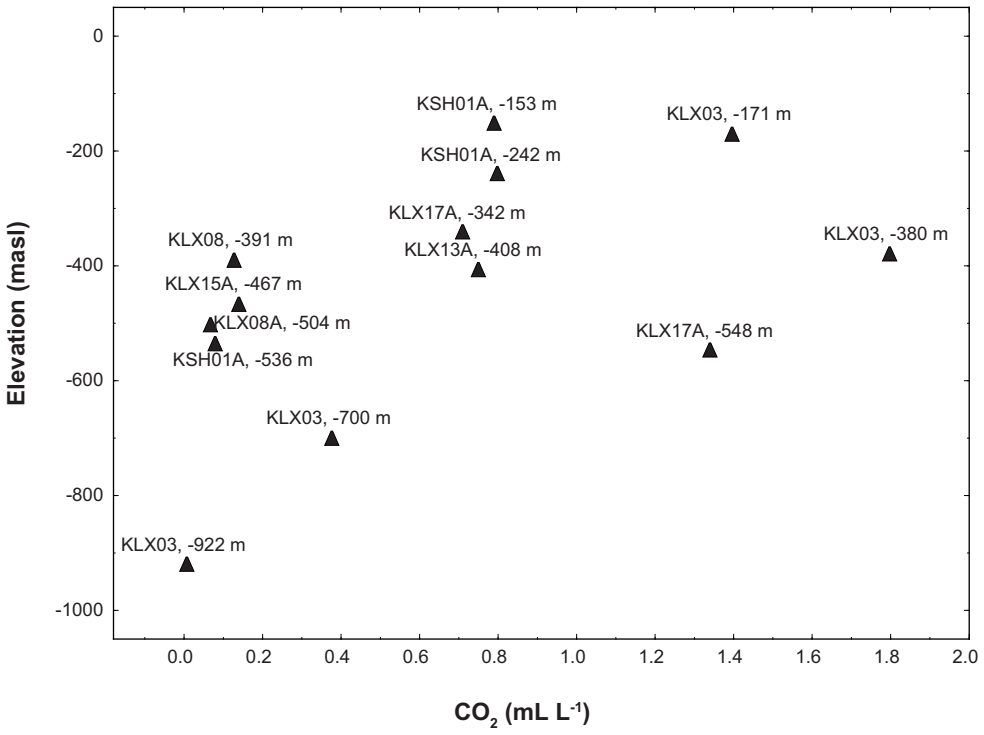

Figure 3-5. *Carbon dioxide concentration versus depth in samples from boreholes in the Laxemar–Simpevarp area.*

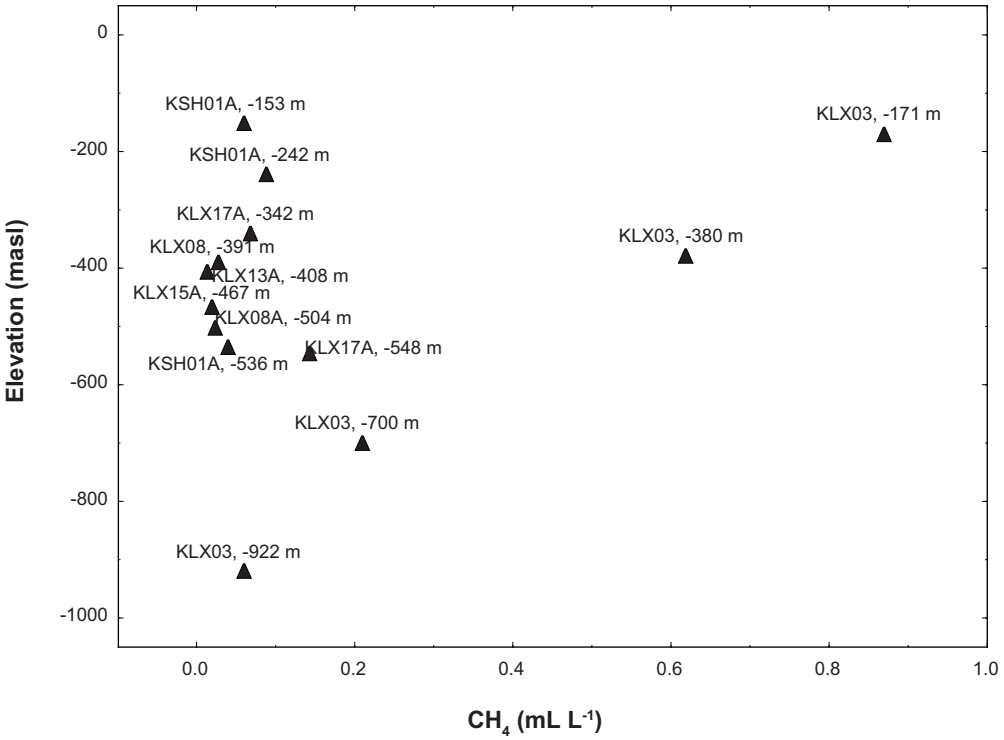

Figure 3-6. *Concentration of dissolved methane in samples from boreholes in the Laxemar–Simpevarp area versus depth.*

Abiogenic methane is produced, for example, in hydrothermal systems during water–rock interactions involving the Fischer–Tropsch synthesis reaction (Equation 3-2). Methane can act as a precursor for polymerization to higher hydrocarbons, such as short-chain alkanes (see below).

The isotopic carbon signature of methane can reveal its source, but no such data are available in Sicada. However, calculating the C1/(C2 + C3) ratio can also provide evidence regarding the origin of the methane (see below).

Table 3-3. The C1/(C2 + C3) ratio in groundwater from the Laxemar area.

Borehole and depth	∑ C2 + C3 (μL L^{-1})	CH4 (μL L^{-1})	C1/C2 + C3
KSH01A, 153 m	2.73	60	22
KSH01A, 242 m	4.31	90	21
KSH01A, 536 m	3.46	40	12
KLX03, 171 m	0.25	870	3,480
KLX03, 380 m	0.12	620	5,166
KLX03, 700 m	0.70	210	300
KLX03, 922 m	2.85	60	21
KLX08, 320 m	0.62	25	40
KLX08, 391 m	0.21	29	130
KLX08, 504 m	0.57	15	214
KLX13A, 408 m	0.07	21	8
KLX15A, 467 m	2.54	70	111
KLX17A, 342 m	0.63	145	1,208
KLX17A, 548 m	0.12	25	44

The concentrations of hydrocarbons other than methane in Laxemar-Simpevarp groundwater remained relatively constant with depth, being below 1 µL L^{-1} (see Figure 3-7). Four samples had higher concentrations, but were all below 4 µL L^{-1}. Calculations of the C1/(C2 + C3) ratio can reveal the source of the methane found, as stated above. A high ratio of over 10^3 is considered to indicate microbiological methanogenesis, while thermogenic and abiogenic methanogenesis will give a ratio of approximately 10 /Sherwood Lollar et al. 1993ab, 2002, Clark and Fritz 1997, Whiticar 1990/. Such calculations made using data from Laxemar and Simpevarp gave ratios ranging from 8 to 5,166. Samples from three sections had ratios over 10^3, namely borehole KLX03, at 171 and 380 m depth, and KLX17A at 342 m. The ratios in the other sections indicated that most of the methane originated from an abiogenic source, though some of the methane may be of biogenic origin. To be certain as to the origin of this gas, more hydrocarbon data must be generated, together with stable isotope values for methane and other hydrocarbons.

3.4.5 Argon

The amount of argon in Laxemar and Simpevarp groundwater was almost constant, increasing only slightly with depth, and no detected value exceeded 2 mL L^{-1} (see Figure 3-8). Argon is the most common of the noble gases, accounting for 0.93% of air. It has three isotopes and 99.6% of all argon is ^{40}Ar, an isotope continuously produced in bedrock by the radioactive decay of ^{40}K. Argon is considered to be a "deep geogas" /Marshall and Fairbridge 1999/.

3.4.6 Hydrogen

Hydrogen is an important gas in several anaerobic microbial metabolisms, such as methanogenesis and acetate production by acetogens. Autotrophic iron- and sulphate-reducing bacteria also can use hydrogen as an energy and electron source, concomitant with iron or sulphate reduction.

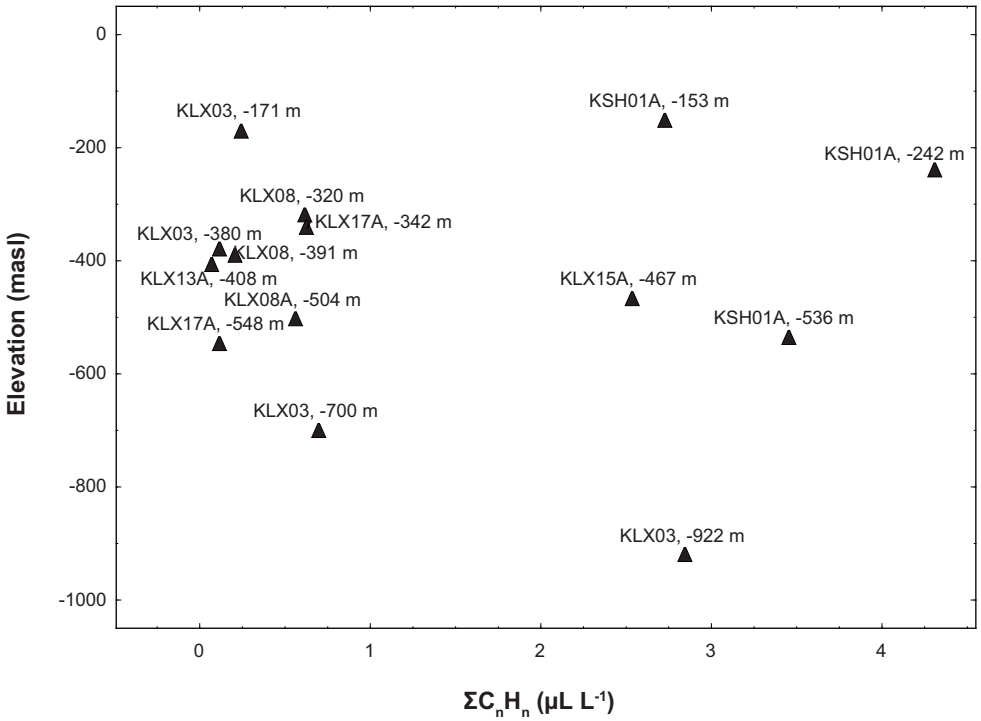

Figure 3-7. *Total concentrations of hydrocarbons (except methane), versus depth in boreholes in the Laxemar-Simpevarp area.*

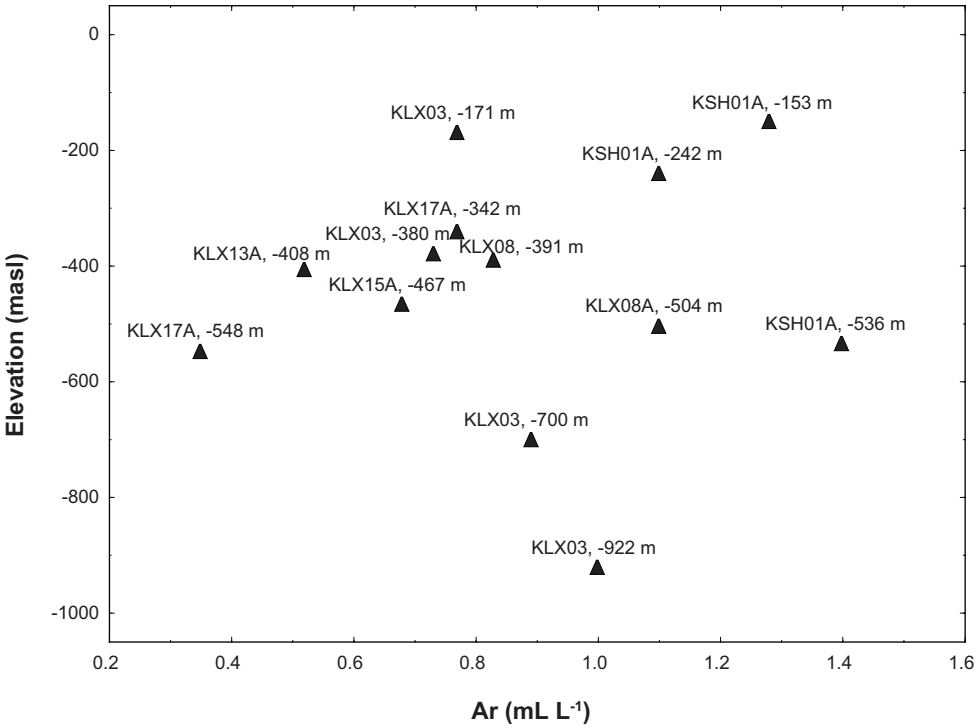

Figure 3-8. *Argon concentration plotted versus depth in samples from boreholes in the Laxemar–Simpevarp area.*

Measuring hydrogen in deep groundwater using a thermal conductivity detector, as was done here, commonly returns below detection results, because the concentrations of hydrogen in such water are relatively low. This accounts for the below detection results found in eight of 12 analysed samples. When the samples were sent to another laboratory for analysis, however, the results indicated 0.5 and 0.7 µL L^{-1} of hydrogen, below the detection limit of the analysis done by the first consulted laboratory. The highest amounts of hydrogen were found in borehole KSH01A at depths of 242 and 536 m, where they reached 85 and 81 µL L^{-1}, respectively. In KLX03 at depths of 380 and 700 m, 110 and 190 µL L^{-1} were found, and in groundwater from KLX08, at 391 m depth, 46 µL L^{-1} was found.

There are at least six possible processes by which crustal hydrogen is generated: (1) reaction between dissolved gases in the C-H-O-S system in magmas, especially in those with basaltic affinities; (2) decomposition of methane to carbon (graphite) and hydrogen at temperatures above 600°C; (3) reaction between CO_2, H_2O, and CH_4 at elevated temperatures in vapours; (4) radiolysis of water by radioactive isotopes of uranium and thorium and their decay daughters and by radioactive isotopes of potassium; (5) cataclasis of silicates under stress in the presence of water; and (6) hydrolysis by ferrous minerals in mafic and ultramafic rocks /Apps and Van de Kamp 1993/. The radiolysis of water has been proposed by /Lin et al. 2005/ as a possible hydrogen-generation process occurring in the granitic system in the Fennoscandian Shield. In addition, hydrogen is biologically produced in microbial fermentation processes. It is important to explore the scale of these processes and the rates at which the produced hydrogen becomes available to deep microbial ecosystems. The information gained thus far from the site investigation is insufficient for such investigation; to be able to do this, more gas data are needed, complemented by the isotopic composition together with studies of the transport rate of hydrogen from deep sources.

3.5 Ratios

Some samples from Laxemar and Simpevarp might have been contaminated with nitrogen, as discussed above. It was also seen that the distributions and concentrations of gases differed between the Simpevarp and Laxemar subareas. The lack of stable isotope data for the analysed gases complicates the interpretation of the dataset – they would have been very helpful in separating the effects. For now, the only analytical tool available is comparing the ratios of analysed gases.

3.6 Nitrogen to argon

A scatter plot of the nitrogen/argon ratios indicates that all samples had nitrogen/argon ratios greater than the water/air equilibrium value (Figure 3-10). The atmospheric nitrogen/argon ratio is 83.54 and four samples exceeded this value. High ratios above this value suggest nitrogen of a very deep, thermogenic origin /Andrews et al. 1989/, but stable isotopes are needed to be able to draw a valid conclusion. An alternative explanation of the high nitrogen/argon ratios is contamination of the sample with pressure vessel nitrogen (cf. Table 3-2), which, depending on the nitrogen gas quality (unknown at present), would have been depleted in argon. From Figure 3-9 it can be seen that samples from boreholes KLX13A at 408 m depth, KLX15A at 467 m, and KLX17A at 548 m have high N_2/Ar ratios. Recalling Figures 3-1 and 3-2, total gas and nitrogen versus depth, the samples from KLX15A and KLX17A had high total gas volumes and nitrogen volumes. These data together, with the high nitrogen/argon ratio, support these samples having been contaminated with nitrogen from the pressure vessel. The sample from borehole KLX17A at 548 m depth, on the other hand, did not contain a high volume of total gas or nitrogen. The high nitrogen/argon ratio in this sample is more likely dependent on cross contamination of groundwater with surface water, as explained in the microbe section.

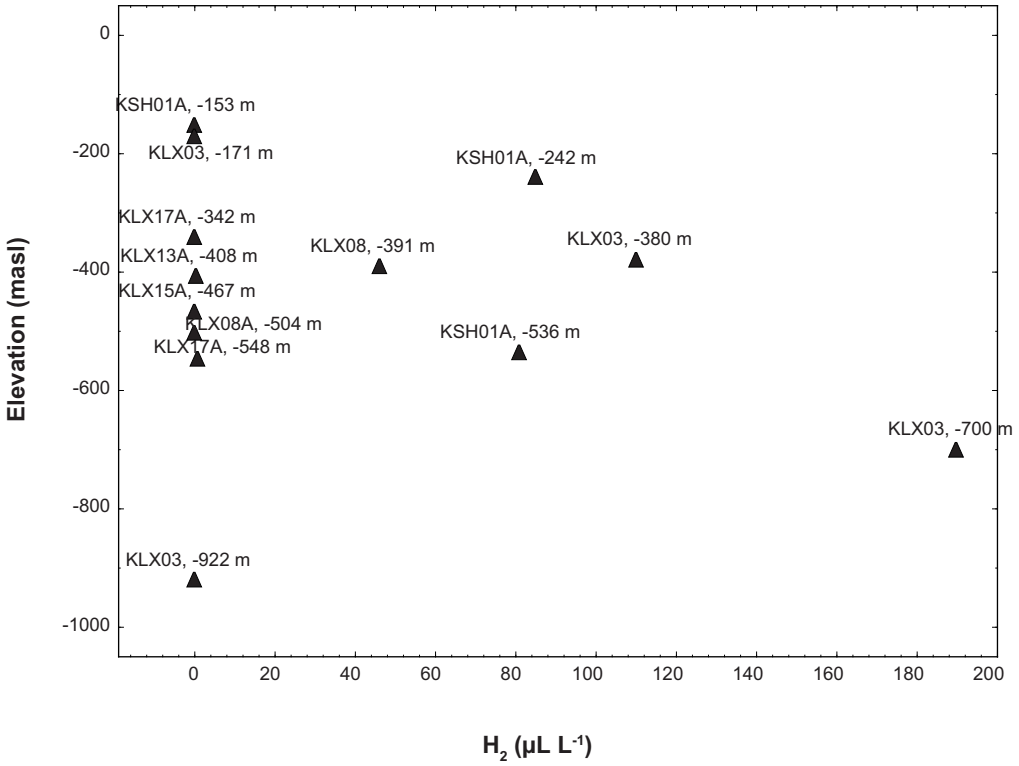

Figure 3-9. *Hydrogen concentration in groundwater from boreholes in the Laxemar-Simpevarp area.*

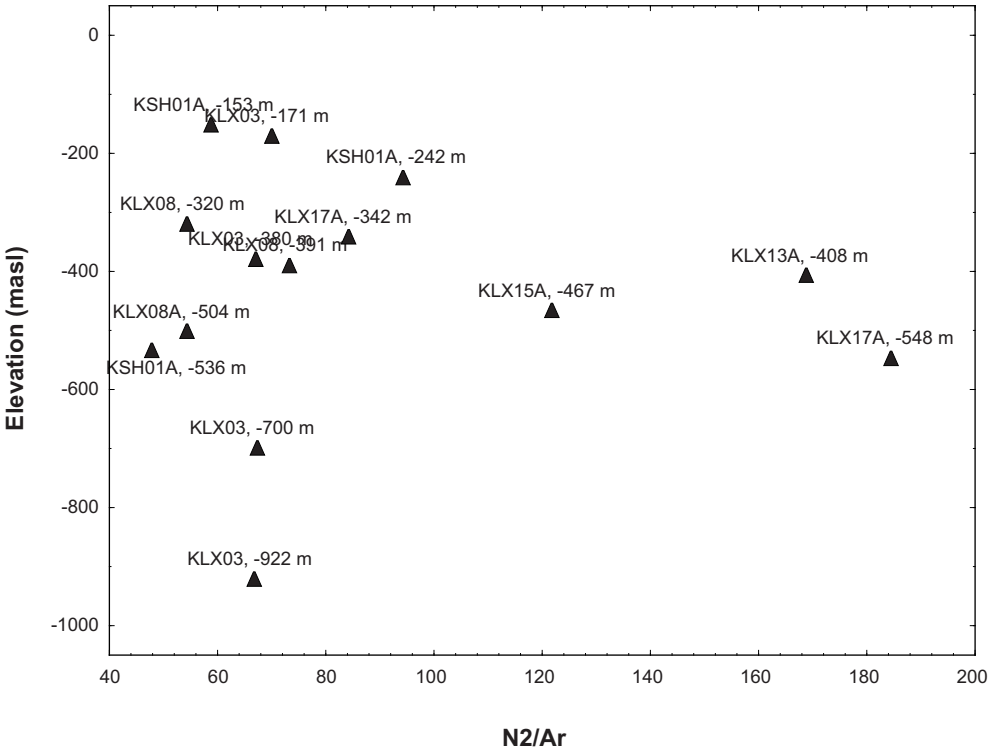

Figure 3-10. *The nitrogen/argon ratios for Laxemar groundwater gas samples.*

3.7 Nitrogen to helium

Comparing nitrogen with helium identifies nine samples with relatively stable ratios versus depth of 8 to 69 (Figure 3-11). Three of the samples displayed higher ratios. One of these is the sample from borehole KLX13A at a depth of 408 m, which further indicates that this sample was contaminated with nitrogen from the pressure vessel. The sample from KLX03 at 171 m depth had an extremely low helium value, which explains the high nitrogen/helium ratio. The sample from KLX17A at 342 m does not have an extremely high nitrogen/argon ratio, though it is nevertheless higher than the others. The helium value from borehole KLX17A at 548 m depth was below the detection limit and was not included in Figure 3-10.

If the nitrogen/helium ratios are similar over depth, here approximately 10, this suggests that the nitrogen comes from deep sources. Helium is known to be produced at great depths due to radioactive decay and also to diffusion from the mantle, as discussed above in relation to Figure 3-11. Nitrogen may also be produced in a similar process. However, stable isotope data and tight PVB vessels are required before any meaningful conclusions can be drawn.

3.8 Methane to helium

If nitrogen is assumed to originate from deep sources, as suggested above, nitrogen/methane ratios should remain constant over depth if the methane is also produced at depth. This is true of all samples in the Laxemar-Simpevarp area, apart from the sample from borehole KLX03 at 171 m depth. This is the sample with the very low helium value and also the highest amount of methane, explaining the high methane/helium ratio in this sample. Three samples were indicated to contain a significant amount of biogenic methane, as determined by the C1/C2 + C3 ratio, but stable isotopes data are needed for confirmation. The possible dilution effect of the presence of nitrogen in the PVB would not upset the ratios in Figure 3-12, as it would equally dilute both helium and methane.

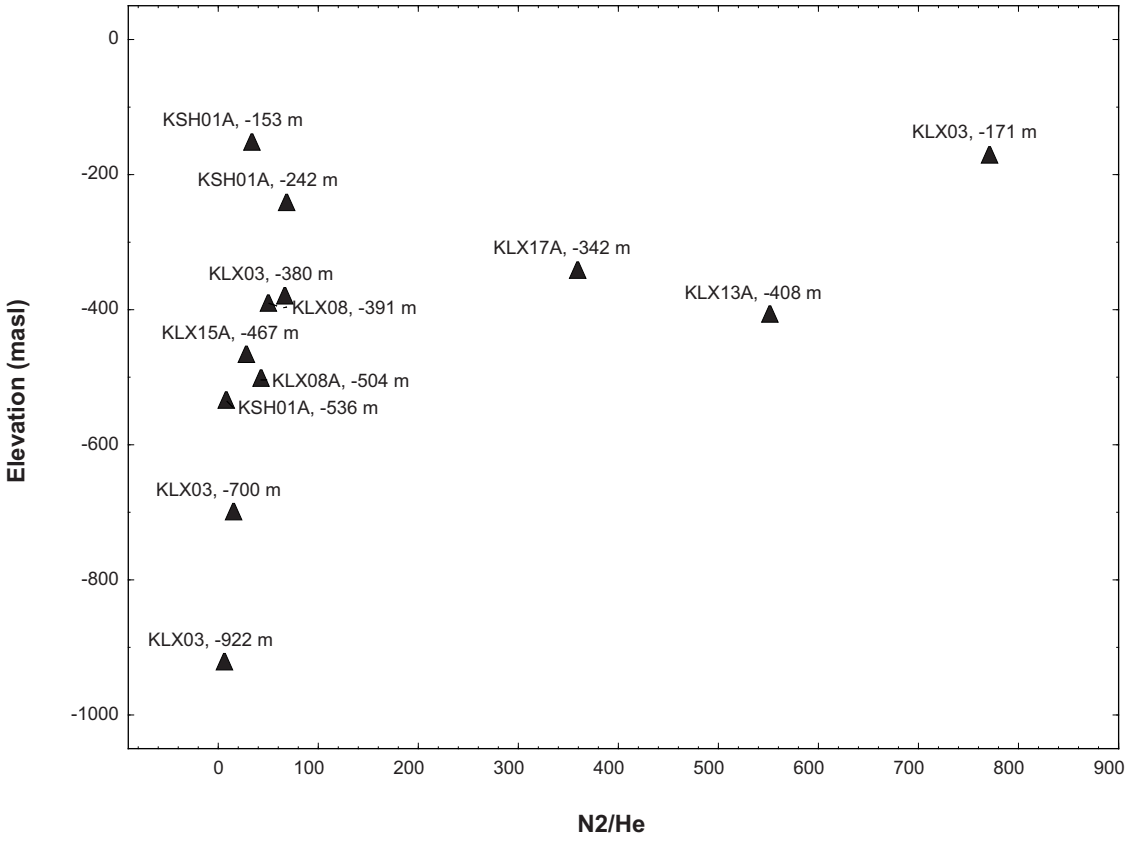

Figure 3-11. *The nitrogen/helium ratios for the Laxemar–Simpevarp groundwater gas samples.*

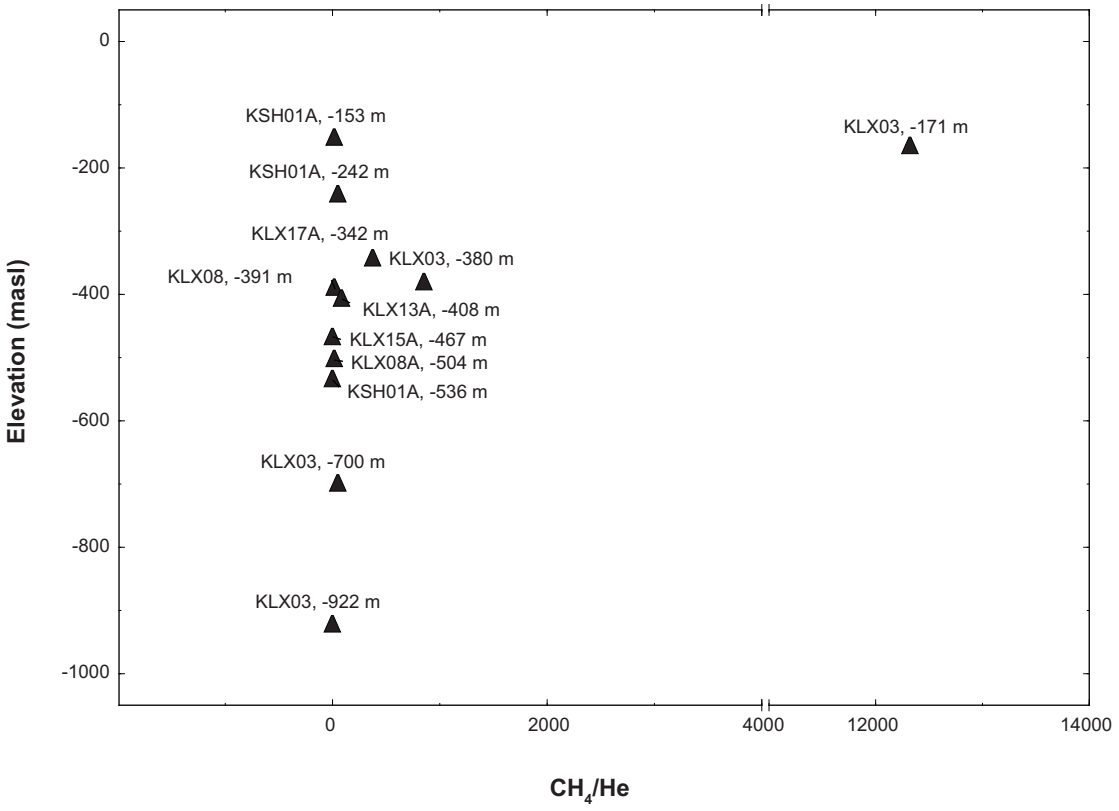

Figure 3-12. *The methane/helium ratios for the Laxemar-Simpevarp groundwater gas samples.*

3.9 Conclusions

- The main gas in samples from Laxemar and Simpevarp groundwater is nitrogen, followed by carbon dioxide in the shallower groundwaters and helium in the deeper parts of the system. Other gases present are helium, methane, argon, hydrogen, and traces of higher hydrocarbons up to three carbon atoms.
- The available data regarding dissolved gas in groundwaters in the Laxemar-Simpevarp area indicate that the total gas content is in the lower range of what could be expected in Fennoscandian Shield groundwater.
- Although their concentrations generally increase with depth, the gases are not oversaturated at the depths at which they were sampled.
- The samples that display indications of biologically produced methane were from borehole KLX03, 171 and 380 m depth, and KLX17A, 342 m depth. The methane in all other samples appears to come from abiotic sources (unless anaerobic methane oxidation is operating).
- Clarifying the origins of methane, helium, argon, and nitrogen calls for more data regarding deeper sections coupled with isotopic studies.

4 References

Andrews J N, Hussain N, Youngman M J, 1989. Atmospheric and radiogenic gases in groundwater from the Stripa granite. Geochimica et Cosmochimica Acta, 53, 1831–1841.

Apps J A, van de Kamp P C, 1993. Energy gases of abiogenic origin in the Earth's crust. The future of energy gases. U.S. Geological Survey Professional Papers. United States Government Printing Office, Washington, pp. 81–132.

Aylward G H, Findley T J V, 2002. SI Chemical Data, 5th ed. John Wiley & Sons Australia, Ltd, Milton, Australia.

Bennett P C, Rogers J R, Choi W J, Hiebert F K, 2001. Silicates, silicate weathering, and microbial ecology. Geomicrobiology Journal, 18, 3–19.

Berg C, Bergelin A, Wacker P, Nilsson A-C, 2006. Forsmark site investigation. Hydrochemical characterisation in borehole KFM08A. Results from the investigated section at 683.5–690.8 m. SKB P-06-63, Svensk Kärnbränslehantering AB.

Boetius A, Ravenschlaug K, Schubert C J, Rickert D, Widdel F, Gleseke A, Amann R, Jörgensen B B, Witte U, Pfannkuche O, 2000. A marine microbial consortium apparently mediating anaerobic oxidation of methane. Nature, 407, 623–626.

Chapoy A, Mohammadi A H, Tohidi B, Richon D, 2004. Gas solubility measurements and modelling for the nitrogen + water system from 274.18 K to 363.02 K. Journal of Chemical Engineering data. 49, 1110–1115.

Clark I, Fritz P, 1997. Environmental Isotopes in Hydrogeology. Lewis Publishers, Boca Raton, FL, 328 p.

Drake H L, Küsel K, Matthies C, 2002. Ecological consequences of the phylogenetic and physiological diversities of acetogens. Antonie van Leeuwenhoek, 81, 1203–1212.

Degueldre C, Pfeiffer H-R, Alexander W, Wernli B, Breutsch R, 1996. Colloid properties in groundwater from crystalline formation. I. Sampling and characterization. Applied Geochemistry, 11, 677–695.

Ekendahl S, Pedersen K, 1994. Carbon transformations by attached bacterial populations in granitic groundwater from deep crystalline bed-rock of the Stripa research mine. Microbiology, 140, 1565–1573.

Etiope G, 1998. Transport of radioactive and toxic matter by gas microbubbles in the ground. Journal of Environmental Radioactivity, 40, 11–13.

Eydal H S C, Pedersen P, 2007. Use of an ATP assay to determine viable microbial biomass in Fennoscandian Shield groundwater from depths of 3–1,000 m, Journal of Microbiological Methods, 70, 363–373.

Fenchel T, King G M, Blackburn T H, 1998. Bacterial Biogeochemistry: The Ecophysiology of Mineral Cycling, 2nd ed. Academic Press, San Diego, CA.

Flodén T, Söderberg P, 1994. Shallow gas traps and gas migrations models in crystalline bedrock areas offshore Sweden. Baltica, 8, 50–56.

Goodfield M, Rodwell W R, 1998. "Geogas" Microbubbles: A Literature Review with Reference to their Potential to Contribute to the transport of Contaminants from a Radioactive Waste Repository. Nirex Science Report S/98/016. Cumbria, UK.

Greenberg A E, Clesceri L S, Eaton A D, 1992. Estimation of Bacterial Density: Standard Methods for the Examination of Water and Wastewater, 18th ed. American Public Health Association, Washington, DC.

Hallbeck L, Pedersen K, 2008. Characterization of microbial processes in deep aquifers of the Fennoscandian Shield. Applied Geochemistry 23, 1796–1819.

Haveman S H, Pedersen K, Routsalainen P, 1999. Distribution and metabolic diversity of microorganisms in deep igneous rock aquifers of Finland. Geomicrobiology Journal, 16, 277–294.

Haveman S A, Pedersen K, 2002a. Distribution of culturable anaerobic microorganisms in Fennoscandian Shield groundwater. FEMS Microbiology Ecology, 39, 129–137.

Haveman S A, Pedersen K, 2002b. Microbially mediated redox processes in natural analogues for radioactive waste. Journal of Contaminant Hydrology, 55, 161–174.

Johnsson A, Arlinger J, Ödegaard-Jensen A, Albinsson Y, Pedersen K, 2006. Solid-aqueous phase partitioning of radionuclides by complexing compounds excreted by subsurface bacteria. Geomicrobiology Journal, 23, 621–630.

Kotelnikova S, Pedersen K, 1998. Distribution and activity of methanogens and homoacetogens in deep granitic aquifers at Äspö Hard Rock Laboratory, Sweden. FEMS Microbiology Ecology, 26, 121–134.

Kyle J E, Eydal H S C, Ferris G, Pedersen K, 2008. Viruses of the deep subterranean biosphere. The ISME Journal, 2, 571–574.

Laaksoharju M, Degueldre C, Skårman C, 1995. Studies of colloids and their importance for repository performance assessment. SKB TR 95-24, Svensk Kärnbränslehantering AB.

Laaksoharju M, Wold S, 2005. The colloid investigation conducted at the Äspö Hard Rock Laboratory during 2000–2004. SKB TR-05-20, Svensk Kärnbränslehantering AB.

Laaksoharju M, Smellie J, Tullborg E-L, Gimeno M, Hallbeck L, Molinero J, Waber N, 2008a. Hydrogeochemistry Laxemar. Site descriptive modelling. SDM-Site Laxemar. SKB R-08-93, Svensk Kärnbränslehantering AB.

Laaksoharju M, Smellie J, Tullborg E-L, Gimeno M, Hallbeck L, Molinero J, Waber N, 2008b. Hydrogeochemistry Forsmark. Site descriptive modelling, SDM-Site Forsmark. SKB R-08-47, Svensk Kärnbränslehantering AB.

Lin L-H, Slater G F, Sherwood Lollar B, Lacrampe-Couloumbe G, Onstott T C, 2005. The yield and isotopic composition of radiolytic H_2, a potential energy source for the deep subsurface biosphere. Geochimica et Cosmochemica Acta, 69, 893–903.

Madigan M T, Martinko J, 2006. Brock Biology of Microorganisms, 11th ed. Prentice Hall, London.

Malmqvist L, Kristiansson K, 1984. Experimental evidence for an ascending microflow of geogas in the ground. Earth & Planetary Science Letters, 70, 407–416.

Marshall C P, Fairbridge R W, 1999. Encyclopedia of Geochemistry. Kluwer Academic Publishers, Dordrecht, the Netherlands.

Meyers C R, Nealson K H, 1990. Respiration-linked proton translocation coupled to anaerobic reduction of manganese (IV) and iron (III) in *Shewanella putrefaciens* MR-1. Journal of Bacteriology, 172, 6232–6238.

Nilsson A-C, Degueldre C, 2007. Forsmark Site Investigation: Granitic Groundwater Colloids Sampling and Characterisation. Colloid analysis from KFM11A. SKB P-07-169, Svensk Kärnbränslehantering AB.

Nilsson A-C, Hedqvist I, Degueldre C, 2008. Granitic groundwater colloids sampling and characterization: the strategy for artefact elimination. Analytical and Bioanalytical Chemistry, accepted for publication.

Pedersen K, Ekendahl S, 1990. Distribution and activity of bacteria in deep granitic groundwaters of southeastern Sweden. Microbial Ecology, 20, 37–52.

Pedersen K, Ekendahl S, 1992a. Incorporation of CO_2 and introduced organic compounds by bacterial populations in groundwater from the deep crystalline bedrock of the Stripa mine. Journal of General Microbiology, 138, 369–376.

Pedersen K, Ekendahl S, 1992b. Assimilation of CO_2 and introduced organic compounds by bacterial communities in ground water from Southeastern Sweden deep crystalline bedrock. Microbial Ecology, 23, 1–14.

Pedersen K, 2001. Diversity and activity of microorganisms in deep igneous rock aquifers of the Fennoscandian Shield. In: Fredrickson J. K, Fletcher M. (Eds.), Subsurface Microbiology and Biogeochemistry. Wiley-Liss, New York, pp. 97–139.

Pedersen K, 2004. Total numbers and metabolic diversity of microorganisms in borehole KSH01A. Results from three investigated sections, 158.5–167 m, 245–261.6 m and section 548–565 m. Oskarshamn site investigation. SKB P-04-276, Svensk Kärnbränslehantering AB.

Pedersen K, 2005a. Äspö Hard Rock Laboratory. The MICROBE framework. Site descriptions, instrumentation, and characterisation. SKB IPR 05-05, Svensk Kärnbränslehantering AB.

Pedersen K, 2005b. Äspö Hard Rock Laboratory. MICROBE. Analysis of microorganisms and gases in MICROBE groundwater over time during MINICAN drainage of the MICROBE water conducting zone. SKB IPR 05-29, Svensk Kärnbränslehantering AB.

Pedersen K, 2005c. Numbers and metabolic diversity of microorganisms in borehole KLX03. Results from sections 193.0–198.0 m, 408.0–415.3 m, 735.5–748.0 m and 964.5–975.2 m. Oskarshamn site investigation. SKB P-05-182, Svensk Kärnbränslehantering AB.

Pedersen K, 2007. Microorganisms in groundwater from borehole KLX08 – numbers, viability, and metabolic diversity. Results from sections 197.0–206.7 m, 396.0–400.9 m and 476.0–485.6 m. Oskarshamn site investigation. SKB P-07-59, Svensk Kärnbränslehantering AB.

Pedersen K, 2008. Microbiology of Olkiluoto groundwater, 2004–2006. POSIVA report 2008-02. Posiva OY, Olkiluoto Finland.

Pitkänen P, Partamies S, Luukonen A, 2004. Hydrochemical interpretation of baseline groundwater conditions at the Olkiluoto site. Posiva Report 2003-07. Posiva, Olkiluoto, Finland.

Pitkänen P, Partamies S, 2007. Origin and implications of dissolved gases in groundwater at Olkiluoto. Posiva Report 2007-04. Posiva OY, Olkiluoto, Finland.

Sherwood Lollar B, Frape S K, Fritz P, Macko S A, Welhan J A, Blomqvist R, Lahemo P W, 1993a. Evidence for bacterially generated hydrocarbon gas in Canadian Shield and Fennoscandian Shield rocks. Geochimica et Cosmochimica Acta 57, 5073–5085.

Sherwood Lollar B, Frape S K, Weise S M, Fritz P, Macko S A, Welham J A, 1993b. Abiogenic methanogenesis in crystalline rocks. Geochimica et Cosmochemica Acta 57, 5087–5097.

Sherwood Lollar B, Westgate T D, Ward J A, Slater G F, Lacrampe-Couloume G, 2002. Abiogenic formation of gaseous alkanes in the Earth's crust as a minor source of global hydrocarbon reservoirs. Nature 416, 522–524.

SKB, 2006a. Hydrochemical evaluation: preliminary site description Laxemar subarea – version 1.2. SKB R-06-19, Svensk Kärnbränslehantering AB.

SKB, 2006b. SR-CAN TR-08-19, Svensk Kärnbränslehantering AB.

Smellie J, Tullborg E-L, 2009. Documentation related to categorisation of the extended data freeze Laxemar 2.3 groundwater samples. In Kalinowski (ed) Complementary hydrogeochemical studies. SKB R-08-111, Svensk Kärnbränslehantering AB.

Staley J T, Konopka A, 1985. Measurements of in situ activities of non-photosynthetic microorganisms in aquatic and terrestrial habitats. Annual Review of Microbiology, 39, 321–346.

Stumm W, Morgan J, 1996. Aquatic Chemistry, 3rd ed. John Wiley, New York.

Söderberg P, Flodé T, 1991. Pockmark development along a deep crustal structure in the northern Stockholm Archipelago, Baltic Sea. Beitrage Meereskunde, 62, 79–102.

Söderberg P, 1993. Seismic stratigraphy, tectonics and gas migration in the Åland Sea, northern Baltic Proper. Stockholm Contributions in Geology, 43, 1–67.

Vilks P, Miller H, Doern D, 1991. Natural colloids and suspended particles in the Whiteshell Research area, Manitoba, Canada, and their potential effect on radiocolloid formation. Applied Geochemistry, 8, 565–574.

Wacker P, Bergelin A, Nilsson A-C, 2003. Forsmark Site Investigation. Complete hydrochemical characterisation in KFM01A. SKB P-03-94, Svensk Kärnbränslehantering AB.

Wacker P, Bergelin A, Nilsson A-C, 2004a. Forsmark Site Investigation. Hydrochemical characterisation in KFM02A. SKB P-04-70, Svensk Kärnbränslehantering AB.

Wacker P, Bergelin A, Nilsson A-C, 2004b. Forsmark Site Investigation. Complete hydrochemical characterisation in KFM03A. SKB P-04-108, Svensk Kärnbränslehantering AB.

Whiticar M J, 1990. A geochemical perspective of natural gas and atmospheric methane. Organic Geochemistry, 16, 531–547.